(2)

US Army Corps of Engineers

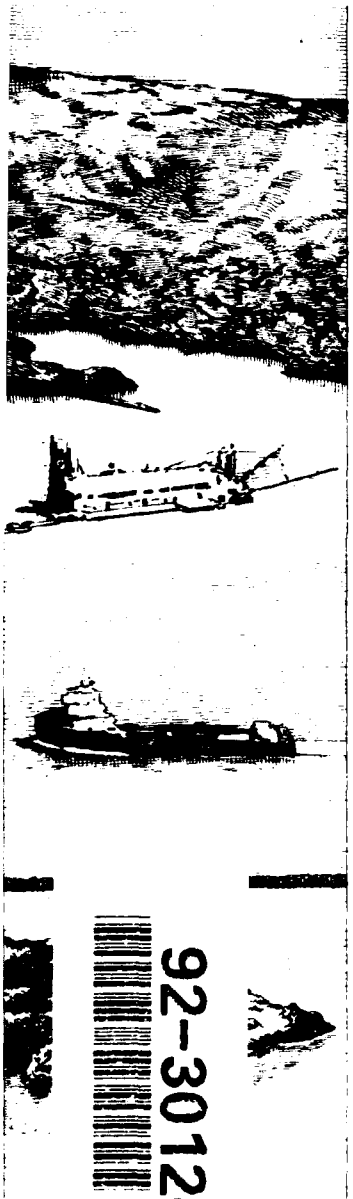

DREDGING RESEARCH PROGRAM

TECHNICAL REPORT DRP-92-5

ANALYSIS OF CROSS-SHORE MOVEMENT OF NATURAL LONGSHORE BARS AND MATERIAL PLACED TO CREATE LONGSHORE BARS

by

Magnus Larson

Department of Water Resources Engineering
Lund Institute of Technology
University of Lund
Box 118, Lund, Sweden S-221 00

and

Nicholas C. Kraus

Coastal Engineering Research Center

DEPARTMENT OF THE ARMY
Waterways Experiment Station, Corps of Engineers
3909 Halls Ferry Road, Vicksburg, Mississippi 39180-6199

September 1992

Final Report

Prepared for DEPARTMENT OF THE ARMY
US Army Corps of Engineers
Washington, DC 20314-1000

Under Work Unit 32463

The Dredging Research Program (DRP) is a seven-year program of the US Army Corps of Engineers. DRP research is managed in these five technical areas:

Area 1 - Analysis of Dredged Material Placed in Open Water

Area 2 - Material Properties Related to Navigation and Dredging

Area 3 - Dredge Plant Equipment and Systems Processes

Area 4 - Vessel Positioning, Survey Controls, and Dredge Monitoring Systems

Area 5 - Management of Dredging Projects

REPORT DOCUMENTATION PAGE

Form Approved
OMB No. 0704-0188

1. AGENCY USE ONLY (Leave blank)	2. REPORT DATE	3. REPORT TYPE AND DATES COVERED
	September 1992	Final report

4. TITLE AND SUBTITLE

Analysis of Cross-Shore Movement of Natural Longshore Bars and Material Placed to Create Longshore Bars

5. FUNDING NUMBERS

Work Unit 32463

6. AUTHOR(S)

Magnus Larson, Nicholas C. Kraus

7. PERFORMING ORGANIZATION NAME(S) AND ADDRESS(ES)

USAE Waterways Experiment Station, Coastal Engineering Research Center 3909 Halls Ferry Road, Vicksburg, MS 39180-6199 and Department of Water Resources Engineering, Lund Institute of Technology, University of Lund, Box 118, Lund, Sweden S-221 00

8. PERFORMING ORGANIZATION REPORT NUMBER

Technical Report DRP-92-5

9. SPONSORING/MONITORING AGENCY NAME(S) AND ADDRESS(ES)

US Army Corps of Engineers
Washington, DC 20314-1000

10. SPONSORING/MONITORING AGENCY REPORT NUMBER

11. SUPPLEMENTARY NOTES

Available from National Technical Information Service, 5285 Port Royal Road, Springfield, VA 22161.

12a. DISTRIBUTION/AVAILABILITY STATEMENT

Approved for public release; distribution is unlimited.

12b. DISTRIBUTION CODE

13. ABSTRACT *(Maximum 200 words)*

This study develops empirical predictive expressions for design of nearshore berms formed of dredged material. Such berms are placed in the form of long linear sand bars and are expected to behave as natural bars. The study examines the cross-shore movement of natural longshore bars at Duck, North Carolina. Beach profile survey data are available at approximately 2-week intervals from 1981 to 1989, together with measurements of the wave conditions. Two bars are typically present at Duck, an outer bar at approximately the 4- to 5- m depth and an inner bar at 1- to 2-m depth. These bars tend to move offshore during storms and onshore during periods of lower waves.

A method is introduced to define bar-type features unambiguously for analysis of field data. The method uses an equilibrium profile shape defined in terms of decreasing grain size with distance offshore. Analysis is made of bar movement, and criteria previously developed by the authors to predict beach erosion and accretion are found applicable if the value of a multiplicative empirical coefficient in each criterion is modified. The results show that onshore movement of bars is more

(Continued)

14. SUBJECT TERMS			15. NUMBER OF PAGES
Bars	Beach Erosion	Cross-Shore Sand Transport	115
Dredged Material	Longshore Bars	Nearshore Berms	16. PRICE CODE
Sediment Transport	Surf Zone		

17. SECURITY CLASSIFICATION OF REPORT	18. SECURITY CLASSIFICATION OF THIS PAGE	19. SECURITY CLASSIFICATION OF ABSTRACT	20. LIMITATION OF ABSTRACT
UNCLASSIFIED	UNCLASSIFIED		

13. (Concluded)

probable than previously estimated, indicating a wider possible range of wave conditions favorable for beach nourishment through creation of nearshore berms.

The predictive criteria developed from the east coast beach successfully described the observed onshore movement of a berm placed at Silver Strand Park, California. The criteria, expressed as nondimensional parameters, appear to have applicability to sites where bars and constructed submerged berms are modified primarily by wave action.

PREFACE

This study was conducted jointly at the Department of Water Resources Engineering, Lund Institute of Technology, University of Lund (UL), Sweden, and the Coastal Engineering Research Center (CERC), US Army Engineer Waterways Experiment Station (WES). Contract coordination was provided by the European Research Office of the US Army in London under contract DAJA45-90-C-0020. The work described herein was authorized as part of the Dredging Research Program (DRP) of Headquarters, US Army Corps of Engineers (HQUSACE) and performed under the Calculation of Boundary Layer Properties (Noncohesive Sediments) Work Unit 32463 which is part of DRP Technical Area 1, Analysis of Dredged Material Placed in Open Water. Messrs. Robert Campbell and Glenn R. Drummond were DRP Chief and TA1 Technical Monitors from HQUSACE, respectively. Mr. E. Clark McNair, Jr., CERC, was DRP Program Manager (PM), and Dr. Lyndell Z. Hales, CERC, was Assistant PM. Dr. Nicholas C. Kraus, Senior Scientist, CERC, was Technical Manager for DRP TA1 and Principal Investigator for Work Unit 32463.

This study was performed and the report prepared over the period 1 January 1991 through 30 June 1991 by Dr. Magnus Larson, Assistant Professor, UL, and Dr. Kraus. The beach profile data from Duck, North Carolina, were supplied by Mr. William A. Birkemeier, Chief, Field Research Facility (FRF), Engineering Development Division (EDD), CERC, and he and the FRF staff are acknowledged for their professionalism and efforts in acquiring these field data. Mr. Birkemeier reviewed this report. Mr. Mark Hansen, formerly of the Coastal Evaluation and Design Branch, EDD, CERC, provided the grain size information from Duck. Mses. Allison Abbe, Dawn Abbe, Marsha W. Darnell, and Holley Messing, Research Division, CERC, assisted in text formatting and figure preparation. Ms. Janean Shirley, Information Technology Laboratory, WES, edited the final report.

At the time of publication of this report, Director of WES was Dr. Robert W. Whalin. Commander and Deputy Directory was COL Leonard G. Hassell, EN.

Additional information can be obtained from Mr. E. Clark McNair, Jr., Program Manager, at (601) 634-2070 or Dr. Nicholas C. Kraus, Principal Investigator, at (601) 634-2018.

TABLE OF CONTENTS

LIST OF TABLES

LIST OF FIGURES

SUMMARY

The purpose of the study is to develop empirical predictive expressions for the effective placement of nearshore berms formed of dredged material. Such berms are placed in the form of long linear sandbars, and they are expected to behave similarly to natural bars, both in their movement and interaction with waves. The present report mainly examines the movement of natural longshore bars. An intensive data analysis is performed to quantify the cross-shore movement of natural longshore bars at Duck, North Carolina. Beach profile survey data are available at approximately 2-week intervals for a continuous period from 1981 to 1989, together with accurate measurements of the wave conditions. Two bars are typically present at Duck, an outer bar at approximately the 4- to 5-m depth and an inner bar at the 1- to 2-m depth. These bars tend to move offshore during storms and onshore during periods of lower waves. Analysis results for bar properties in the field are compared with previous results obtained in large wave tanks with monochromatic waves to test the range of applicability of the tank data sets for representing natural conditions.

A method is first introduced to define bar-type features unambiguously for analysis of field data. This method centers on a newly introduced equilibrium profile shape that is defined in terms of decreasing grain size with distance offshore. A detailed analysis is made of bar movement, and criteria previously developed by the authors to predict beach erosion and accretion are found to be applicable if a single multiplicative empirical coefficient in each criterion is modified. The results show that onshore movement of bars is more probable than previously estimated, indicating a wider possible range of wave conditions favorable for beach nourishment through creation of nearshore berms.

The methodology developed is examined with data documenting the behavior of a nearshore berm constructed of dredged material off Silver Strand State Park, in Southern California. It is found that the predictive criteria developed from the east coast beach successfully describe the observed onshore movement of the berm at Silver Strand. The criteria, expressed as nondimensional parameters, appear to have applicability to any site where longshore bars and constructed submerged berms are modified primarily by wave action.

ANALYSIS OF CROSS-SHORE MOVEMENT OF NATURAL LONGSHORE BARS AND MATERIAL PLACED TO CREATE LONGSHORE BARS

PART I: INTRODUCTION

Problem Statement and Objectives

1. The beach is a dynamic system that resists inundation and erosion by two processes, storage of material on the foreshore and dune complex, and storage of sand offshore through creation of longshore bars that also act to reduce erosive energy reaching the beach by breaking the incident waves. In the cross-shore plane, sediment moves between the shore face and bars according to the wave and water level conditions, grain size of the beach material, and other factors. During storms, which are characterized by higher waves and water levels, sediment moves from the beach face and, possibly, from dunes to form bars, whereas under lower waves, bars tend to lose volume and move onshore. Sediment also moves alongshore in a direction mainly controlled by the angle of the incident waves. In the present study, only cross-shore sediment transport processes are considered, and the reader is referred to Hanson and Kraus (1989) and Gravens, Kraus, and Hanson (1991) for calculation of beach planform change produced by wave action.

2. In recognition of the positive effects of bars for promoting beach growth and protecting beaches, a limited number of field profile nourishment projects have been performed to construct bars or "nearshore berms or mounds" from dredged material with the intent of the placed bars to either serve as a wave break and/or to supply the beach with material. If a nearshore berm is not intended to move, it is referred to as a "stable berm," whereas if the bar is expected to move it is called an "active" or "feeder berm" with reference to its potential action of supplying material to the littoral zone of the beach, either increasing visible beach volume or reducing erosion by serving as a supplemental source of material. Stable berms need not be of beach-quality material and have beneficial uses as wave breaks and fish habitats. Feeder berms must be of beach-quality material compatible with the native material, meaning they should have a substantial grain size fraction equal to or greater than the native sediments. McLellan (1990) discusses the concept of nearshore berms and their performance from an engineering perspective,

and Smith and Jackson (1990) compare various alternative placement locations and means of placement from the perspectives of public perception and physical factors controlling performance.

3. In many situations, handling costs for constructing feeder berms can be significantly less than the cost of direct placement on the beach or disposal far offshore. In any case, it is almost always preferable to retain beach quality sand in the littoral zone in dredging activities. Questions arising in the design of feeder berms include whether the placed sediment will act as a stable or feeder berm, whether it will move onshore (to the beach) or offshore, the time frame of the material movement, the wave and water level conditions that promote movement, and potential adverse impacts of the berm on the beach or surf conditions. Knowledge to estimate the interaction of both natural and artificial bars with waves and their potential for onshore or offshore movement is rudimentary. Hands and Allison (1991) describe a criterion to estimate whether a berm will be stable, based on statistical properties of the wave climate. They found that a statistically defined near-bottom horizontal component of the wave orbital velocity as calculated from linear-wave theory was a good predictor of whether a berm was active or stable for fine to medium sands.

4. McLellan and Kraus (1991) introduced a systematic methodology and guidance for designing nearshore berm projects by applying a beach accretion and erosion prediction criterion developed by Larson and Kraus (1989) (and further verified by Kraus, Larson, and Kriebel 1991) to the prediction of onshore or offshore movement of material placed in the active littoral zone. Timing (as in season of placement), depth, length of the berm, location of placement, and suitable grain size were discussed in general and through an example for Bald Head Island, North Carolina. Based on statistical summaries of a wave hindcast for the site, the potential performance of a berm was evaluated and guidance provided for the maximum depth of placement and appropriate grain size. McLellan and Kraus (1991) did not evaluate their methodology by direct observation of nearshore berms or natural bars, however. Recently, Foster, Healy, and de Lange (1991) applied the criterion given in Kraus et al. (1991) (that is further studied in the present report) to a dredged material mound placed off Mount Maunganui Beach, New Zealand. The criterion predicted onshore movement, in agreement with observation.

5. The main objective of the present study is development of rational criteria and a procedure for predicting the movement of material placed in the nearshore zone to perform as an

active or feeder berm. In order to derive such criteria, extensive analysis of data on the movement and characteristics of natural sand bars was carried out. Thus, a wide range of geometric properties describing longshore bars and their movement were determined based on field data, and these properties were related to the prevailing wave climate. Geometric properties such as depth to bar crest, maximum bar height, bar volume, location of bar mass center, and speed of bar movement were calculated for a large number of consecutively surveyed profiles at Duck, North Carolina, at the Field Research Facility (FRF) operated by the Coastal Engineering Research Center of the US Army Engineer Waterways Experiment Station. These data are supplemented by other limited data and a case study of a berm placed off Silver Strand State Park, California.

Procedure

6. Beach profile survey data obtained at the FRF (see Birkemeier et al. 1985) were analyzed for examining quantitative features of profile change with focus on the time evolution of bar properties and their relation to the measured wave climate. The nearshore bathymetry at the FRF has been surveyed, on the average, every 2 weeks from 1981 to 1989 along four lines located far from the disturbing influence of the research pier (profile Lines 58, 62, 188, and 190; see Howd and Birkemeier 1987a). Approximately 200 to 300 surveys exist for individual lines, with 20 to 50 distance-elevation measurement pairs for each survey. During limited periods, such as during major field experiments, and along some of the profile lines, surveying at shorter time intervals was carried out, encompassing several profile measurements in a day.

7. During the 8-year period of available profile survey data, the wave height and period, determined as the energy-based significant wave height and the peak spectral period, respectively, were recorded every 6 hr in the 18-m water depth by a waverider buoy. However, during the latter part of the 8-year measurement period, more frequent recording of the wave height and period was made with a time resolution of up to 1 hr.

8. Analysis of the general response of the beach profile to the incident waves at the four survey lines showed quite similar long-term behavior. In analysis of geometric bar properties, only data from Line 62 were used, since this line encompassed the largest number of profile surveys and displayed the most representative response in terms of bar movement. Bar

properties were calculated with respect to a reference profile which was determined from the average profile at Line 62, and encompassed:

a. Depth to bar crest.

b. Maximum bar height.

c. Bar volume.

d. Bar length.

e. Location of bar center of mass (direction of bar movement).

f. Bar speed.

An effort was made in this study to correlate these properties with the wave conditions associated with the observation interval between any two profile surveys being compared.

9. At Duck, two bars typically appear along the profile, an inner bar in shallower water closer to shore that is almost constantly exposed to breaking waves, and an outer bar where the waves only break during significant storms. In the present analysis, it was considered appropriate to separately examine the response of these two types of bars, especially with reference to the time scale of bar movement for respective features. Also, from the analysis of the time evolution of bar properties, criteria were derived for determining the direction of bar movement (direction of sand transport) in terms of the wave properties and the beach characteristics.

10. Much of the profile shape analysis procedures and insights into bar behavior obtained in this report follow from previous work performed by the authors in examination of macro-scale beach profile change generated in laboratory programs involving Large Wave Tanks (LWT). Two major LWT laboratory projects were studied, one performed in the United States in the 1950s and 1960s (Saville 1957, Kraus and Larson 1988) and the other performed in Japan (Kajima et al. 1982). The results of the LWT analysis are documented in Kraus and Larson (1988), Larson, Kraus, and Sunamura (1988), and Larson and Kraus (1989). These and subsequent related publications will be discussed below in comparison of procedures used and in the study of the behavior of bars and beaches in the field.

11. The analysis procedures adopted in this report as summarized above are applicable if two assumptions are satisfied. First, the analyzed profile change must be dominated by cross-shore processes and transport, meaning that longshore homogeneity exists. The second assumption is that short-period incident waves are the direct and dominant sediment-transport

driving mechanism. Engineering studies have long recognized the appearance of three-dimensional patterns in beach morphology in the surf zone (Hom-ma and Sonu 1962). Intensive high-resolution beach profile surveys (Howd and Birkemeier 1987a, 1987b) and inference of morphology through long-term remote sensing (Lippman and Holman 1990) at the FRF indicate that bars tend to become linear (two-dimensional) during storms and rhythmic (three-dimensional) 5 to 16 days following the peaks of storms. Care was taken in the present study to recognize potential occurrences of three-dimensionality, mainly through comparison of the shapes of the profiles at different survey lines and through censoring of the data by, for example, imposing threshold values to consider only large changes.

12. Bars formed by high breaking waves during storms are located seaward of the surf zone during more frequent times of milder wave conditions. Wright et al. (1991) collected field data over a 3-year period to investigate cross-shore sediment fluxes on the shore face seaward of the surf zone. They isolated and made relative comparisons of several sediment-transport driving mechanisms. Among their findings were that incident waves were the major source of bed shear stress and that mean flows contributed both to onshore and offshore fluxes during fair weather. Although incident waves may be one contributing mechanism to the mean flow, other forcing mechanisms such as the tide and wind-generated currents also enter in the total mean flow. Thus, during times of mild wave conditions in particular, correlations between bar movement and incident waves, such as sought in the present study, may be weak and should be viewed with caution.

Scope of Report

13. Part I describes the objectives of the study and gives an overview of the analysis procedure used to study longshore bars. Part II reviews the field data sets employed, and Part III describes the investigation of basic properties of the beach profile at the FRF, with emphasis on the equilibrium profile and definition of a bar for the field situation. Parts IV and V respectively describe analysis results for basic properties, such as volume and speed of movement, for the inner and outer bars at the FRF. Main results of the study are contained in Part VI, which relates bar movement to the measured wave conditions and contains criteria developed for predicting whether a natural or constructed longshore bar composed of sand of a certain grain size

will move on- or offshore under specified wave action. Part VII contains an application of the predictive criteria, developed from measurements on an east-coast beach, to a west-coast beach (Silver Strand Beach, located in southern California). Conclusions and a summary of results are given in Part VIII. Appendices A through D contain listings of calculated bar and wave properties for the inner and outer bars. Mathematical notation used in this report is listed in Appendix E.

PART II: DATA EMPLOYED IN THIS STUDY

14. Beach profile data collected at the FRF were analyzed to provide information on the spatial and temporal properties of natural longshore bars in the nearshore zone (depth less than approximately 15 m). This data set encompasses profile surveys with the associated wave and water level climate from a measurement period extending from 1981 to 1989. Understanding of the characteristics and response of natural longshore bars provides a foundation for predicting the behavior of artificial bars or berms constructed by placing dredged material in the nearshore zone. One important aspect requiring study is whether such a berm will move onshore to nourish the beach or whether the material will be lost to the offshore.

Beach Profile Data

15. The beach profile was surveyed approximately biweekly along four shore-normal lines from 1981 to 1989, where each survey extended from a base line behind the dune region out to a typical water depth of about 9 m. The locations of the four profile lines (Lines 58, 62, 188, 190) are shown in Figure 1, together with the location of the FRF Research Pier. No influence from the pier on profile evolution along the survey lines is expected since the lines are located far away from the pier where depth contour lines are typically straight and parallel (see Figure 1). All profile elevation data given in this report are referenced to the 1929 National Geodetic Vertical Datum (NGVD), the datum customarily used to report bathymetry data at the FRF, and cross-shore distances refer to the FRF baseline unless otherwise stated. The relationship between NGVD and Mean Sea Level (MSL) at the FRF is given as MSL = NGVD + 0.067 m (Kraus, Gingerich, and Rosati 1989).

16. The profile data from the time period 1981 to 1984 have been tabulated by Howd and Birkemeier (1987a), whereas the data from the period 1985 to 1989 have been compiled but not yet published. In the present analysis, the profile data were made available to the authors on magnetic media directly from the FRF*. Table 1 summarizes the data for each survey line that were available for this study.

---

* Personal Communication, June 1990, Mr. W. A. Birkemeier, Chief, FRF.

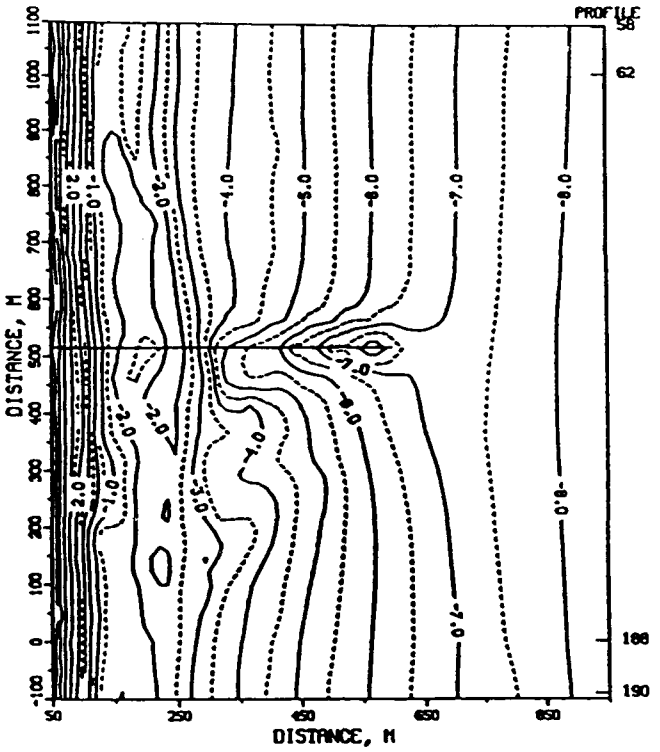

Figure 1. FRF bathymetry on 27 Nov. 1984 (after Howd and Birkemeier 1987a)

Table 1

Summary of Data for the Four Profile Survey Lines at the FRF

Line No.	No. of Surveys	First Survey	Last Survey
58	267	810717	891228
62	300	810126	891228
188	256	810120	891228
190	255	810717	891228

The larger number of surveys for profile Line 62 is partly related to an increased survey effort in this area during the field experiment DUCK85 (Mason, Birkemeier, and Howd 1987). Typically between 20 and 50 distance-elevation pairs were recorded during each individual survey. The surveys were in general carried out to a water depth exceeding the measured depth of profile

closure (Hallermeier 1978, Birkemeier 1985) with the exception of some surveys taken during special research efforts such as DUCK85. All profiles in the data set were surveyed using the Coastal Research Amphibious Buggy (CRAB) (Birkemeier and Mason 1984).

Wave and Water Level Data

17. The wave data used in this study were taken by a waverider buoy located in the 18-m water depth directly off the FRF research pier (originally named Gage 620 in the FRF instrument identification system; during the latter part of the measurement period it was renamed Gage 630). A wave staff gage (Gage 625) is located at the seaward end of the pier, but data collected by this gage were not used because wave breaking occurs shoreward of this point during large storms. The maximum height for an unbroken wave at the seaward end of the pier is approximately 3 m (Howd and Birkemeier 1987a). In analysis of bar response to the prevailing wave climate, it was desirable to use simple descriptors of the wave characteristics such as deepwater quantities, avoiding the additional complexity of wave transformation in connection with breaking.

18. Wave height was obtained as energy-based significant wave height calculated as four times the standard deviation for a 20-min water level record. The wave period was determined as the period corresponding to the peak in the energy spectrum. Wave height and period were typically recorded every 6 hr but were recorded more frequently during the end of the 8-year observation period, for which hourly values are available.

19. Hourly values for the water level are available from a National Oceanic and Atmospheric Administration tide gage located at the end of the research pier at approximately the 4-m depth contour. The measurement represents the total water level including both tide and possible surge. The influence of water level was not included in this study, because its typical period of variation was significantly shorter than the time elapsed between surveys, and the variation in most cases was almost symmetrical about the mean value. In between most surveys, several tidal cycles occurred with an approximate variation around the mean water level, making it difficult to assess the influence of this variable.

Accuracy of Profile Surveys

20. The accuracy of profile surveying by CRAB is discussed in detail in Howd and Birkemeier (1987a), together with the most common types of errors that can occur during a survey. The accuracy of elevation measurements with the CRAB is on the order of 5 cm. For the profile data from the measurement period 1981-1984, extensive error checking and correction were performed by Howd and Birkemeier (1987a), whereas for the period 1985 to 1989 only spot checking has presently been made. Thus, it is expected that the latter part of the measurement period is more affected by survey errors than the first part. However, an effort was made to use as many profile surveys as available in the original database, and no additional systematic error checking and corrections were implemented.

PART III: BASIC PROPERTIES OF PROFILE CHANGE

21. In this chapter, some general properties of beach profiles and the variability in profile shape are discussed as background for the definition and analysis of longshore bars. A representative profile (equilibrium profile) is introduced as a reference for the definition of the spatial extent of a bar. Volumetric profile change and contour movement are described primarily for the subaerial portion of the profile in order to quantify profile variability and establish typical time scales of profile change. Beach change on the foreshore is closely linked to the formation and movement of bars located near to shore because an exchange of material continually takes place between these areas, depending on the nearshore wave conditions. Also, an overall analysis of the temporal change in profile volume above selected contours displays possible long-term trends regarding evolution of the profile; that is, if accretion or erosion takes place. In the study of bar properties, interpretations are more easily done for a beach with no net long-term change, and it is easier to define a reference profile for the definition of bar properties.

Representative Beach Profile

Average profile and profile variability

22. The average profile was computed for each line (Lines 58, 62, 188, and 190) by averaging all profile surveys for the entire period 1981 to 1989. Because individual survey points were taken at varying distances from the baseline, (linear) interpolation was employed between measured points to derive the average profile. Table 1 summarizes the number of surveys used for each line in the averaging procedure. The surveys extended to different maximum depths (distance offshore), with fewer surveys extending to deeper water. Thus, the average profile is based on fewer surveyed depths in the offshore region of the profile in comparison to the inshore. In the offshore region of the profile, changes are smaller than closer to shore, implying that a more accurate estimate of average offshore depths may be obtained based on a smaller number of surveys than along the inshore region of the profile.

23. The maximum and minimum depth recorded at any point were determined across-shore together with the standard deviation of the depth (see Howd and Birkemeier 1987a). These quantities indicate profile variability during the measurement period and the areas along the

profile where the most active sand transport occurred. Figures 2 to 5 display the aforementioned quantities for survey Lines 58, 62, 188, and 190, respectively. The minimum and maximum depths do not represent a specific profile but originate from a number of surveys describing the limiting envelopes for profile change at points across shore. Thus, the minimum and maximum profile envelopes display an uneven shape with abrupt change in depth at neighboring points.

24. Average profiles are very similar for the four survey lines, having a steep foreshore that joins to a gently sloping profile a small distance seaward of the shoreline. Because longshore bars are usually present at the profiles from the FRF, the average profiles are influenced by these features, and the computed average profiles have two regions where the beach gradient is not monotonically decreasing. These regions are related to the inner and outer bar feature commonly occurring at the FRF. The similarity between the average profiles from respective survey lines is illustrated in Figure 6, which shows the four average profiles displayed together. The offshore region is almost identical for the four average profiles, whereas the region around the shoreline differs slightly. North of the FRF research pier the two survey lines (58 and 62) have a subaerial profile that is located somewhat more seaward with respect to the

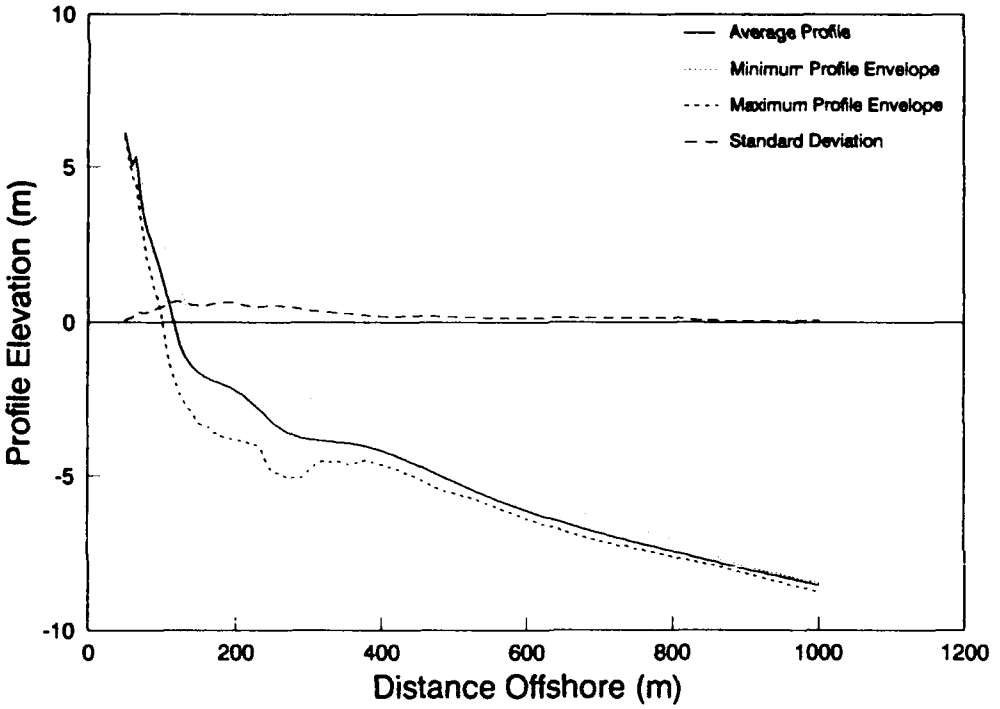

Figure 2. Average profile and profile variability for Line 58

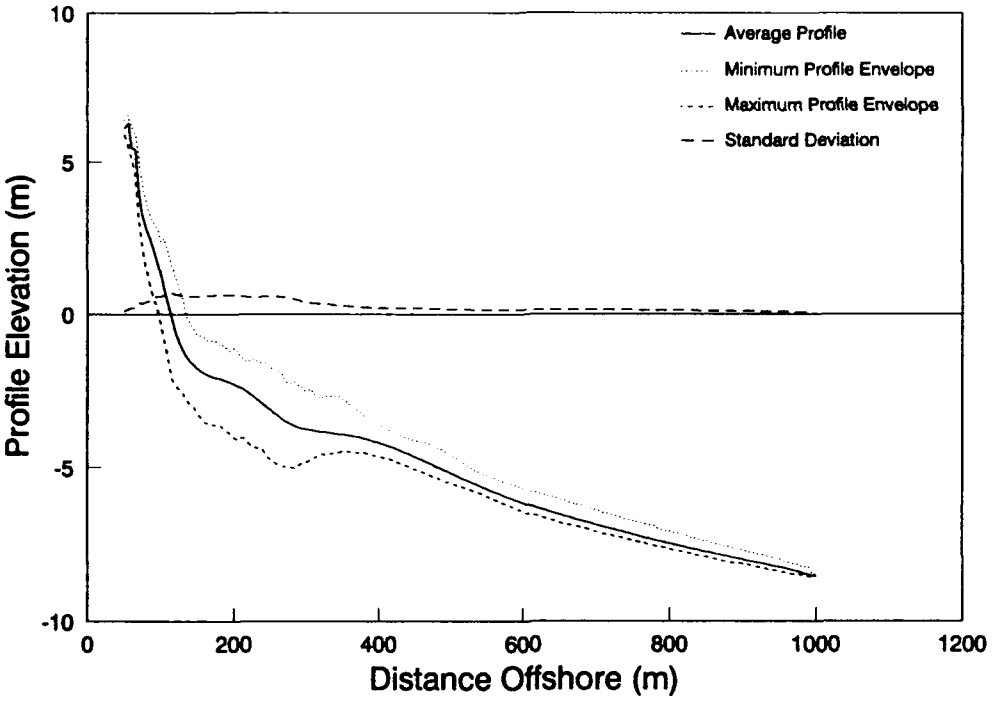

Figure 3. Average profile and profile variability for Line 62

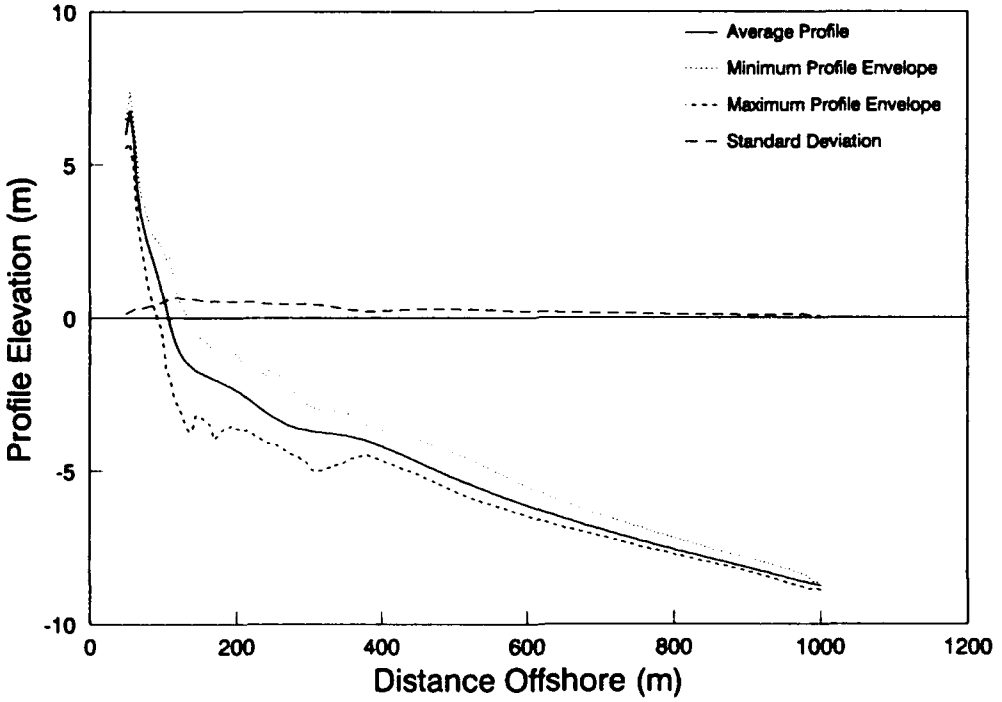

Figure 4. Average profile and profile variability for Line 188

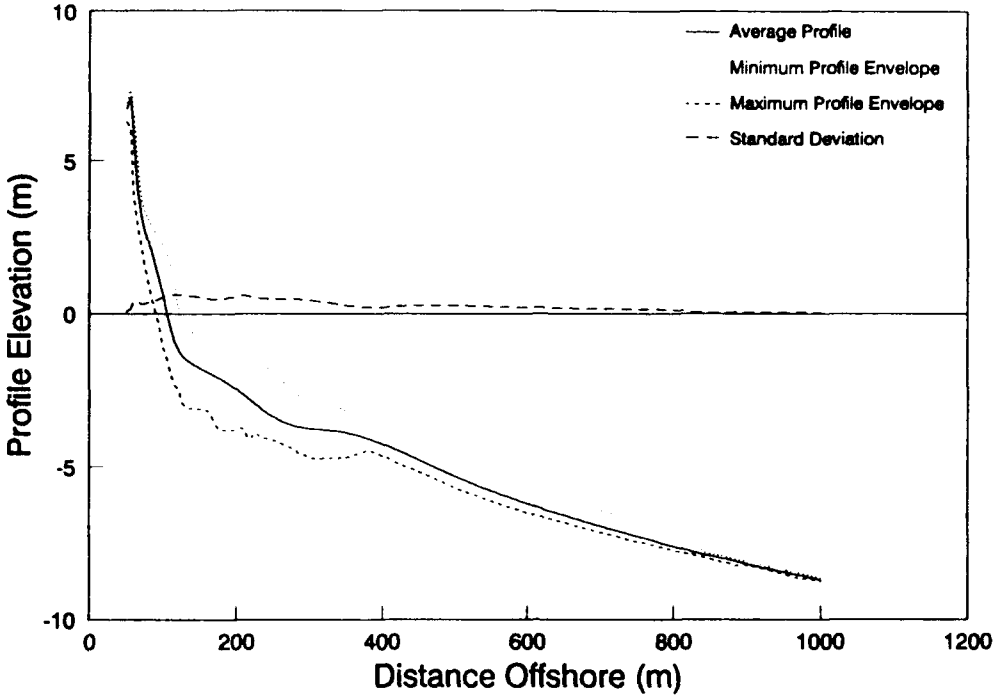

Figure 5. Average profile and profile variability for Line 190

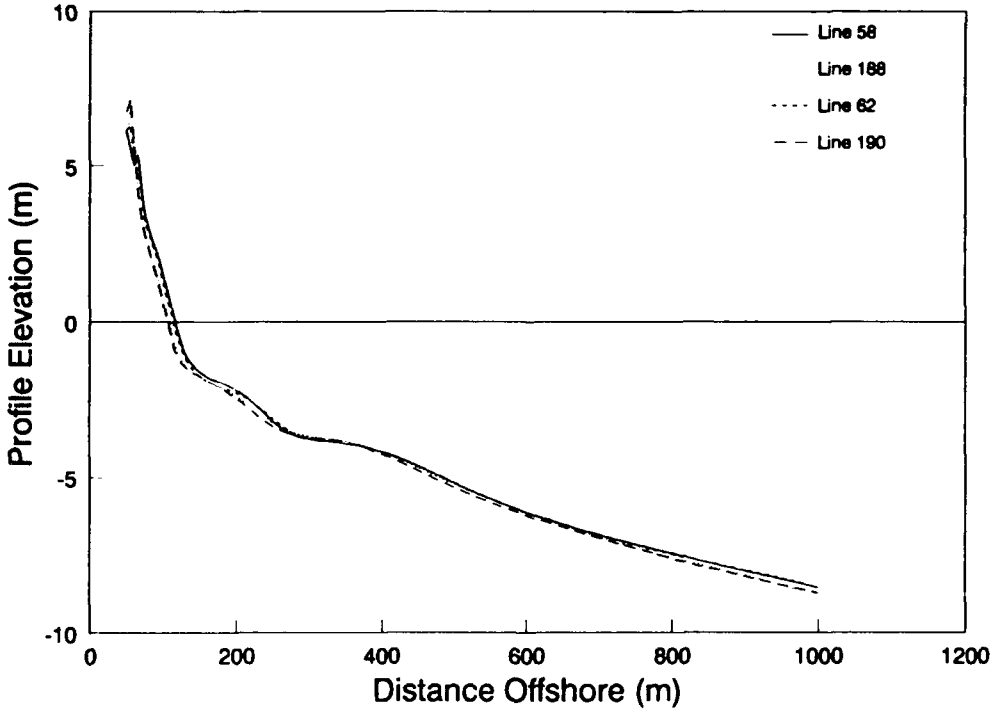

Figure 6. Comparison of average profiles from the four FRF survey lines

FRF baseline in comparison with the survey lines to the south of the pier (188 and 190). An alignment of the average profiles with respect to the shoreline location would bring the profile shapes to almost perfect agreement.

25. Variability in profile elevation is greatest at distances from about the shoreline out to 400 m for all survey lines, representing the region of most active sand transport. Further seaward, depth changes are still noticeable, especially with regard to the minimum profile depth. It should be noted, however, that survey errors may strongly influence the location of the envelope, as it is defined by single survey points. Profile elevation variation (distance between minimum and maximum depth envelope) decreases significantly at a depth between 4 and 5 m, which approximately corresponds to the location of the break point for the higher waves during a severe storm. At this depth, the standard deviation also drops off for all the survey lines, as shown in Figures 2-5.

Equilibrium beach profile

26. A useful concept in the study of beach profile change is the equilibrium profile (Bruun 1954, Dean 1977), which for field conditions represents the characteristic shape of the profile with respect to the average forcing conditions at the site. Dean (1977) theoretically derived an equilibrium shape of a beach profile assuming constant energy dissipation per unit water volume (equilibrium energy dissipation), arriving at a 2/3-power curve,

$$h = Ax^{2/3} \tag{1}$$

in which

h = water depth

A = an empirical (shape) parameter

x = distance offshore (measured from the shoreline, $h = 0$)

The shape parameter A has been empirically related to the median grain size of the beach (Moore 1982) or to the average fall speed of the sand (Dean 1987; Kriebel, Kraus, and Larson 1991).

27. The equilibrium profile equation (Equation 1) was least-square fitted to the computed average profiles, determining the optimum value of the shape parameter as $A = 0.09$ m$^{1/3}$. The corresponding median grain size using the relationship of Moore (1982) is 0.20 mm. In the

least-square procedure, the location of the shoreline was also estimated in order to achieve the best overall fit by the expression

$$h = A(x - x_s)^{2/3} \tag{2}$$

where x_s is the location of the shoreline. Figure 7 shows an example of the agreement between the least-square fitted Dean equilibrium profile and the average profile for Line 62. For this case, the root-mean-square (rms) deviation in profile depth between the average profile and the power curve was $\Delta h_{rms} = 0.20$ m. Offshore, the agreement is satisfactory; however, close to the shoreline the basic equilibrium profile equation (Equation 1) provides a poor fit, because the average profile is considerably steeper in this region. The larger beach gradient at the shoreline is due to the coarser grain size found to be present in this region. The typical median grain size on the foreshore at the FRF is 1.0 mm, whereas the grain size in the offshore region of the profile approaches 0.1 mm (Howd and Birkemeier 1987a).

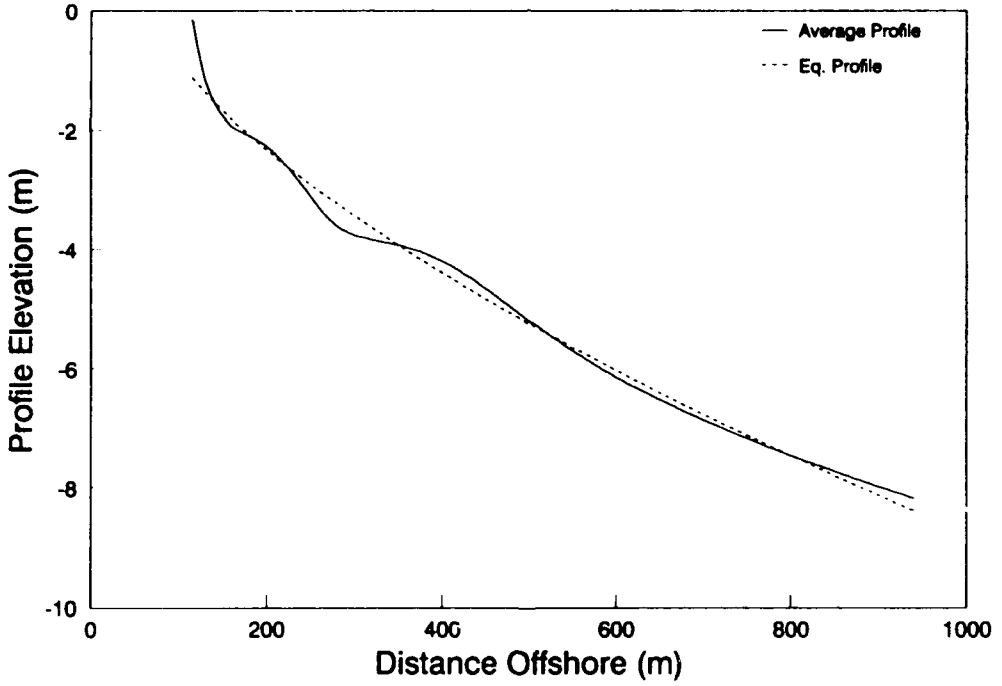

Figure 7. Average profile at Line 62 and least-square fitted equilibrium profile

28. In order to account for variable grain size as general fining of sediment across the profile, and thus achieve a better description of the shape of the equilibrium profile, a modified version of the Dean profile equation was employed to allow for a varying equilibrium energy dissipation across shore (Larson 1991);

$$h = A_* \left[x + \frac{1}{\lambda} \left(\frac{D_o}{D_\infty} - 1 \right) (1 - e^{-\lambda x}) \right]^{2/3} \tag{3}$$

in which

A_* = shape parameter in the offshore region of the profile

D_o = equilibrium wave energy dissipation per unit volume in the inshore

D_∞ = equilibrium wave energy dissipation per unit volume in the offshore

λ = characteristic length describing rate at which D_o approaches D_∞

In this approach the equilibrium energy dissipation per unit volume of breaking waves is assumed to decrease exponentially with distance offshore, approaching a constant value far away from the shoreline.

29. An improved fit to the average profiles was achieved using the modified equation, although additional parameters had to be introduced to characterize the variation in median grain size with distance offshore. Figure 8 displays a comparison between the average profile at Line 62 and a least-square fit of the modified equilibrium profile equation according to Larson (1991). In the offshore, the agreement is similar to that achieved with the 2/3-power curve, but closer to shore the approach involving a varying grain size across shore gives a superior fit. The overall profile shape, involving a steep inshore and a gently sloping offshore, is better reproduced by the modified equilibrium equation.

30. The optimum parameter values in the modified equilibrium profile equation for Line 62 were $A_* = 0.09$ m$^{1/3}$, $D_o/D_\infty = 3.3$, and $\lambda = 0.039$ m^{-1}, with $\Delta h_{rms} = 0.15$ m. This least-square fit gave a grain size at the shoreline of about 0.7 mm, which is in the correct range for the material on the foreshore at the FRF. The estimated grain size in the offshore part of the profile was about 0.20 mm (from $A_* = 0.09$) as for the case with the classical 2/3-power curve. The optimum value of the parameter λ indicates that the grain size decreases sharply with distance offshore to reach a constant value quite close to the shoreline.

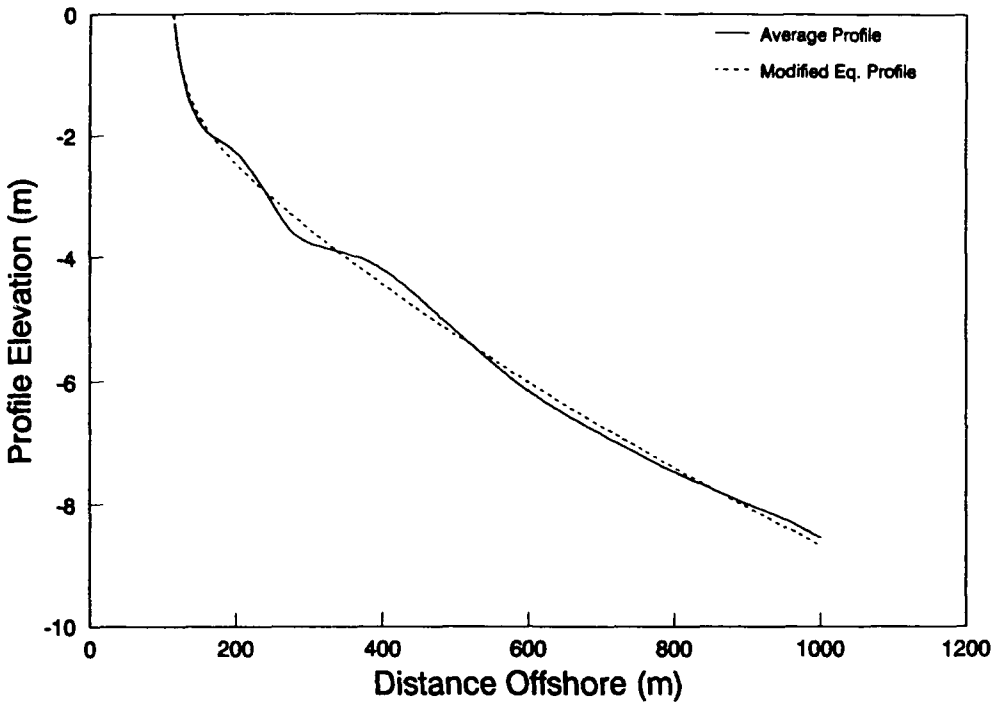

Figure 8. Average profile at Line 62 and least-square fitted equilibrium profile modified for varying grain size across shore

Median grain size across the profile

31. Information* derived from sand samples collected during 1984 and 1985 was used to determine the grain-size variation across the profile. Figure 9 illustrates the variation in the median grain size as a function of distance across the shore for collected subaqueous sand samples (209 samples shown). Although there is large scatter in the data, coarser material is identified close to the shoreline, and the median grain size is steeply decreasing with distance offshore and becomes approximately constant about 200 m from the shoreline. In the offshore part of the profile, the median grain size is slightly less than 0.2 mm, whereas the material at the shoreline in general is coarser, although the scatter is wide. The sediment samples confirm the cross-shore trend in grain size derived from the least-square fit of the modified equilibrium profile equation.

* Personal Communication, January 1991, Mark Hansen, formerly Physical Scientist, CERC.

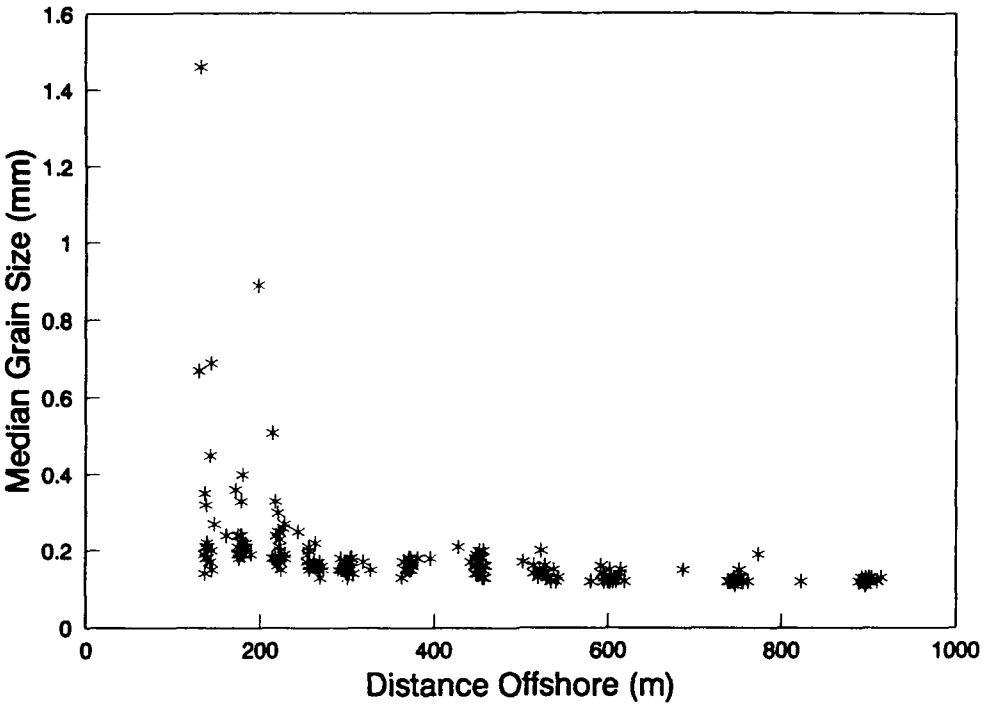

Figure 9. Median grain size as a function of distance across shore at the FRF

Definition of Bar Properties

32. In order to describe and quantify bar formation and movement, a consistent definition of the bar feature is needed. Previous investigations involving laboratory data have defined the bar with reference to the initial profile (Larson and Kraus 1989). Areas along the subaqueous part of the profile where material accumulates with respect to the initial profile were regarded as bar features. Crossings between a specific profile and the initial profile defined the beginning and the end of the bar. However, in the field, such a definition is not operational due to the absence of a well-defined "initial profile," and thus a different method must be employed. In the present study, several methods were tested for defining bar features and carefully evaluated to estimate the method that was most suitable for defining a bar. The two main methods evaluated in this study were:

a. Define a bar with respect to a reference profile, and assume that the area above the reference profile constitutes the bar.

b. Define a bar by determining the beginning and the end of the bar, linearly connect these points, and assume that the area above the straight line constitutes the bar.

33. Method 1 is identical to that employed in laboratory studies and introduces the difficulty of specifying a representative profile for a natural beach. Three different representative profiles were evaluated in this study, namely: (a) the calculated average profile, (b) the Dean equilibrium profile, and (c) the modified equilibrium equation taking into account a varying grain size. Use of the average profile is not convenient because the shape is decisively influenced by the presence of longshore bars for most of the surveyed profiles. Employing the Dean equilibrium profile equation gave a description close to the shoreline that was not satisfactory, and one that caused difficulties in describing the movement of the inner bar. The modified equilibrium equation, however, was found to provide a useful definition of a bar feature. As an example, Figure 10 illustrates a surveyed profile (Line 62, survey date 870303 at time 0929; dates are given as year-month-day and time in hour-minute). The hatched areas represent the extent of the two bars on the surveyed profile. Unless otherwise specified in this report, the location of a bar is defined with respect to the modified equilibrium profile.

34. The method of defining a bar by determining the beginning and the end of the bar (typically by locating local minima), linearly connecting these points, and then assuming that the area above the straight line constitutes the bar, was also investigated. This definition was employed by Keulegan (1945, 1948) in the study of longshore bars in the field. In order to identify bar features, the beginning and the end of the bar must be established, either subjectively or through some criterion. Manually selecting these points by studying individual surveys is, however, time-consuming and to a large degree arbitrary. Another technique for determining the starting and ending points of a bar that was investigated was through the change in the sign of the second spatial derivative along the profile. A well-behaved profile shape would show such a sign change going from the trough seaward towards the bar crest, but determining the seaward limit of the bar proved to give ambiguous results with this technique and it was abandoned.

35. In summary, the modified equilibrium profile equation was demonstrated to give the most reliable reference profile for definition of a bar and was employed in the following analysis. With this definition it proved possible to identify the formation and movement of both the inner and outer bars in a consistent and objective manner. Furthermore, evaluation of the large

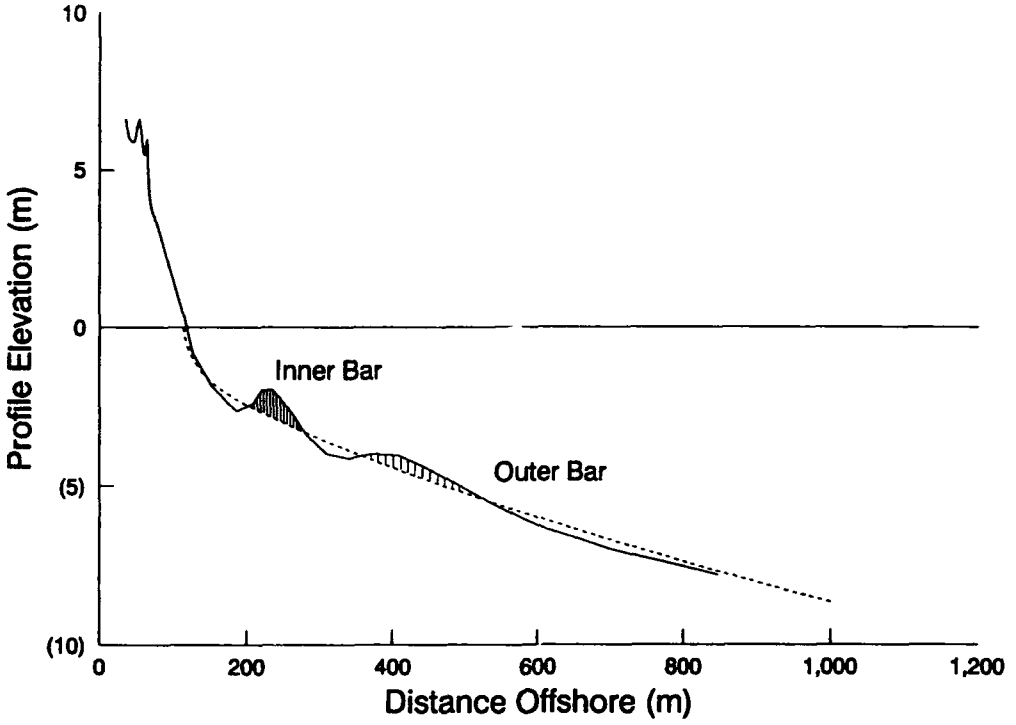

Figure 10. Definition of longshore bar extent using the modified equilibrium profile equation (hatched areas represent bars)

number of surveys available could be carried out automatically by the reference-profile method without time-consuming manual analysis. However, for a small number of profile surveys made during the end of the measurement period, no crossing between the surveyed profile and the reference profile was obtained for the most seaward bar, with the surveyed profile leveling out in parallel with the reference profile. In these cases, the location of the seaward end of the bar had to be determined manually by visually examining each such profile. The seaward end of the bar was determined from the break in slope that typically occurred as the profile leveled out seaward of the bar.

Volumetric Profile Change and Contour Movement

Subaerial sand volume

36. To determine and characterize the long-term beach evolution at the FRF, the time variation in subaerial sand volume above selected elevation contours was calculated. During a typical seasonal cycle, exchange of sand occurs between the foreshore and the bar region, with

less sand residing in the subaerial part of the profile in the winter and more sand in the summer. However, if sand is removed from the upper berm and dune region, recovery can only take place through wind-transported sand, which promotes dune buildup. Another cause of short- and long-term changes in beach topography is a differential in the longshore sand transport.

37. Over the 8-year interval encompassed by the data set, the subaerial part of the beach at the FRF displayed a slight trend of accretion, especially at Line 62, indicated primarily by a long-term increase in the sand volume above NGVD. Strong seasonal variations, including large storm events, were superimposed on this trend, with the subaerial sand volume mainly below the average value during the first part of the measurement period, and above it during the second part. Figure 11 displays the variation in the amount of sand above NGVD as a function of elapsed time for Line 62. The time scale is given in consecutive days starting at 810101, and the sand volume is referenced to the average volume above NGVD from a point located 66 m seaward of the FRF baseline. This average volume in the subaerial profile was 104 m^3/m for the measurement period, for which the shoreward point was chosen as the most seaward starting point appearing in the surveys. Linear interpolation between survey points was used to integrate the sand volume.

38. As seen in Figure 11, the subaerial sand volume fluctuates at many different time scales, but there is a trend for the volume to increase with time. Occasional storms caused rapid decrease in the volume, although the figure tends to suggest a more gradual change because the curve represents linear interpolation between measurement points, and the points are usually separated in time by 1 to 2 weeks. The other survey lines displayed a similar trend, although Lines 58 and 62 north of the FRF pier displayed a stronger tendency for accretion than Lines 188 and 190 south of the pier. Figure 12 illustrates the temporal variation in subaerial volume for Line 188, south of the pier, where the sand volume is referenced to the average volume for the entire time series. The sand volume was calculated above NGVD from a point 72 m seaward of the baseline, and the average sand volume was 60 m^3/m. A comparison of Figure 11 and Figure 12 shows the typical difference in subaerial volume change between survey lines north and south of the pier. Neighboring survey lines showed high correlation with respect to the amount of sand contained in the subaerial profile, whereas the lines north and south of the pier could have exhibited very different volume change during the same time period.

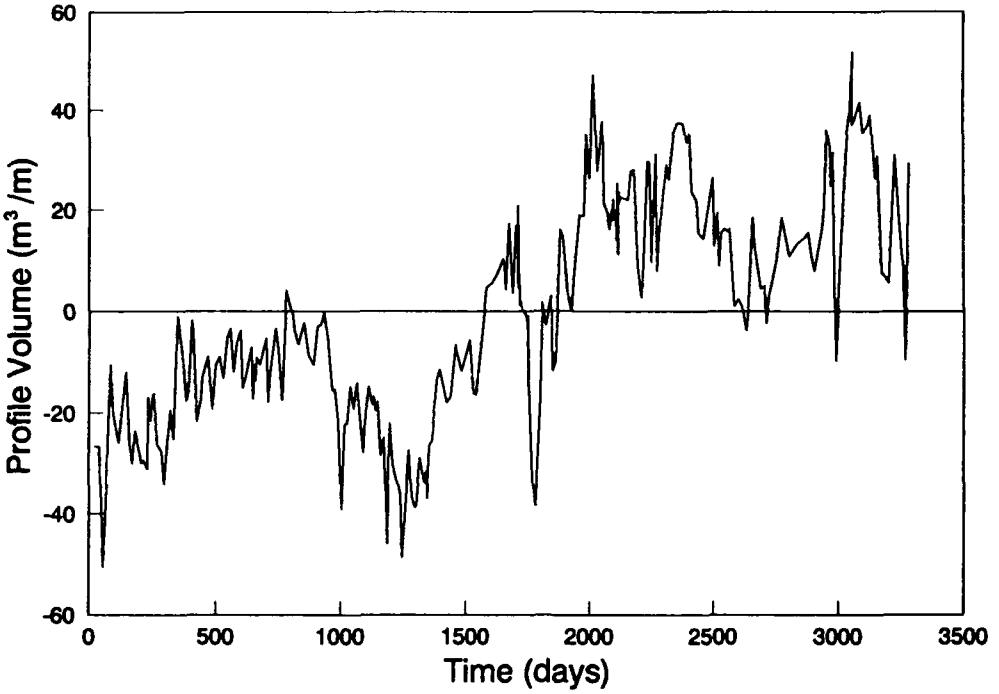

Figure 11. Temporal variation in subaerial sand volume at Line 62

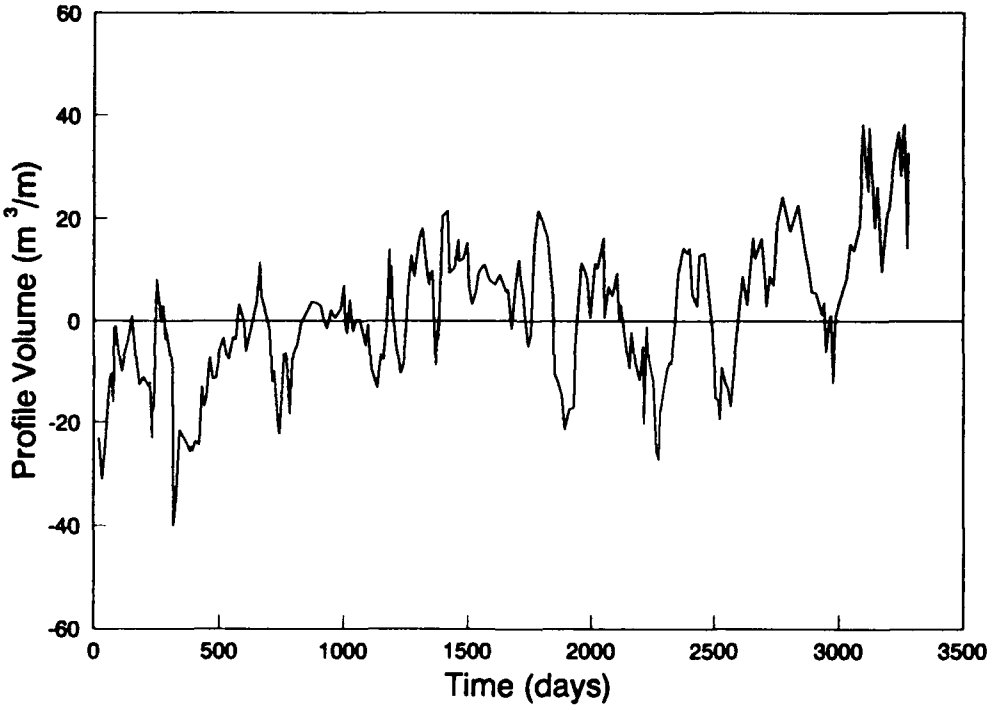

Figure 12. Temporal variation in subaerial sand volume at Line 188

39. The temporal variation in sand volume above elevation contours other than NGVD was also studied for the subaerial part of the beach. At higher elevations the variation became less pronounced because this portion of the profile is only subject to sand transport during extreme conditions. Also, at high elevations the volume calculation was more sensitive to the measurement resolution on the dune face. For a limited number of surveys, where very few points were taken along the dune face, the volume calculation could display significant changes as an artifact of inadequate measurement resolution. The dune portion of the profile was surveyed infrequently and with varying quality. Although significant effort was exerted to address this problem in the database, it was concluded that dune change should not be studied unless the change is marked.

Subaqueous sand volume

40. Although it is more difficult to estimate the amount of sand in the subaqueous portion of the profile because the profile surveys were carried out to different depths on each measurement occasion, no particular long-term trends were apparent in the profile data. Thus, the beach at the FRF had, on the average, a fairly constant subaqueous sand volume during the measurement period, but experienced a slight accumulation of sand in the upper berm and dune region. From the point of view of studying bar formation and movement, it is of considerable value that the subaqueous sand volume is approximately conserved and no net long-term change in volume exists. This simplifies the data analysis by removing potential complicating factors such as a differential in longshore transport.

41. Contour movement. The movement of specific elevation contour lines was computed to further identify long-term trends in the profile data. The temporal variation in shoreline position defined with respect to NGVD exhibited a small trend for seaward displacement, indicating accretion, but not as significant an increase as for the subaerial volume. Figures 13 and 14 show the mean shoreline location with time elapsed for profile Line 62 (x_s = 113.9 m) and Line 188 (x_s = 108.6 m), respectively, where the time evolution is quite different for the two survey lines. Thus, the shoreline position at the survey lines north and south of the pier displayed distinctly different temporal patterns of change, as was the case for the subaerial sand volume. There seemed to be more large-scale fluctuations in the shoreline position at Line 62 than at Line 188, which exhibited mainly higher frequency variation.

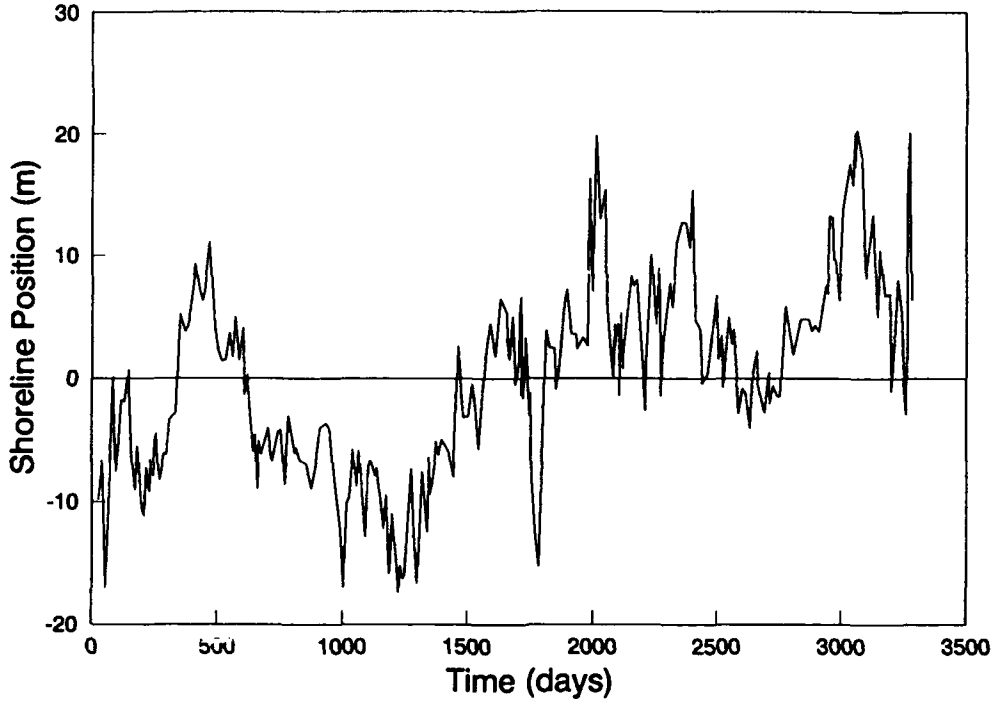

Figure 13. Shoreline position change for Line 62

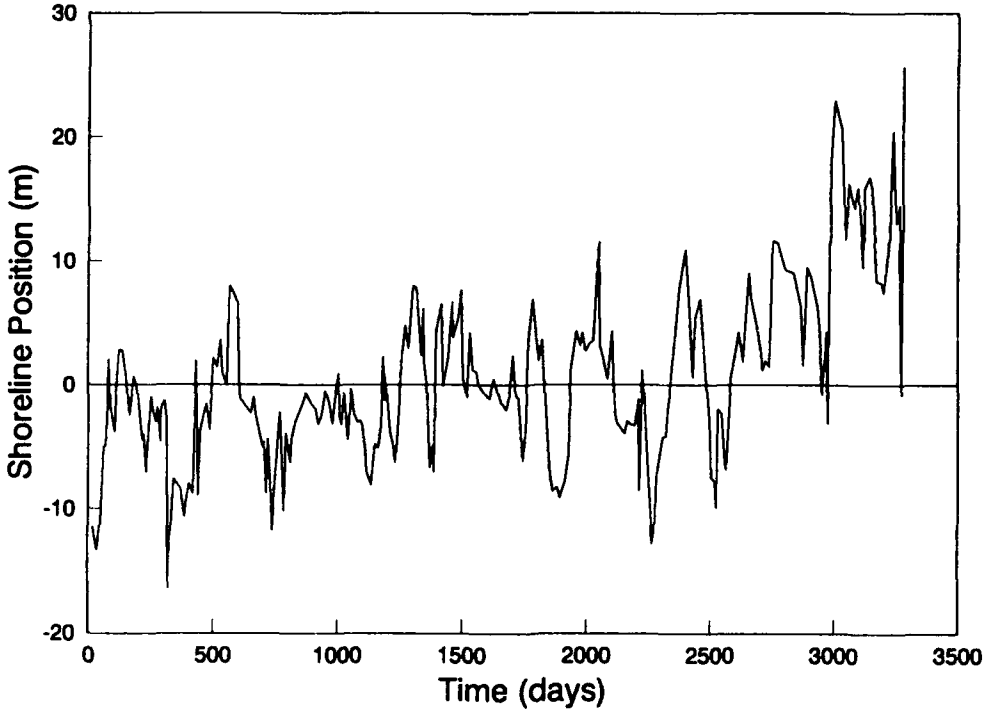

Figure 14. Shoreline position change for Line 188

42. In order to detect possible trends in the subaqueous portion of the profile, the movement of selected depth contours below NGVD was calculated, studying mainly contours close to the shoreline in order to maximize the number of measurement points in time. As an example, the most shoreward position of the 1-m depth contour is shown in Figure 15 as a

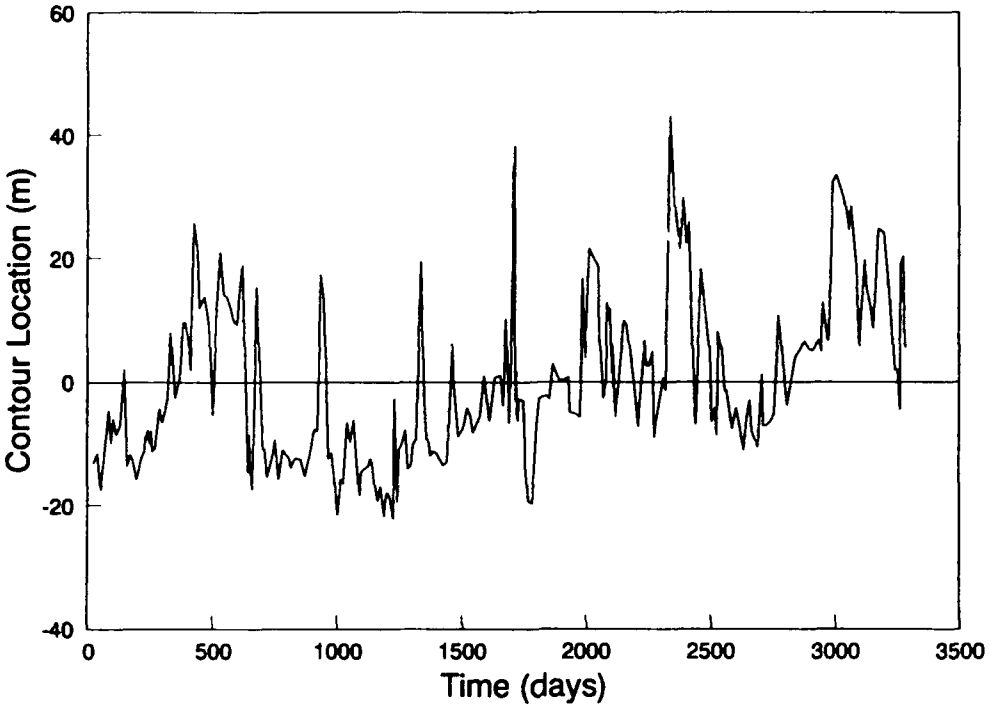

Figure 15. Change in position of 1-m depth contour for Line 62

function of elapsed time for Line 62. No particular trend may be detected visually in the figure, indicating that on a long-term basis the profile is stable without experiencing a net change. The other survey lines displayed a similar behavior as Line 62 for depth contours close to the shoreline.

43. In summary, the analysis of volumetric profile change and contour movement showed that the beach at the FRF accreted somewhat above NGVD for the measurement period, but no long-term change in the subaqueous portion of the beach could be detected. The survey lines north of the FRF research pier (Lines 58 and 62) experienced slightly more accretion than south of the pier (188 and 190). The increase in subaerial sand volume is probably due to sand transport by wind and associated dune buildup. A stable subaqueous beach profile indicates no

long-term differential in the longshore sand transport or no significant loss of material to the offshore. Thus, the profile data from the FRF should provide a good basis for analysis of natural longshore bar properties because the data set is not strongly influenced by a net alongshore drift. However, short-term longshore effects could still influence profile evolution when strong longshore currents are generated during storms. Because the forcing conditions appear to be relatively uniform during storms when significant bar movement occurs, no large-scale alongshore differentials are expected.

Time scales of subaerial volume change

44. The box-counting method was employed to determine the characteristic time scales of sand volume change on the foreshore (Hentschel and Procaccia 1983). This procedure can be used to analyze patterns of fluctuations in time and space, and to determine if these fluctuations display fractal properties. If the pattern may be characterized with a single fractal dimension, fluctuations at various scales are following the same basic pattern, only differing through a scale transformation. Processes that are governed by the same physical mechanisms at all scales are expected to exhibit fluctuations with fractal properties.

45. The general procedure in the box-counting analysis is to divide the studied data series into gradually decreasing, non-overlapping segments (boxes) of size r, and for every r, count the number of boxes, $N(r)$, in which a specific phenomenon occurs. If the data set may be characterized by the expression $N(r)=r^{-d}$, it is an indication that the pattern of fluctuation is of fractal nature. The exponent d, called the box dimension, is associated with the fractal dimension and is estimated as the slope of the straight line in plotting $\log[N(r)]$ as a function of $\log(r)$. In the present study, the phenomenon investigated was whether the subaerial portion of the profile was eroding or not during the measurement period. However, in order to perform the analysis, data at fixed time increments were needed, requiring linear interpolation to be carried out between the time of surveys. This assumes smooth changes in the profile shape between the surveys, which is not the case when storms impact the beach. Thus, the box-counting analysis will only provide information on time scales exceeding the typical time interval between surveys, which was about 10 days for survey Line 62 used as the example in the following.

46. The resulting curve obtained from the box-counting analysis, shown in Figure 16, could be well described by two straight lines in a logarithmic diagram, with the break in the slope occurring for a time increment of about 60 days. The presence of two lines with different

slopes indicates that a single fractal dimension is not appropriate to characterize the temporal pattern of fluctuations in subaerial sand volume, implying physical mechanisms with different temporal scales are governing the volume change. The steeper slope had $d = 1$, whereas the gentler slope for shorter time periods (box sizes) corresponded to $d = 0.77$. A slope of $d = 1$ indicates that for a corresponding box size (time period), subaerial erosion will always occur. However, for a slope milder than $d = 1$, time periods will be found where no erosion occurs. The break point between the two lines may thus be interpreted as the typical maximum duration between storms that causes erosion on the foreshore.

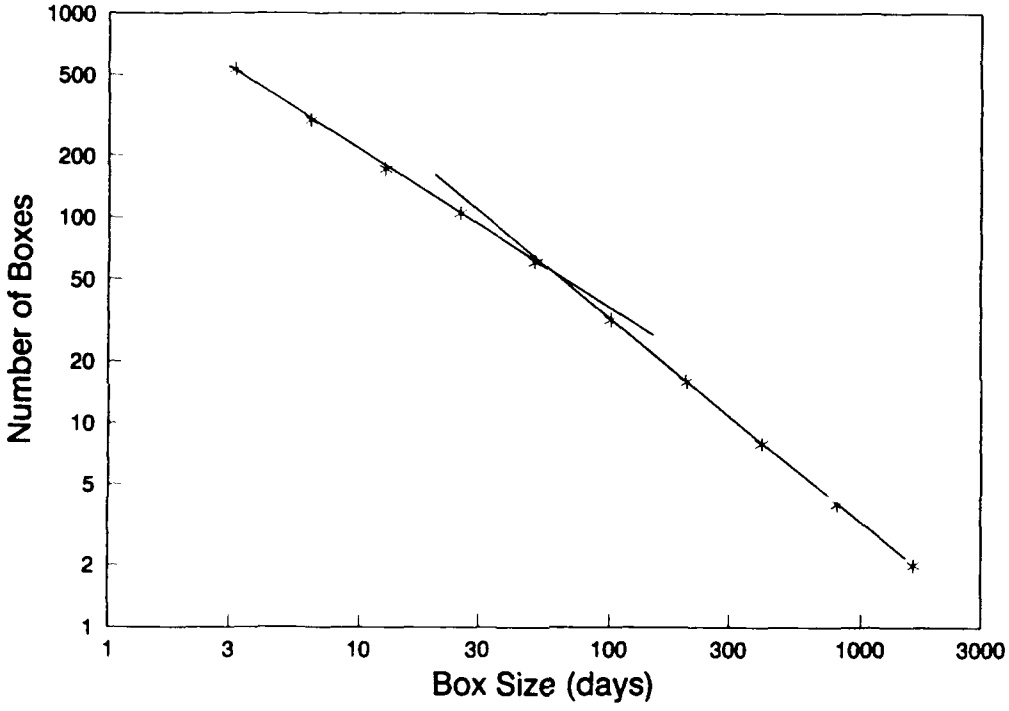

Figure 16. Box-counting curve for decrease in subaerial sand volume, Line 62

Overview of Studied Bar Properties

47. Because the four studied profile survey lines displayed similar overall long-term behavior, it was decided to restrict analysis of bar properties to profile survey Line 62. Profile Line 62 has the largest number of surveys (300) and was judged to exhibit the most representa-

tive response in terms of bar formation and movement. Each profile survey was visually examined for bar features, for which the shore- and seaward boundaries of the bar were determined from the crossings between the specific profile and the modified equilibrium profile, as previously discussed. Thus, a bar was defined as the volume of sand above the modified equilibrium profile, in accordance with the concept of a bar being a feature where sand is deposited. Also, such a volume definition is in accordance with the purpose of using the bar property analysis for predicting the response of placed dredged material along a profile. If a profile is close to its equilibrium shape and dredged material is placed in the form of a mound or a bar, the present bar definition will produce good agreement between calculated bar volume and the volume placed along the profile.

48. The following properties were calculated for every identified bar of each individual profile survey:

V_b = bar volume

l_b = bar length

h_c = minimum bar depth (subscript c denotes bar crest)

z_m = maximum bar height

x_{cg} = location of bar mass center

dx_{cg}/dt = speed of bar movement

49. Figure 17 illustrates the definition of the above-listed properties for a typical profile survey from the FRF data set. Bar volume was calculated as the volume of sand above the reference profile (m^3/m) and bar length as the horizontal distance between the start and the end points of the bar. The minimum bar depth, or depth to bar crest, was determined as the smallest depth across the bar, whereas the maximum bar height was given by the largest vertical difference between the surveyed profile and the reference profile. Bar speed was determined from the change in location of the bar mass center between two profile surveys divided by time elapsed between the surveys. In the analysis of bar properties, the accuracy of the calculations is closely linked to the measurement resolution across the bar. For most surveys the resolution was judged to be satisfactory to ensure a reliable estimate of the bar properties. All horizontal distances in the calculated properties refer to the baseline at the FRF unless otherwise stated.

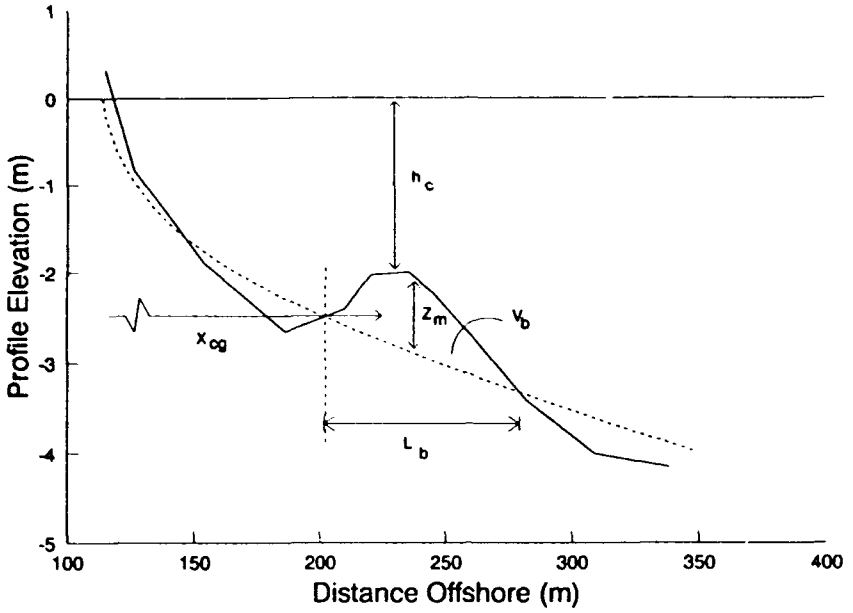

Figure 17. Definition sketch of bar properties calculated for each survey

50. In most profile surveys from the FRF, two bar features could be identified along the profile, namely an inner bar and an outer bar (Howd and Birkemeier 1987a; see Figure 10). During extended periods of low waves, the outer bar would disappear and only the inner bar existed. In some rare cases, and only for a short period of time, three bars were present with the most shoreward bar being small and located close to the shoreline. In this report, the focus of the analysis will be on the inner and outer bars, where the outer bar is of primary interest with respect to predicting the behavior of placed dredged material. The typical depth at the outer bar corresponds to water depths where placement of dredged material in the nearshore is expected to occur.

51. The mass center of the outer bar was typically located about 300 m from the shoreline, whereas the mass center location of the inner bar varied more, with a characteristic distance of 100 m from the shoreline. The outer bar experiences breaking waves only during large storms, in contrast to the inner bar, which is exposed to wave breaking during most of the year, resulting in greater variability in its position. Thus, the inner and outer bars displayed significantly different behavior and were studied separately in analysis of bar properties. Short characterizations of the inner and outer bars follow, to provide a background for the bar analysis.

Inner bar

52. As noted in the preceding section, short-term variability in bar properties was considerably greater for the inner bar in comparison with the outer bar. Because the inner bar was frequently located in the breaker zone, the bar frequently experienced significant sand transport, and thus exhibited changes on a shorter time scale than the outer bar. On several occasions, the inner bar moved onshore as a unit and welded on to the shoreline, and, during a few storms, the inner bar moved offshore to become, or merge with, the outer bar.

Outer bar

53. Volume growth and offshore movement only occurred for the outer bar during more energetic storms. Between storms, bar volume typically decreased gradually under the influence of non-breaking waves, and the mass center of the bar moved slightly onshore. The outer bar never showed a tendency to move a significant distance onshore as a unit, but it appeared to experience steady onshore transport across its body under the action of non-breaking waves.

54. Although it was appropriate to distinguish between the inner and outer bar for most of the analysis, in some cases difficulties were encountered in making this distinction. For example, on two occasions the inner bar moved offshore to become the outer bar, and on some occasions when the bar was located in the area between the locations where the inner and outer bar are typically found, this division became somewhat artificial. Also, in some cases the employed bar definition implied an inner bar that extended far offshore because the crossing between the specific survey and the reference profile was located more seaward than the typical extent of the inner bar.

PART IV: INNER BAR PROPERTIES

55. In this section, results from the calculation of properties of the inner bar are presented. Appendix A gives a summary of the calculated values of the different bar properties for each of the individual surveys of Line 62. The start and end points defining each bar are also given as determined from crossings between the specific survey and the reference profile. A distinct inner bar was identified in 200 of the 300 surveys of Line 62. Occurrences of offshore movement to the inner bar to merge or to form an outer bar are discussed in Part V, which describes the properties of the outer bar. Table 2 lists time periods when an inner bar was identified and the reason for its disappearance. Time periods were based on the first and last survey that exhibited a distinct inner bar feature for each series of consecutive profile surveys with an inner bar present.

56. Calculated properties for the inner bar were compared with results from the LWT experiments because typical dimensions of this bar and the local wave climate are similar to the

Table 2

Time Periods with Inner Bar Present on Line 62

Time Period		Reason for Disappearance
810126 0850	810928 1135	Bar moved offshore
821007 1505	830725 1155	Bar welded on to shore
830826 1230	840811 800	Bar welded on to shore
840906 1310	841213 1508	Bar flattened out
850105 1125	850821 0735	Bar welded on to shore
850913 1640	860602 1430	Bar welded on to shore
860818 1115	860912 1235	Bar welded on to shore
861011 0840	870511 0916	Bar welded on to shore
870901 0605	880909 1015	Bar moved offshore

conditions prevailing in the laboratory experiments. Identification of similarities between the LWT experiments and field data is of great value because it increases the applicability of the LWT data sets, which encompass much more detailed measurements in time and space, and in a controlled environment for a wide range of wave conditions and different grain sizes. Thus, it is much easier to establish firm cause-effect relationships for LWT data than for field data.

Depth to Bar Crest

57. Figure 18 displays the minimum depth over the bar, or the depth to the bar crest h_c through time. The time is given in consecutive days from 810101, and periods when no distinct inner bar existed (Table 2) have been left blank. The average depth to bar crest was about 1.6 m for the 200 inner bar observations. With the assumption that breaking waves are the main cause of bar formation and movement (or a limiting factor in determining h_c), the depth to the bar crest should be on the same order as the breaking wave height H_b, yielding a mean breaking wave

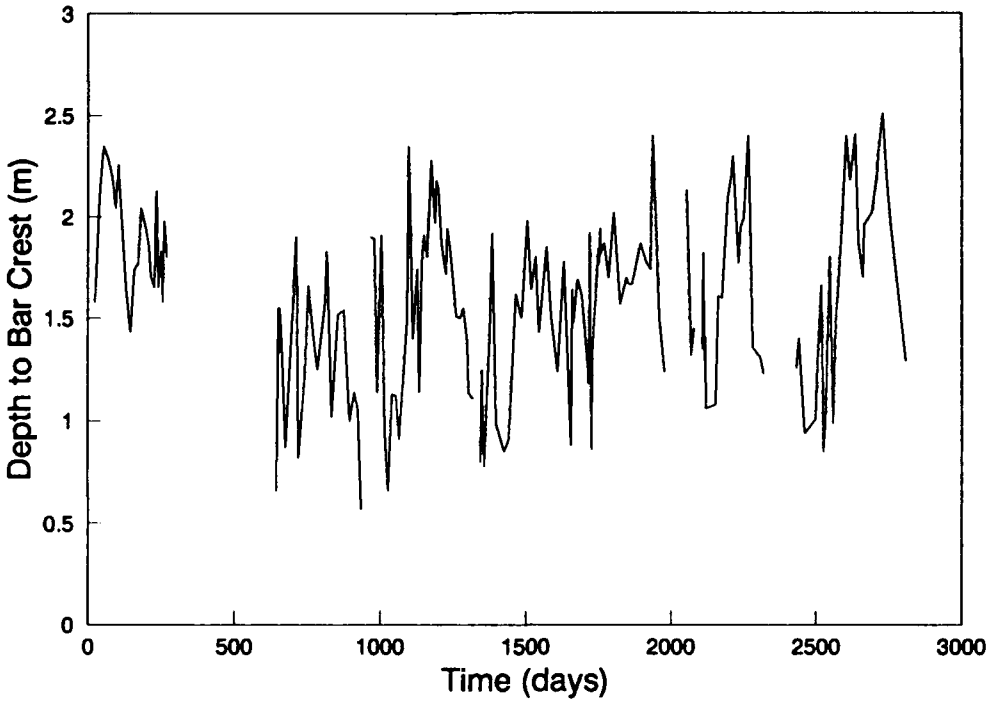

Figure 18. Depth to bar crest as a function of time for the inner bar

height of about 2 m as a first-order estimate. Larson and Kraus (1989) found the relationship $h_c = 0.66H_b$ based on analysis of profile change in the LWT experiments under near-prototype wave and beach conditions, but for regular (monochromatic) waves. This relationship gives an $H_b = 2.4$ m as a characteristic value for the inner bar. The minimum depth to bar crest recorded was about 0.6 m and the maximum depth to crest was about 2.5 m. These values depend, however, on determination of when the inner bar welds on to the shore or becomes the outer bar as it moves offshore.

Maximum Bar Height

58. The maximum bar height, determined as the maximum vertical distance across the bar between a specific survey and the reference profile, is displayed in Figure 19 as a function of time for the measurement period. The average maximum bar height $(z_m)_{mean}$ for the inner bar was about 0.9 m, whereas the minimum and maximum were $(z_m)_{min} = 0.2$ m and $(z_m)_{max} = 1.4$ m. In the LWT experiments, z_m typically ranged between 1 and 2 m (Larson and Kraus 1989) for incident deepwater waves with heights of 1 to 2 m. Regular waves are expected to produce much more peaked bars than random waves because there is no smoothing effect from a randomly varying breakpoint location. The tidal variation (range of about 1 m at the FRF) will also smooth beach profile morphologic features. Thus, the maximum bar height is, in general, larger for the monochromatic-wave LWT data for a specific set of wave conditions than for the field data.

Bar Volume

59. The average volume for the 200 inner bars identified was about 42 m^3/m, and the variation in the bar volume with time is displayed in Figure 20. The notable variability in bar volume indicates considerable sensitivity of the inner bar to changes in the nearshore wave conditions and to the existence of a rapid response rate. This variability is attributed to the high exposure of the inner bar to breaking waves that have a large potential for transporting sand, and thus for changing the beach profile shape. The calculated maximum bar volume was 98 m^3/m

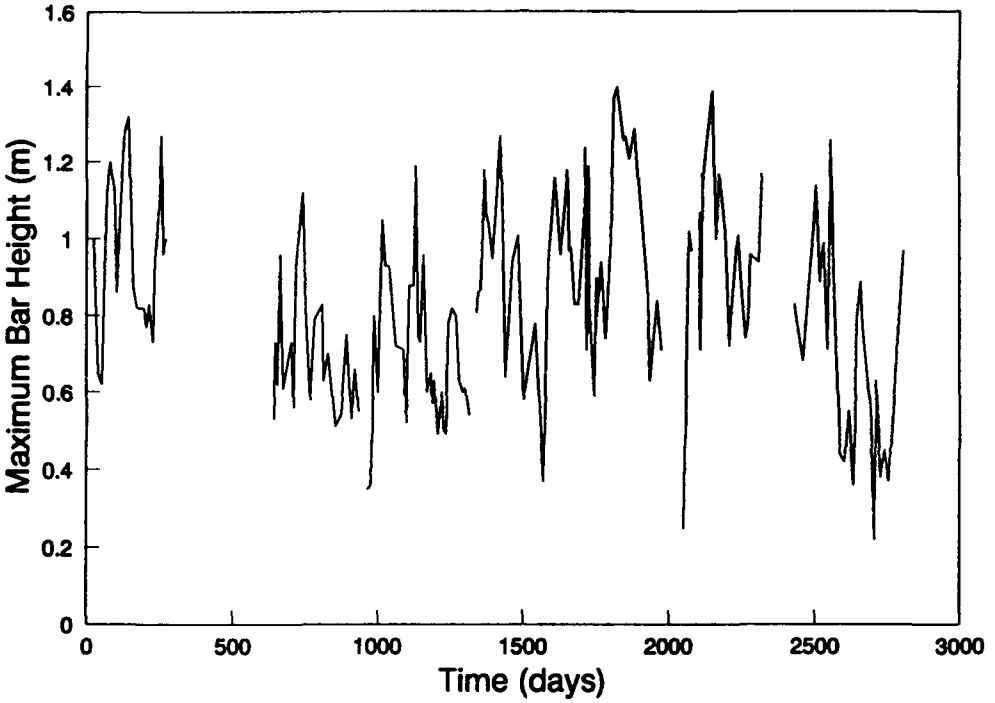

Figure 19. Maximum bar height as a function of time for the inner bar

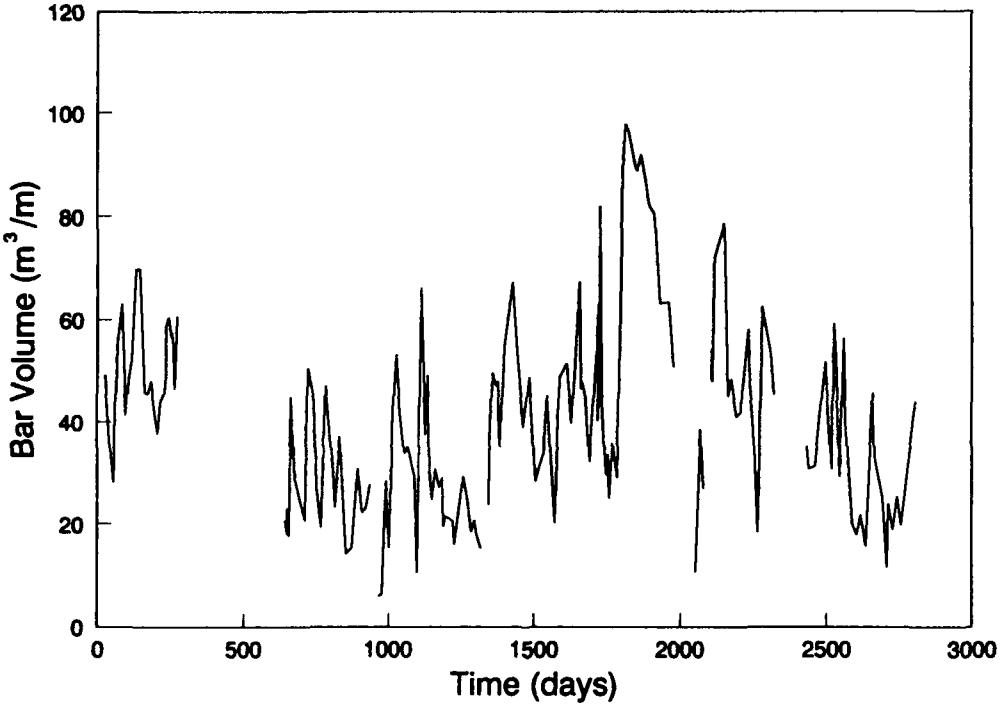

Figure 20. Bar volume as a function of time for the inner bar

and the minimum bar volume was 6 m^3/m. For occurrences where the inner bar moved offshore to become an outer bar, bar volume continued to grow as the bar moved seaward.

Location of Bar Center of Mass

60. The average distance to the center of mass of the inner bar was about 213 m from the FRF baseline, approximately 100 m seaward of the average shoreline location at survey Line 62. Figure 21 shows the temporal variation in the location of the bar center of mass referenced to the baseline. Numerous small-scale fluctuations in bar location occur that encompass movements in the range 10 to 20 m. During severe storms, however, significantly larger movement of the inner bar occurred. Another relevant measure for determining the variation in bar location would be the distance from the shoreline to the bar mass center. Such a measure could possibly better reflect the exchange of material between the foreshore and the bar region than the distance to the bar mass center from the baseline.

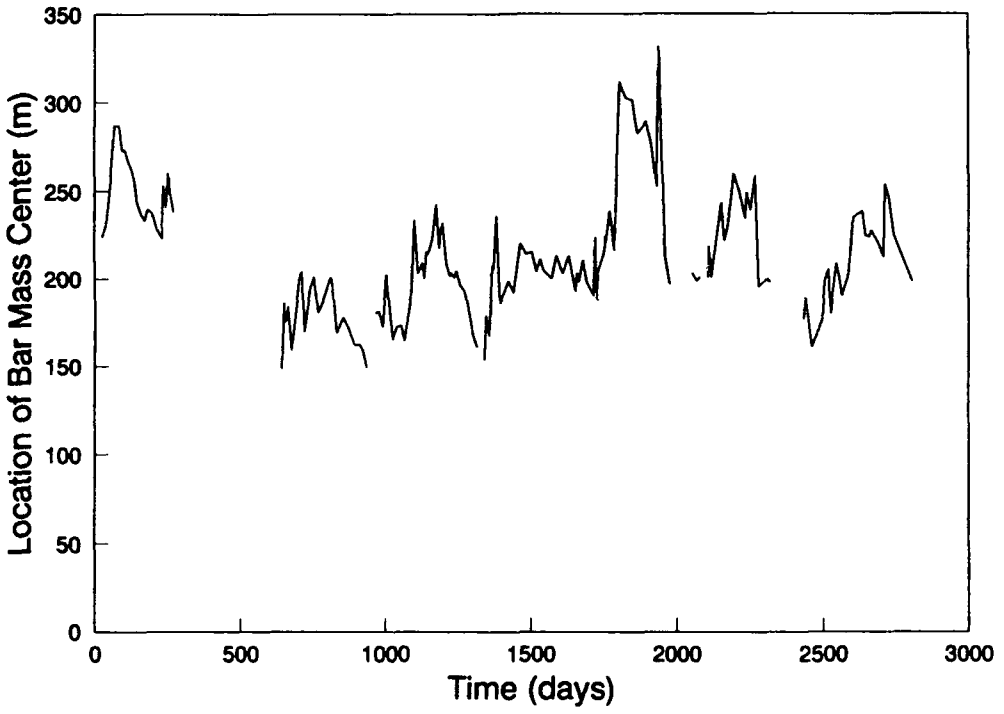

Figure 21. Location of mass center as a function of time for the inner bar

Speed of Bar Movement

61. The speed of bar movement was determined for the inner bar as the distance the bar mass center moved between two consecutive surveys divided by the time elapsed between the two surveys dx_{cg}/dt. However, because bar movement in general is rapid (Sallenger, Holman, and Birkemeier 1985; Sunamura and Maruyama 1987; Larson and Kraus 1989) and associated with storms, such a calculation method typically underestimates the bar speed in the assumption that the movement is constant during the time between surveys. In the presently used database, the average time interval between profile surveys at Line 62 was about 10 days, although more frequent surveying sometimes occurred. A storm with a typical time scale of days that moves a bar offshore would produce a rapid bar movement not apparent in the calculation if the surveying were done at a much longer time scale. If the bar is outside the region of breaking waves, profile changes are more regular under the action of non-breaking waves, and the estimated bar speed should be more representative. Thus, the calculated speed of the outer bar during onshore movement is more credible than offshore movement of the inner bar (the same conclusion is valid for the outer bar).

62. Onshore and offshore bar movements were analyzed separately, and in the 191 events where movement of the mass center was recognized, the inner bar moved onshore on 99 occasions and offshore on 92 occasions. The average speed of onshore bar movement was 1.5 m/day and the maximum onshore bar speed was 8.7 m/day. Corresponding values for offshore bar movement were an average speed of 2.9 m/day and a maximum speed of 18 m/day. Thus, on the average, offshore bar speed is about twice as great as onshore bar speed, and approximately the same ratio is valid for the maximum speed. No restrictions were placed on the number of days between surveys in calculating the bar speed, and all surveys were used in the analysis.

63. A comparison was also made between the speed of onshore and offshore bar movement for the larger events. A threshold bar speed of 2 m/day was employed, and only events above this cutoff were included in the calculation. For these events, a larger number of occurrences with offshore movement were recorded (33) than for onshore movement (20). The calculated average bar speed was 4.5 m/day and 6.7 m/day for onshore and offshore bar movement, respectively, for these faster events.

Characteristic Time Scales of Bar Evolution

64. The box-counting method was used to analyze characteristic patterns of offshore movement of the inner bar with time. As a measure of bar movement, either change in bar volume or location of the bar mass center provided indicators of onshore or offshore movement. Growth in bar volume and movement of the bar center of mass in the seaward direction were regarded as indicators of offshore bar movement. Change in bar volume or mass center movement as the indicator produced about the same result with respect to the box-counting curve. Figure 22 shows the box-counting curve for offshore center of mass movement, which may be schematized by two straight lines in a logarithmic plot. The slopes of the two lines and the location of the break point between the lines are quite similar to the corresponding curve for volume decrease above NGVD (Figure 16). The break point occurs for a box size of about 60 days, which may be interpreted as the typical maximum duration between events that move the inner bar offshore.

65. The agreement between the box-counting curve for volume decrease above NGVD and offshore movement of the inner bar is expected because the inner bar evolution is closely dependent on material exchange between the foreshore and the inner bar. Thus, the representative time scales governing foreshore and inner bar response should be similar.

Summary of Bar Properties

66. In analysis of 200 profile surveys, a distinct inner bar was identified and statistical quantities were computed for the different bar properties. Table 3 summarizes these properties for the inner bar for depth to bar crest, maximum bar height, bar volume, bar length, and location of bar center of mass. Data on individual profile surveys that were used to compute the values in Table 3 are tabulated in Appendix A.

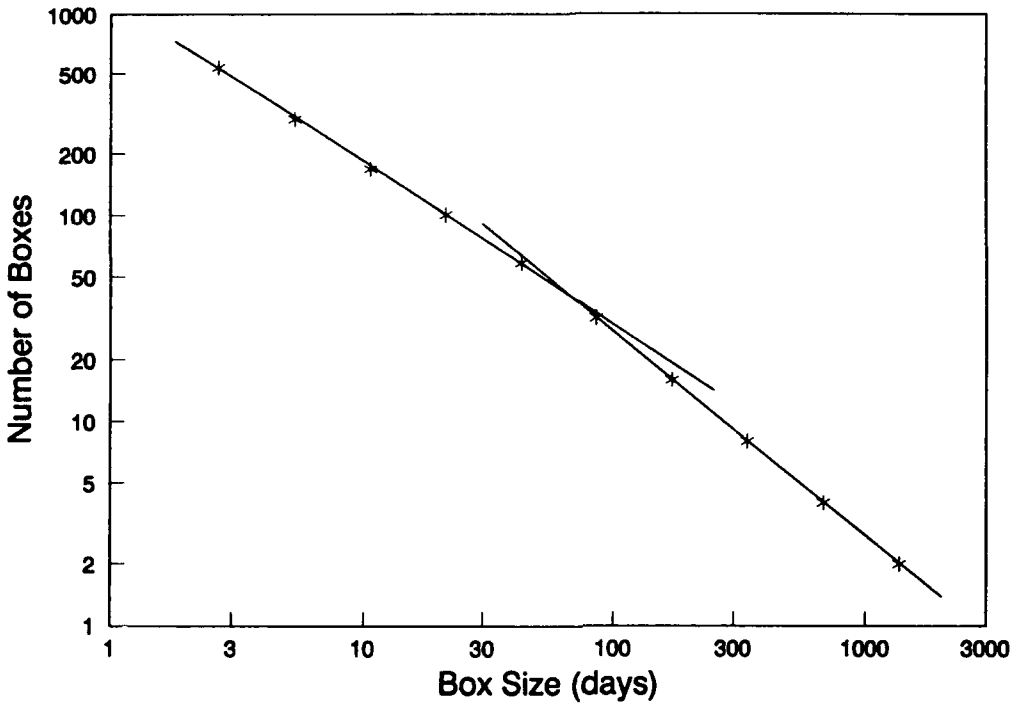

Figure 22. Box-counting curve for offshore mass center movement, inner bar

Table 3

Statistics for Inner Bar Properties

Property	Mean	Minimum	Maximum	Q_{25}*	Q_{75}*
Depth to crest, m	1.6	0.6	2.5	1.3	1.9
Bar height, m	0.9	0.2	1.4	0.7	1.0
Bar volume, m^3/m	42	6	98	27	55
Bar length, m	95	35	280	65	100
Bar mass center, m	215	150	330	195	230

* The quantities Q_{25} and Q_{75} denote the limits which 25 and 75 percent of the values are below, respectively.

PART V: OUTER BAR PROPERTIES

67. In this chapter, calculation results are presented for properties of the outer bar. Appendix B lists calculated values of the different bar properties for each of the individual profile surveys of Line 62. For 221 of the 300 surveyed profiles of Line 62, an outer bar was present, and the periods when a distinct outer bar existed are summarized in Table 4. During extended periods of low waves, the outer bar moved slightly onshore simultaneously with flattening, to finally disappear. In general, the outer bar disappeared as an identifiable morphological feature by flattening before it moved a significant distance onshore as an identifiable unit. As previously mentioned, during some periods between surveys the inner bar moved offshore to become an outer bar. Two such time periods were observed when the inner bar consistently moved offshore to finally reach an offshore position corresponding to the location where the outer bar typically was found. The approximate time periods were 810928 to 820105 and 880909 to 890312, both periods coinciding with the autumn and winter seasons when the severe storms arrive to the coast at the FRF.

Table 4

Time Periods with Outer Bar Present on Line 62

Time Period		Reason for Disappearance
810126 0350	810717 1200	Bar flattened out
810928 1115	840920 1030	Bar flattened out
850125 1200	851121 0820	Bar flattened out
860516 1224	[illegible]0602 1012	Bar flattened out
880909 1015	891228 1550	Bar flattened out

Depth to Bar Crest

68. The average depth to bar crest for the outer bar was 3.8 m, which indicates the presence of individual breaking waves with characteristic heights on the order of 4 to 5 m

associated with modifications of the outer bar. Figure 23 illustrates the depth to bar crest as a function of time for the outer bar. In comparison with depth to crest for the inner bar (see Figure 18), the fluctuations are significantly smaller and much more regular. This is because once the outer bar has formed, it is only exposed to wave breaking and large sand transport during severe storms, and transport induced by non-breaking waves produces less rapid changes in bar shape. Figure 23 also contains the two time periods when the inner bar moved offshore and became the outer bar. The maximum depth to crest recorded was 5.1 m, whereas the minimum depth to crest as determined by the depth over the inner bar as it started moving offshore to become an outer bar was $(h_c)_{min} = 1.3$.

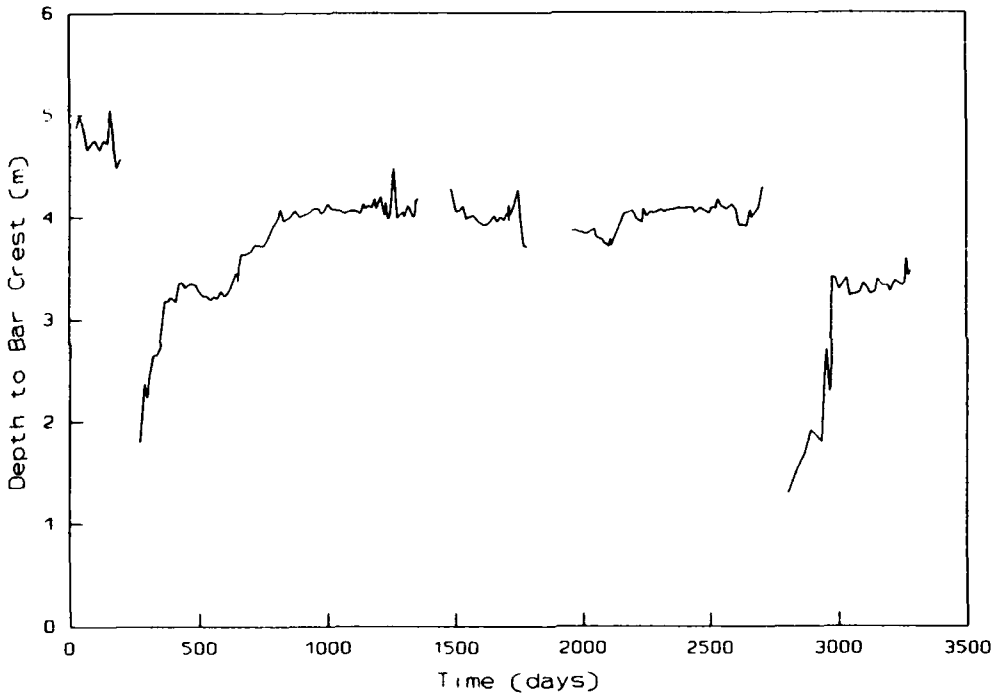

Figure 23. Depth to bar crest as a function of time for the outer bar

Maximum Bar Height

69. Maximum bar height as a function of time for the outer bar is displayed in Figure 24. Regular, long-term variations in maximum bar height are noticeable, where the bar

grows rapidly to maximum size, after which it decreases in volume at a lower rate until it flattens out completely. Approximately five such cycles encompassing outer bar growth and decay may be identified in Figure 24, which implies that a cycle is not necessarily completed during a year. The buildup of the outer bar is related to the severe storms occurring during the autumn and winter. The average maximum bar height was 0.4 m, which is about half the corresponding average height of the inner bar. Furthermore, the profile analysis gave the limiting values $(z_m)_{max}$ = 1.4 m and $(z_m)_{min}$ as negligible.

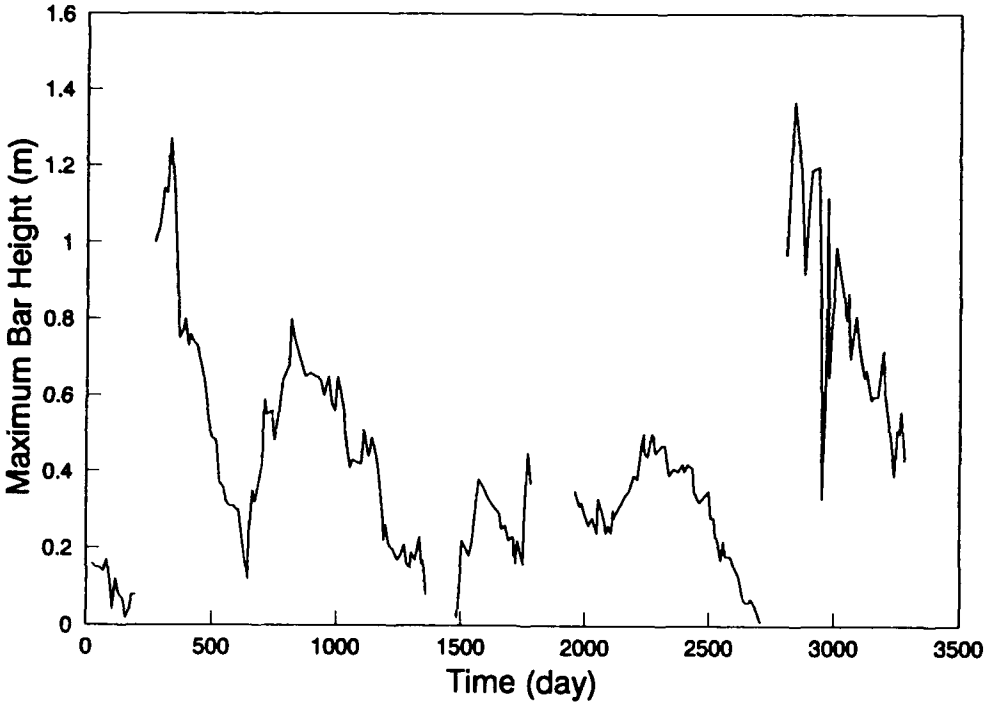

Figure 24. Maximum bar height as a function of time for the outer bar

Bar Volume

70. The average volume for the outer bar was 45 m^3/m, which is approximately the same as the average volume for the inner bar. In Figure 25 the variation in outer bar volume is shown as a function of time. The same principal temporal variation as for the maximum bar height occurred with a number of cycles where the bar experienced regular growth in volume

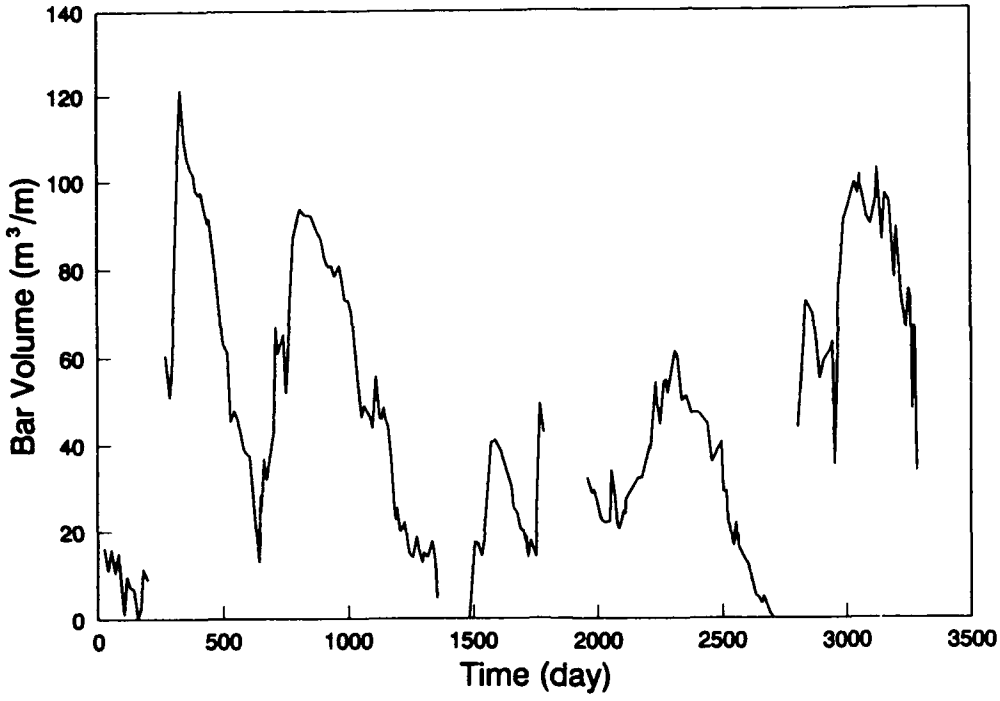

Figure 25. Bar volume as a function of time for the outer bar

followed by a decrease in size until the bar completely disappeared. The maximum bar volume was determined to be 120 m^3/m, whereas the minimum bar volume was reached before the flattening out of the bar, giving a volume close to zero.

Location of Bar Center of Mass

71. Figure 26 shows the location of the center of mass for the outer bar as a function of time. The average location of the bar was 410 m from the FRF baseline, which is approximately 300 m from the average shoreline position. As in Figure 23, the two occurrences when the inner bar moved offshore to form an outer bar are easy to recognize. The maximum offshore location of the outer bar was 520 m, corresponding to a depth of about 5 m, whereas the most nearshore position of the bar occurred as the inner bar started to move offshore with $(x_{cg})_{min}$ = 200 m.

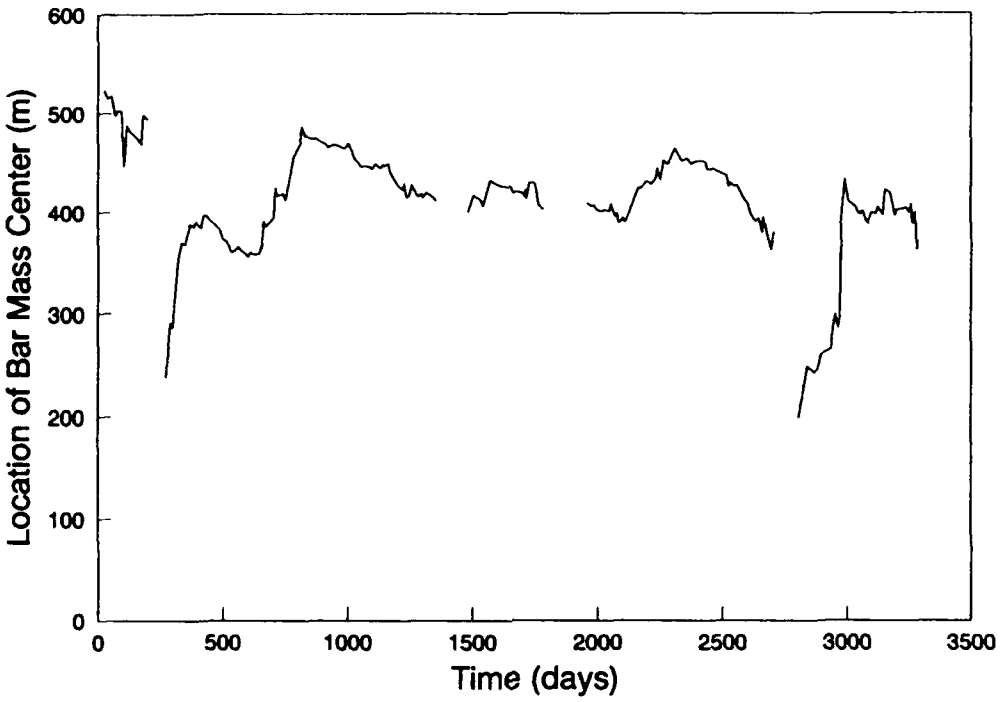

Figure 26. Location of mass center as a function of time for the outer bar

Speed of Bar Movement

72. The speed of bar movement was calculated for the outer bar in the same manner as for the inner bar. Thus, onshore and offshore bar speeds were obtained as averages over time intervals corresponding to periods between surveys, typically underestimating the bar speed. For the total number of events analyzed, 122 displayed onshore bar movement and 90 displayed offshore bar movement. The average bar speed for onshore movement of the outer bar was 0.6 m/day and the maximum speed was 6.1 m/day. For offshore movement, the corresponding values were an average bar speed of 1.1 m/day and a maximum speed of 15.2 m/day.

73. In comparison to the movement of the inner bar, the outer bar exhibited considerably lower average bar speeds, both for the onshore and offshore movement, whereas the maximum values were quite similar for the inner and outer bars. The average bar speed for the outer bar was approximately one third of that for the inner bar. Because the inner bar is more frequently subjected to breaking waves than the outer bar, the average speed of bar movement is

greater for the inner bar. However, in the case of waves breaking on the outer bar, the speed of movement is comparable to that of the inner bar, as shown by the similar maximum bar speed for the inner and outer bars.

74. Bar movement was also analyzed after applying a threshold bar speed of 2 m/day. In this case, the average bar speed was 4.2 m/day (5 events) and 3.9 m/day (14 events) for onshore and offshore bar movement, respectively. Thus, for events involving rapid movement of the outer bar, onshore and offshore bar movement have similar speeds.

Characteristic Time Scales of Bar Evolution

75. Figure 27 illustrates the curve resulting from a box-counting analysis for the outer bar using the location of the center of mass as the indicator of offshore bar movement. The curve is well described by two straight lines, with the break in slope occurring for a box size of about 120 days. As for the inner bar, this break point may be interpreted as the representative maximum duration between storm events that cause offshore movement of the outer bar.

76. In summary, the inner bar moves offshore at least every second month, whereas, for the outer bar, about 4 months could separate wave events producing movement in the seaward direction. Thus, offshore movement of the outer bar displays a distinct seasonality being exposed to significant transport in the seaward direction mainly during the fall and winter seasons.

Summary of Bar Properties

77. For 221 profile surveys, a distinct outer bar was identified and statistical quantities were computed for the different bar properties. Table 5 summarizes these properties for the outer bar, encompassing depth to bar crest, maximum bar height, bar volume, bar length, and location of bar mass center. Data on individual profile surveys that were used to compute the values in Table 5 are tabulated in Appendix B.

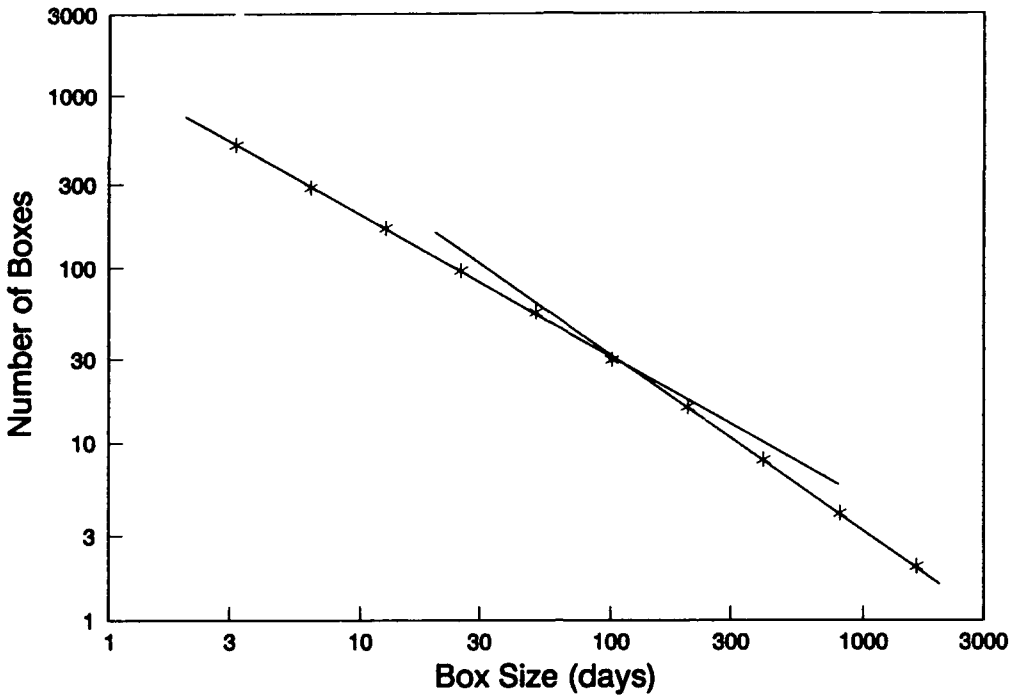

Figure 27. Box-counting curve for offshore mass center movement, outer bar

Table 5

Statistics for Outer Bar Properties

Property	Mean	Minimum	Maximum	Q_{25}*	Q_{75}*
Depth to crest, m	3.8	1.3	5.1	3.4	4.1
Bar height, m	0.4	0	1.4	0.27	0.6
Bar volume, m^3/m	45	0	120	20	67
Bar length, m	170	25	280	150	200
Bar mass center, m	300	85	410	280	330

* The quantities Q_{25} and Q_{75} denote the limits which 25 and 75 percent of the values are below, respectively.

PART VI: RELATIONSHIP BETWEEN BAR AND WAVE PROPERTIES

Relationship Between Bar Properties

Inner bar

78. Correlation analysis was performed for combinations of the different bar properties to determine the linear dependence between the studied properties. The highest positive correlation coefficients r were obtained for:

a. Bar volume versus bar height, $r = 0.82$.

b. Bar volume versus bar length, $r = 0.75$.

c. Depth to bar crest versus distance to bar mass center, $r = 0.70$.

In this analysis, all values were employed without applying a threshold value to the data. A positive correlation coefficient, but with a lower value, was also noted for bar volume versus distance offshore, whereas a small negative correlation was obtained for maximum bar height versus depth to bar crest.

79. Correlation analysis for the inner bar produced high values for the expected combinations of bar properties. As a bar moves offshore and into deeper water, its size grows, and the bar volume, bar length, and maximum bar height increase correspondingly. Thus, a significant correlation should occur between these properties, as was the case. Correlation between depth to bar crest and distance to bar center of mass indicates that inner bars located further offshore have a larger crest depth. In studying the LWT data, Larson and Kraus (1989) concluded that the depth to crest was approximately constant for a bar moving offshore during constant wave conditions, and similar behavior was measured in the field during a storm by Sallenger, Holman, and Birkemeier (1985). However, the present data include many different bars that were formed and influenced by quite different wave conditions, thus producing a depth to crest that varies with the location of the bar center of mass.

80. Figure 28 displays the relationship between volume and height for the inner bar, encompassing 200 measurements. Although there is a considerable scatter in the figure, a positive correlation between the two bar properties is recognized. In Figure 29, the depth to bar crest is shown as a function of the location of the bar center of mass, illustrating a positive

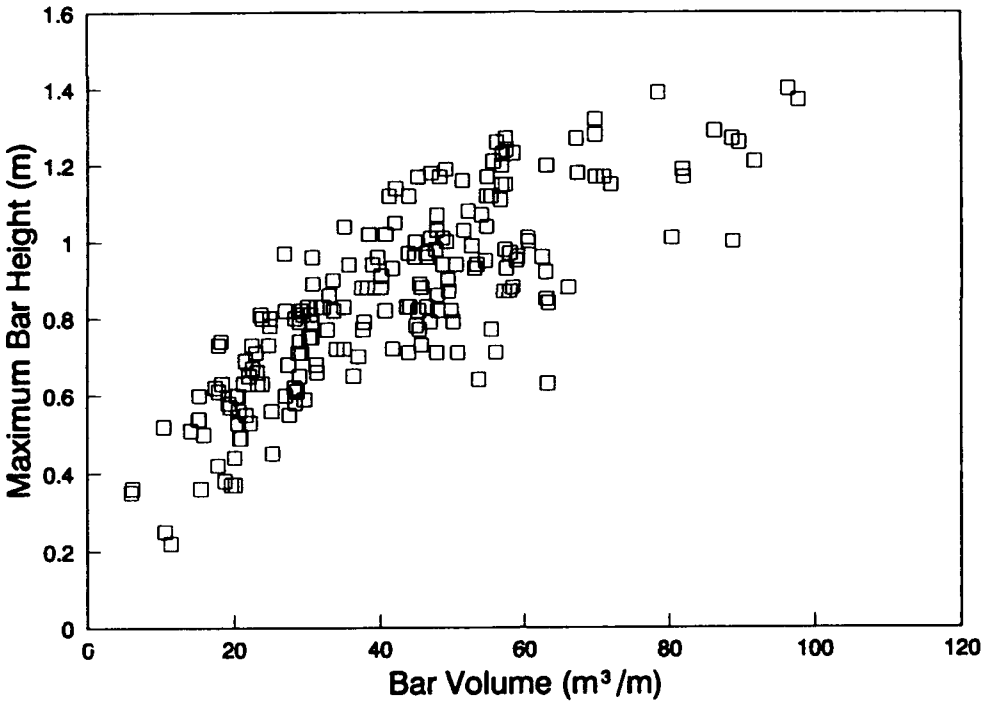

Figure 28. Maximum bar height as a function of bar volume, inner bar

correlation between these properties. The scatter is larger than in Figure 28, largely caused by one sequence of profile surveys where the inner bar was located further offshore than was normally the case. If these measurements were eliminated, a much stronger correlation would be obtained between the properties in Figure 29. This illustrates the difficulty sometimes encountered in distinguishing between the inner and outer bar, as, for example, when the inner bar moves seaward to become the outer bar.

Outer bar

81. The outer bar displayed high correlation between properties similar to those of the inner bar. The highest positive correlation occurred for:

a. Bar volume versus maximum bar height, $r = 0.85$.

b. Bar volume versus bar length, $r = 0.70$.

c. Depth to bar crest versus distance to bar mass center, $r = 0.90$.

A marked negative correlation coefficient was obtained for depth to bar crest versus maximum bar height ($r = -0.78$), which was greater than that for the inner bar. Figure 30 shows the maximum bar height as a function of depth to bar crest, clearly illustrating the negative

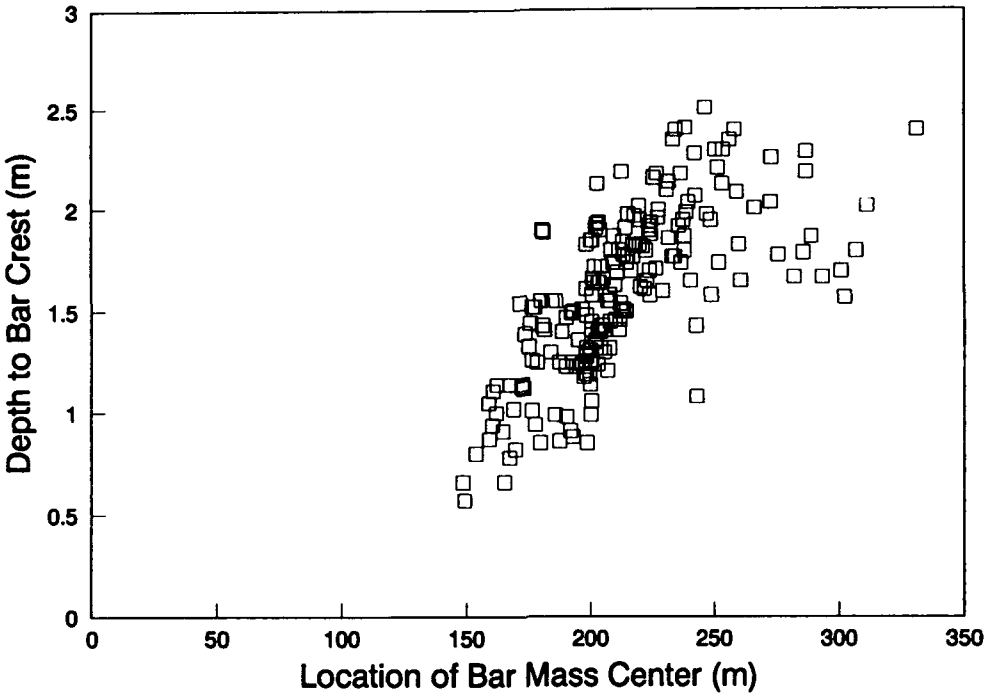

Figure 29. Depth to bar crest as a function of bar mass center, inner bar

correlation between these two properties. Thus, an outer bar located in deeper water is in general flatter, implied by the smaller maximum bar height. However, similar to the data presented in Figure 29, the data in Figure 30 contain cases where the bar was not located in the typical range for the outer bar, but located further inshore (points located to the left in Figure 30). Removing these cases would significantly alter the negative correlation between maximum bar height and depth to bar crest.

Summary of Wave Characteristics

82. The energy-based significant wave height and peak spectral period were available at the measurement depth of 18 m for the studied period (1981 to 1989) with a typical time resolution of 6 hr. However, during the latter half of this period (1985 to 1989), more frequent measurements were available, often at hourly intervals. A summary of the available wave data is given in Table 6 for the first and second half of the measurement period. Howd and Birkemeier (1987a) give a more extensive presentation of wave data obtained at the FRF during the period

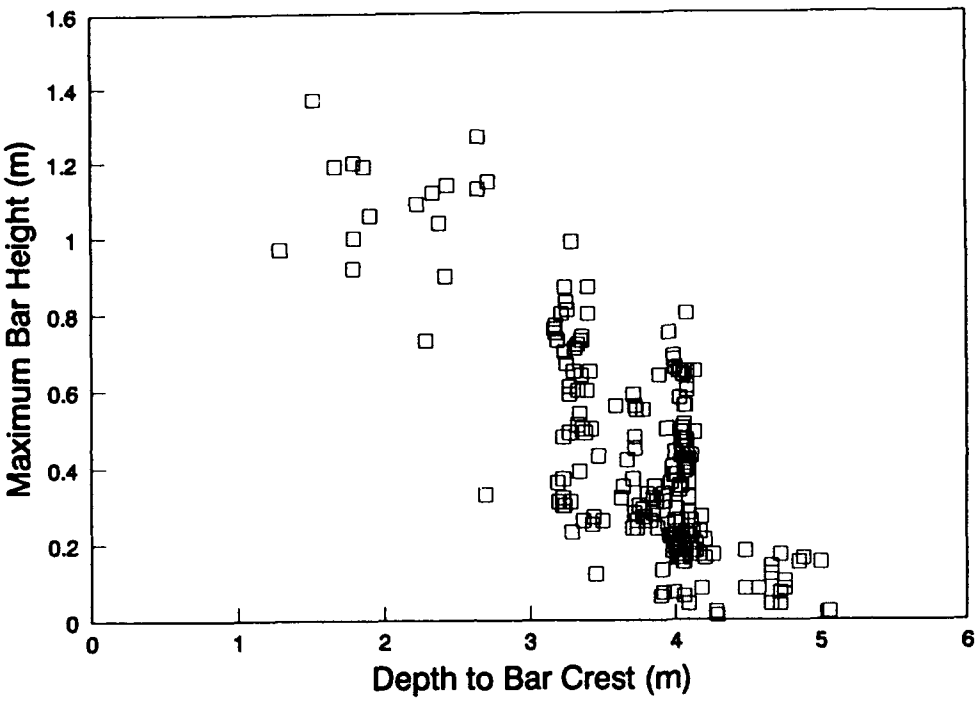

Figure 30. Maximum bar height as a function of depth to bar crest, outer bar

Table 6

Summary of Wave Characteristics for 1981 to 1989 at the FRF Waverider (Gage 62)

Period	Number of Values	H_{mean} (m)	T_{mean} (sec)	H_{max} (m)	T_{max} (sec)
1981-1984	5,173	1.0	8.4	4.7	17
1985-1989	23,926	1.1	8.4	6.8	23

1981 to 1984; however, the measurements discussed therein were mainly obtained by the gage at the end of the FRF pier, and not by the waverider buoy, which is used in this report. In Table 6, H_{mean} denotes the average significant wave height, H, T_{mean} the mean peak spectral wave period, H_{max} the maximum significant wave height, and T_{max} the maximum peak spectral wave period for the respective measurement periods.

83. To further analyze the wave climate at a more convenient time scale, daily mean values were calculated from the measured time series of wave heights and periods by averaging

all measurements from a particular day. The statistical properties of daily significant wave height and peak spectral period are given in Table 7 (covering 3,130 days) for the measurement depth of 18 m. The average significant wave height for the entire measurement period was 1.1 m, and the average peak spectral wave period was 8.4 sec based on 29,098 individual recordings. The average values differ slightly from those calculated using all values in the measurement series, because the number of measurements per day varies.

Table 7

Statistics of Daily Mean Significant Wave Height and Peak Spectral Wave Period

Property	Mean	Minimum	Maximum	Q_{25}^{*}	Q_{75}^{*}
Wave height, m	1.0	0.0	4.5	0.6	1.2
Wave period, sec	8.3	2.3	18.9	6.8	9.5

* The quantities Q_{25} and Q_{75} denote the limits which 25 and 75 percent of the values are below, respectively.

84. Figure 31 displays the time variation in the daily mean significant wave height at the gage for the entire measurement period (3,130 values). The time is given in consecutive days from the start of the studied period (810101). Although the plot is too dense to distinguish individual days, a long-period temporal pattern is apparent, with higher waves occurring during the autumn and winter seasons, and lower waves occurring during the summer. Annual summary reports from the FRF also display this seasonality in time series plots of the wave height.

85. The empirical distribution of the mean significant wave height was determined using the calculated daily wave height, making it possible to estimate the probability of exceedance of a specific daily wave height. Figure 32 displays the distribution of the daily wave height at the measurement point, and the distribution has an approximately log-normal shape.

86. Measurements of the incident wave angle were not available for the full 8-year observation period, and in the simultaneous analysis of bar and wave properties the importance of this variable was not quantified. The wave angle is typically small close to shore, but events may occur when this is not the case. Thus, when deepwater wave quantities were calculated, the waves were backed out to deep water by use of linear-wave theory omitting refraction and

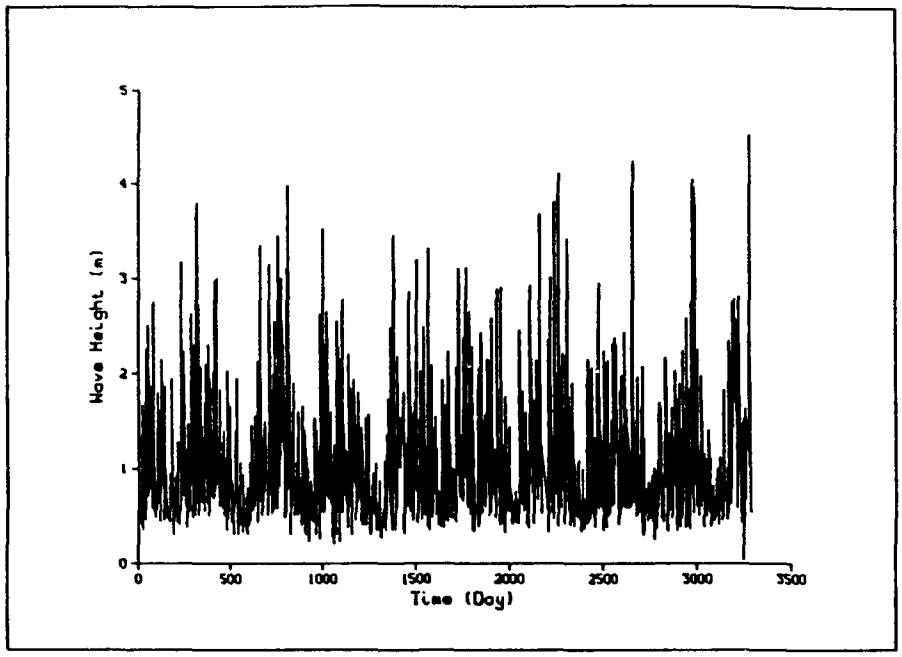

Figure 31. Daily mean significant wave height as a function of elapsed time in the 18-m water depth at FRF Gage 62

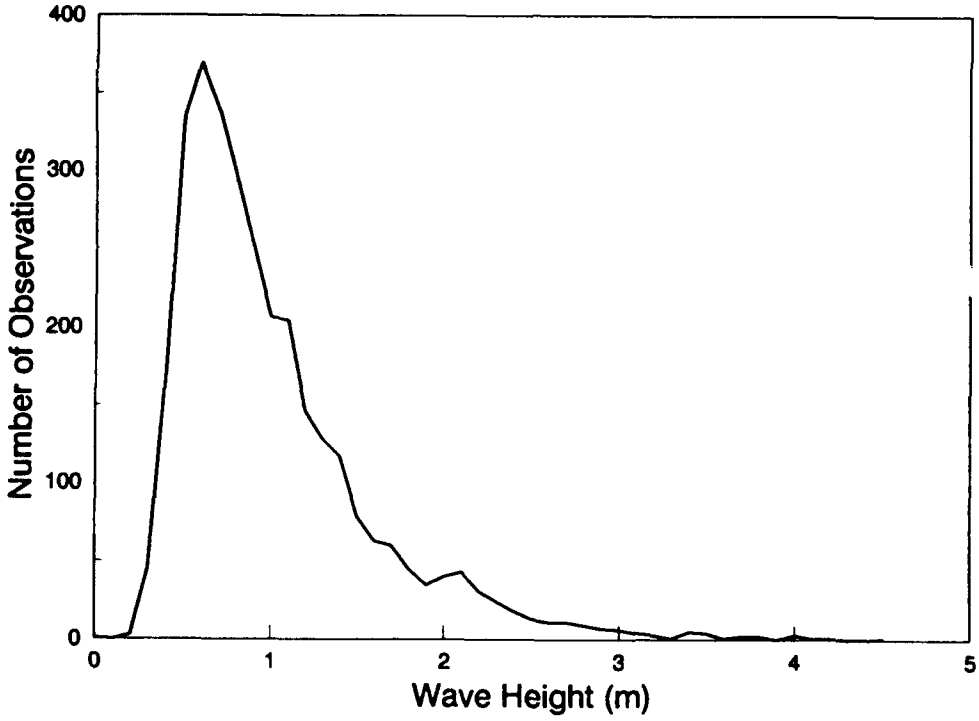

Figure 32. Empirical distribution of daily mean significant wave height in the 18-m water depth at FRF Gage 62

just accounting for shoaling. Omission of refraction in the analysis is one contributing factor to the scatter in relationships between bar and wave properties.

Correlation Between Bar Properties and Wave Measurements

87. With the objective of understanding bar response to incident waves, the aforementioned bar properties were correlated with different measured wave characteristics. The following wave-related quantities were used in the correlation analysis:

H_{mean} = mean significant wave height

H_{max} = maximum significant wave height

T_{mean} = mean peak spectral period

T_{max} = maximum peak spectral period

$(H/L)_{mean}$ = mean wave steepness

$(H/L)_{max}$ = maximum wave steepness

$(H/wT)_{mean}$ = mean fall speed parameter

In these relations, L is the wavelength computed by linear-wave theory with the mean spectral wave period, and w is the sediment fall speed, here taken to be the fall speed associated with the median grain size of the sediment. Fall-speed parameter values were calculated by using mean monthly water temperatures given by Birkemeier et al. (1985). These quantities were determined based on the time period preceding a specific profile survey, encompassing the entire period from the previous survey. In most of the analysis, deepwater quantities were employed; that is, the waves measured in 18 m were backed out to deep water neglecting refraction. Appendix C presents the deepwater wave quantities for the inner bar, determined from the profile survey dates, and Appendix D gives the same quantities for the outer bar. In these appendices, the date associated with the wave quantities represents the time of the last profile survey in the period for which the wave quantities were averaged. The first date of the time period of the averaging pertains to the previous profile survey.

88. In general, little correlation was present between bar properties and wave quantities calculated for the period prior to the profile survey, if all data were analyzed simultaneously. Although this field data set is unique with respect to its high resolution in time and space of the

profile evolution, the average spacing in time for the most intensively surveyed line (Line 62) was about 10 days. As observed by Sallenger, Holman, and Birkemeier (1985) in the field and by Sunamura and Maruyama (1987) and Larson and Kraus (1989) through analysis of LWT data, the time scale of profile response during a storm, both for the erosive phase and the post-storm recovery, is rapid, with significant changes occurring over a few hours. The redistribution of material within the profile, and thus the movement of longshore bars, is a function of not only the wave characteristics, but also of such factors as how far from equilibrium the profile is with respect to the wave conditions (and water level) and the duration of a given set of forcing conditions.

89. Thus, a specific survey represents the integrated result of the wave and water level conditions that have prevailed since the previous profile survey. Characterization of the variable forcing by using a set of statistical parameters is difficult, but necessary, if large amounts of data are to be analyzed and the objective is to derive relationships that can be readily used in engineering design. The above-mentioned wave properties were judged to be the most appropriate at an initial stage of an analysis to derive such relationships. An underlying assumption in the present analysis is that the chosen quantities as a first-order approximation characterize the forcing condition that causes changes along the profile and the associated changes in bar properties. Furthermore, the changes in these quantities should not vary too much in between the surveys in order for mean values to be a good measure of the forcing conditions.

90. In order to derive relationships at an acceptable level of correlation, careful data analysis was required in which only events involving significant changes between profile surveys were included. Thus, a threshold value was often employed in the analysis with respect to the change in bar volume and/or location of the bar center of mass. Application of a threshold for the bar volume partly eliminates events affected by the surveying accuracy, whereas including the movement of the bar center of mass ensures that events where the bar moved but maintained its volume are not discarded. In deriving relationships to be used in engineering applications, and also bearing in mind the type of data that are typically available in such calculations, only events pertaining to significant beach change are of primary interest (Kraus, Larson, and Kriebel 1991).

Inner bar

91. The above-discussed difficulties in establishing simple relationships between bar and wave properties were especially prevalent for the inner bar. The following analysis was performed to establish such relationships:

a. Correlation between geometric bar properties and wave quantities.

b. Correlation between change in geometric bar properties and wave quantities.

c. Distinguishing of mutually exclusive events.

The first method encompassed correlation between the bar properties presented in Appendix A and the wave-related quantities in Appendix C. In this analysis method, it is assumed that bar properties on a specific profile are only a function of the wave conditions preceding the survey and the past profile shape is of minor importance (no "memory" of the past profile). Analysis of LWT data (Larson and Kraus 1989) showed bar development that was rapid in time, and thus the influence of a certain profile shape would be limited in time. However, in the LWT experiments, breaking waves acted at all times in the region around the bar and for a duration corresponding to near equilibrium. The situation of a bar almost continuously exposed to breaking waves is also expected for the inner bar at the FRF, whereas the persistence of constant wave conditions with a duration sufficiently long to achieve equilibrium is rare. In the case of the outer bar, it is only expected to be in the breaker zone during severe storms, thus implying that a specific profile shape persists longer and is of greater importance for the evolution of consecutive profiles.

92. In the second method, changes in the bar properties between two profile surveys were correlated with the associated wave quantities. Because bar properties inferred from the previous survey are included in the analysis, the profile shape is indirectly taken into account. The analysis of mutually exclusive events, such as onshore and offshore bar movement, was aimed at deriving relationships for distinguishing between the occurrence of these events. The results of this analysis are discussed in more detail in the following section dealing with criteria for onshore and offshore bar movement.

93. Figure 33 clearly illustrates the difficulties in deriving simple relationships between bar and wave properties for the present data set without data censoring. The figure displays the depth to bar crest as a function of the maximum wave height for the inner bar involving about

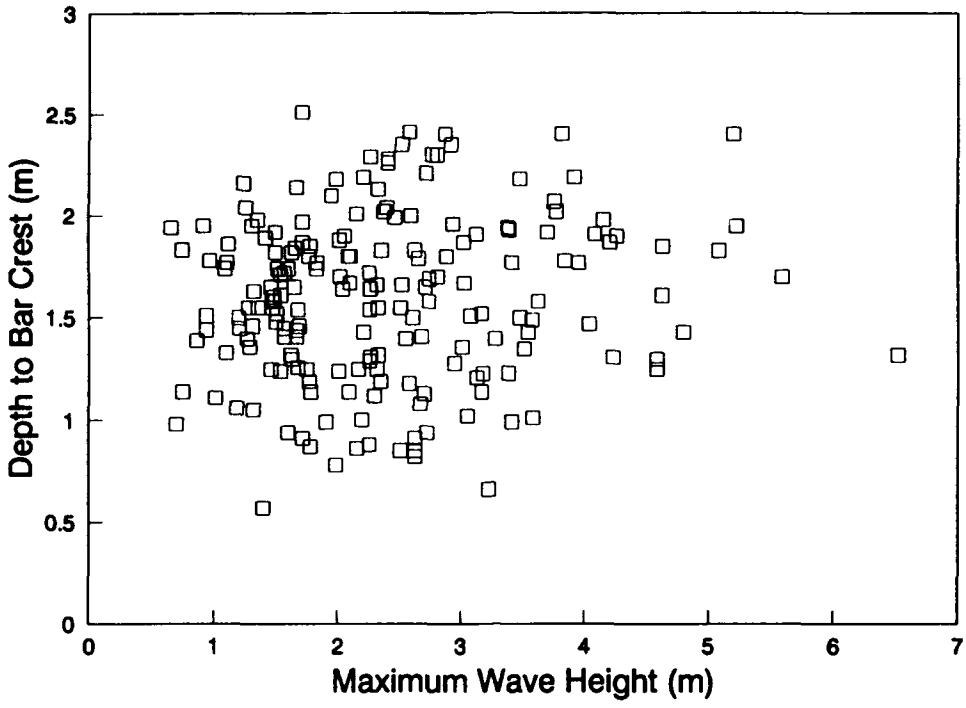

Figure 33. Depth to crest for the inner bar as a function of the maximum wave height occurring between two consecutive profile surveys

200 measurements, and no correlation between these variables is noted. Even though a correlation between the depth to bar crest and the maximum wave height is expected, factors such as variability in wave conditions, absence of profile equilibrium, and neglect of incident wave angle and water level effects contribute to the scatter.

94. In general, no significant correlations could be found between the geometric properties of the inner bar and the investigated wave properties, but results similar to what are displayed in Figure 33 were obtained for other combinations of wave and bar properties. The rapid response of the inner bar probably caused the calculated average wave properties to be poor descriptors of the conditions that were essential to formation of the bar. The length of the time period between profile surveys from which the wave quantities were computed was the main reason for this problem. If this time period was long, the wave conditions could vary considerably, and it was difficult to determine representative wave quantities with respect to the measured profile response. Even with application of a threshold value given by the bar volume or center of mass movement, the degree of correlation only improved marginally.

95. Correlation analysis was also performed for changes in the different bar properties between two consecutive surveys in time and the associated wave properties. By applying a threshold value of 5 m^3/m on the change in bar volume between consecutive surveys, events that could potentially be contaminated by surveying accuracy were eliminated. Using this criterion, relationships between change in bar properties and wave characteristics could be derived, although the correlation coefficients were still low. To further clarify the correlation and include only those events where a distinct bar response was observed (profile change of engineering significance), a criterion was imposed to take into account only the events for which the volume change and the mass center movement indicated a similar trend in the bar response. Thus, only those events were included that simultaneously displayed either volume growth and offshore movement or volume decrease and onshore movement. In the analysis, an effort was made to employ non-dimensional quantities to increase the generality of the results obtained.

96. Figure 34 illustrates the change in bar volume normalized with the mean wave height squared as a function of the mean fall speed parameter (37 measurements). The scatter is still fairly large (r = 0.56), but a clear trend is noted. For higher values of the fall speed parameter, positive bar volume changes occur and the magnitude of the change increases. Another example of the correlation between bar and wave properties, after the previously described data reduction, is shown in Figure 35, which displays $h_c / (H_o)_{max}$ as a function of the mean wave steepness, where the subscript o denotes wave steepness. Also, in this figure the scatter is large (r = 0.66), although the trend is clear with decreasing values in $h_c / (H_o)_{max}$ for decreasing steepnesses. Figure 35 indicates that the crest depth with respect to the maximum wave height decreases for increasing wave steepness; that is, the bar crest is relatively closer to the water surface for erosional waves (higher wave steepness) than for accretionary waves (lower wave steepness).

97. Other, more qualitative, results from the correlation analysis after data reduction were an increase in the change in maximum bar height with increasing $(H_o / L_o)_{mean}$ and $(H_o / wT)_{mean}$, and an increase in the change of the distance to the bar center of mass with increasing $(H_o / L_o)_{mean}$ and $(H_o / wT)_{mean}$. Regression relationships were derived for some combinations of bar and wave properties, but the coefficient of determination was too low to be significant. Thus, the results of the correlation and regression analysis were mostly of a qualitative nature.

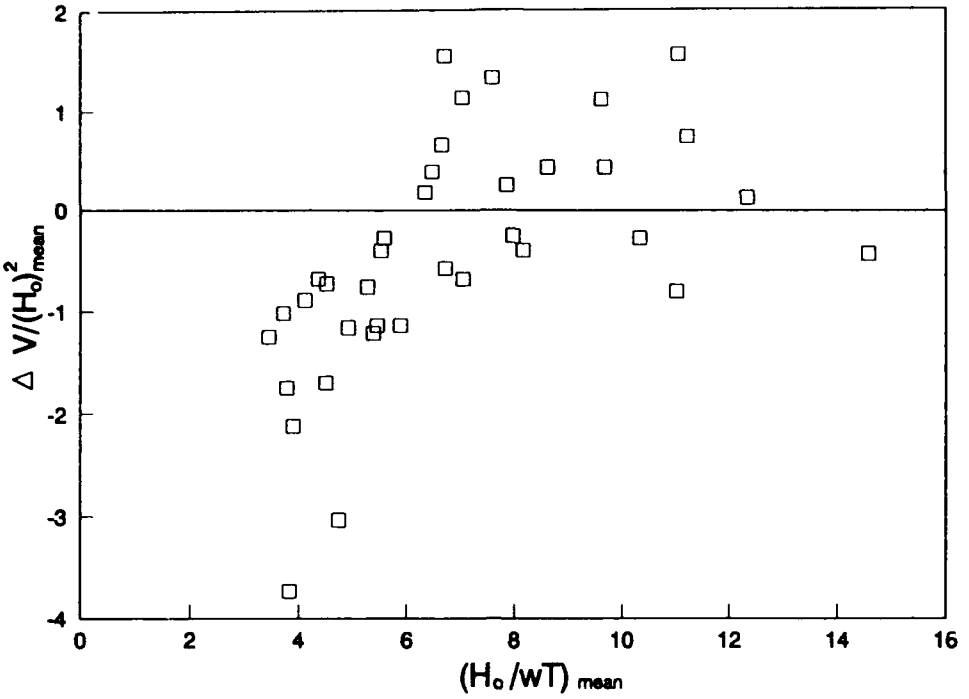

Figure 34. Change in inner bar volume as a function of mean fall speed parameter

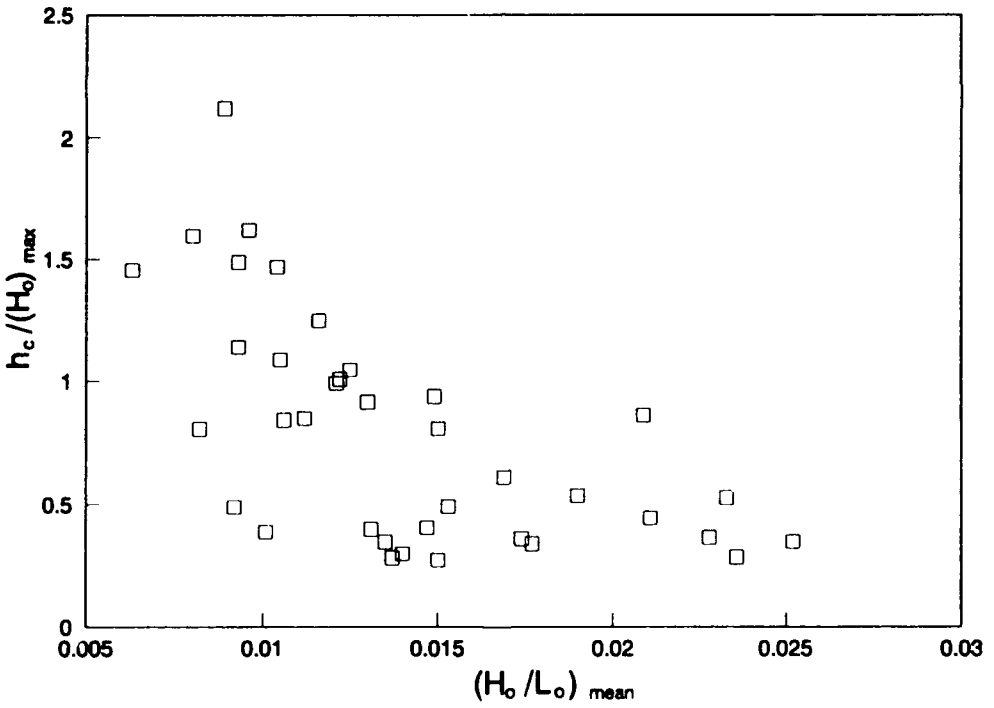

Figure 35. Depth to crest for the inner bar as a function of mean wave steepness

Outer bar

98. Similar correlation analysis as for the inner bar was carried out with reference to outer bar and wave properties. Both the bar properties and changes in these properties were used in the analysis to obtain simple relationships with the previously discussed wave characteristics. The same difficulties as for the inner bar were encountered, and significant correlation only occurred after data reduction in accordance with the criteria described above (employing a threshold value for the change in bar volume, and requiring the same behavior for bar volume change and mass center movement).

99. After censoring of the data, 55 events remained for the correlation analysis. Figu 36 illustrates $h_c / (H_o)_{max}$ as a function of $(H_o / wT)_{mean}$ ($r = 0.78$), and it displays a similar trend as the inner bar shown in Figure 35. The mean wave steepness gave a slightly lower correlation than the mean fall speed parameter, but the overall trend was similar in use of $(H_o / L_o)_{mean}$ and $(H_o / wT)_{mean}$. Other results of the correlation analysis of a more qualitative nature were an increase in the change in maximum bar height with increasing $(H_o / L_o)_{mean}$ and $(H_o / wT)_{mean}$, and an increase in the change of bar volume with increasing $(H_o / L_o)_{mean}$ and $(H_o / wT)_{mean}$.

100. Efforts were also made to perform the correlation analysis by separating events where the bar moved onshore and offshore. Furthermore, threshold values on bar volume change were employed to select events with marked change in bar volume to obtain cases with a well-defined response. However, correlation between bar and wave properties only marginally improved compared to analyzing on- and offshore movements simultaneously. The highest correlation values were in general obtained if consecutive profiles in time were analyzed where a continuous onshore or offshore bar movement occurred.

Criteria for Onshore and Offshore Bar Movement

101. It is of fundamental importance to be able to predict the direction of sand transport for the design of nearshore dredged material berms intended to function as beach nourishment. By studying the response of natural longshore bars with respect to the incident wave conditions, it is possible to derive criteria that should be applicable for predicting the cross-shore direction of movement of mounds placed near shore. In this context, the outer bar at the FRF is of particular

interest because it is located in water depths where available hopper dredges and similar equipment can have access. For that reason, in this study, development of engineering criteria for predicting transport direction focused on the response of the outer bar, although the inner bar was studied as well to assess the generality of the results.

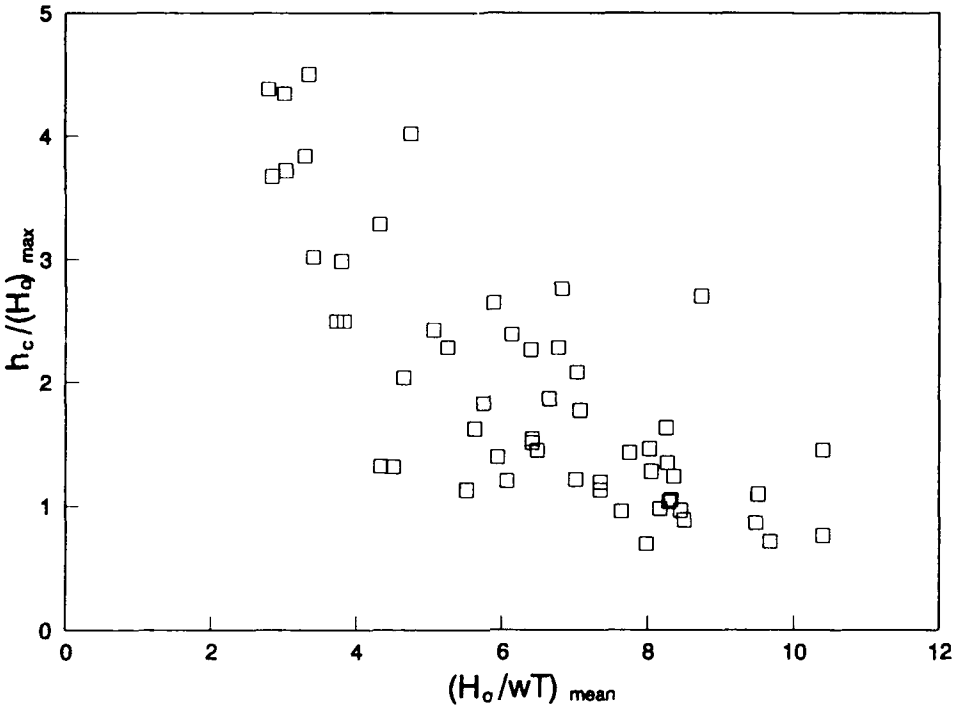

Figure 36. Depth to crest for the outer bar as a function of mean fall speed parameter

102. Several different criteria were derived to determine the onshore and offshore movement of the inner and outer bar. To determine the direction of bar movement, and thus the net direction of the sand transport across the bar, both change in bar volume and change in the location of bar center of mass were employed. Use of bar volume as an indicator of transport direction assumes that bar growth is associated with offshore movement, whereas a decrease in bar volume is caused by onshore movement. In the final analysis for deriving the criteria, a simultaneous increase in bar volume and an offshore movement of the center of mass were required as indicators of offshore transport and vice versa.

103. Furthermore, in order to obtain clearer distinction between onshore and offshore bar movement, different threshold values were evaluated in terms of bar volume and mass center location. As discussed previously, if only values above a certain threshold were included in the

analysis, the disturbing influence by factors such as the survey accuracy were minimized. Thus, a threshold value of 5.0 m^3/m on bar volume change was imposed to eliminate events with minor change that were expected to be sensitive to measurement limitations. Also, events where the inner bar moved offshore to become an outer bar were removed in the analysis, and only those cases were included where the inner and outer bar were located within their typical range of movement.

104. To distinguish accretionary and erosional events, i.e., when sand is transported on- or offshore across the bar, respectively, different combinations of dimensionless parameters were investigated. The parameters examined were: wave steepness H_o/L_o, dimensionless fall speed H_o/wT, wave height over grain size diameter H_o/D_{50}, and a Froude number based on grain size $Fr = w/(gH_o)^{1/2}$. Wave heights and associated wave periods in the analysis were taken as the mean over the analysis interval of the significant wave height. Similar analyses have been performed by Larson and Kraus (1989) primarily for the LWT data sets and limited field data (not examining the Froude number), and by Kraus, Larson, and Kriebel (1991) for the LWT data and an extensive field data set of primarily qualitative observations of beach erosion and accretion (and including the Froude number). All wave-related quantities were evaluated for deepwater conditions, for which the waves measured at the gage depth (18 m) were shoaled to deep water neglecting wave refraction. Initially, criteria for onshore and offshore bar movement were derived based on wave quantities at the gage depth; however, equally good separation of onshore and offshore bar movement was obtained with the unrefracted deepwater waves and, for the sake of generality, the final analysis was performed with deepwater waves. The (energy-based) significant wave height and spectral peak wave period were used in these calculations to provide convenient results for engineering applications. Larson and Kraus (1989) and Kraus, Larson, and Kriebel (1991) have shown that mean wave height should be used to compare field results and LWT results with regular waves.

Inner bar

105. After censoring the data, 41 events remained that were used to derive criteria for the cross-shore movement of the inner bar. The strategy for obtaining the criteria was to plot the data in a diagram encompassing two non-dimensional parameters and subjectively fit a line that best separated accretionary and erosional events (onshore and offshore bar movement, respectively). In the choice of parameter combinations, at least one parameter contained a variable that

characterized the sediment (either the fall speed w or the median grain size D_{50}). Figures 37 to 39 illustrate how well different combinations of parameters distinguished the two types of events and give the criteria derived by separating the accretionary and erosional points in the diagrams.

106. The following parameter combinations were found to provide a satisfactory distinction between accretionary and erosional events for the outer bar (subscript o denotes deepwater conditions): **H_o/L_o versus H_o/wT (Figure 37)**. These parameters have successfully been employed by previous investigators for distinguishing between overall beach accretion and erosion (Larson and Kraus 1989; Kraus, Larson, and Kriebel 1991). Acceptable distinction between on- and offshore bar movement could be obtained by the criterion:

$$\frac{H_o}{L_o} = 3.92 \cdot 10^{-5} \left[\frac{H_o}{wT} \right]^3 \tag{4}$$

The criterion is displayed in Figure 37 as the solid line. In Equation 4 the same power is obtained for H_o/wT as was noted in earlier work but the constant multiplier has a smaller value. This means that applying previous criterion on overall beach response to sand movement in the offshore produces conservative estimates regarding predictions of onshore sand transport across the bar. A reasonable prediction is also given by the simple criterion $H_o/wT = 7.2$, where values above this threshold imply offshore bar movement and vice versa.

H_o/L_o versus H_o/D_{50} (Figure 38). These parameters were combined to yield the following predictive equation:

$$\frac{H_o}{L_o} = 4.5 \cdot 10^{9} \left[\frac{H_o}{D_{50}} \right]^{-3} \tag{5}$$

A threshold value of $H_o/D_{50} = 6{,}400$ also provided an acceptable division between onshore and offshore bar movement. Note that Equation 5 is sensitive to the representative grain size.

H_o/wT versus $w/(gH_o)^{1/2}$ (Figure 39). The predictive equation was expressed as:

$$\frac{H_o}{wT} = 2.34 \cdot 10^{5} \left[\frac{w}{\sqrt{gH_o}} \right]^2 \tag{6}$$

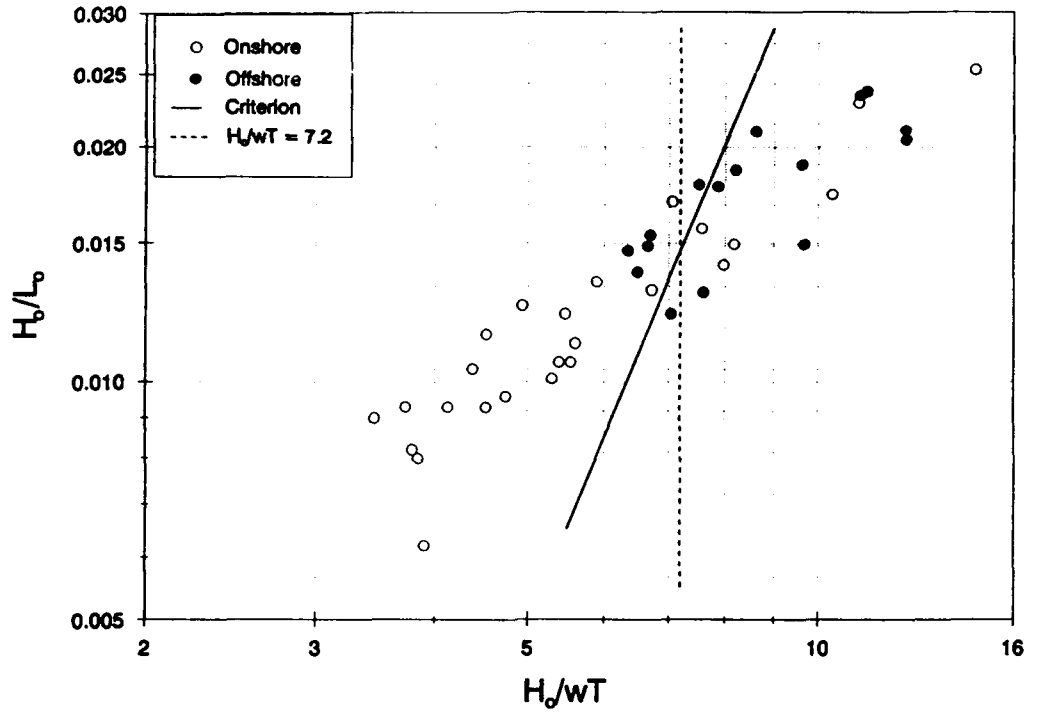

Figure 37. Prediction of cross-shore movement of inner bar using H_o/wT and H_o/L_o

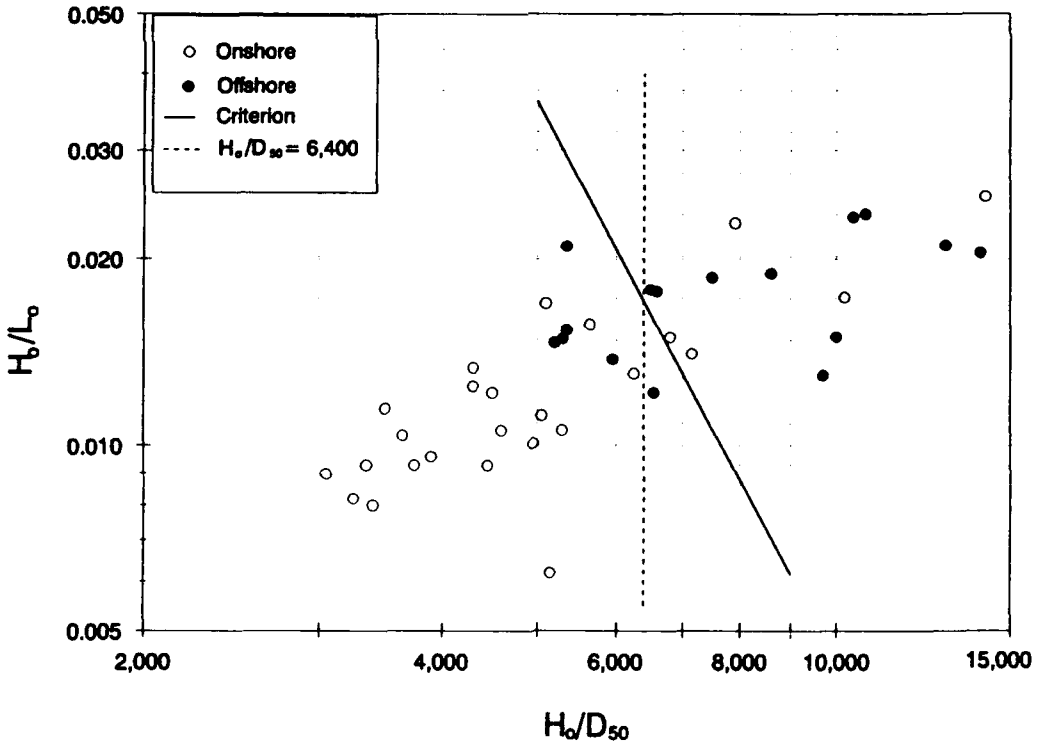

Figure 38. Prediction of cross-shore movement of inner bar using H_o/D_{50} and H_o/L_o

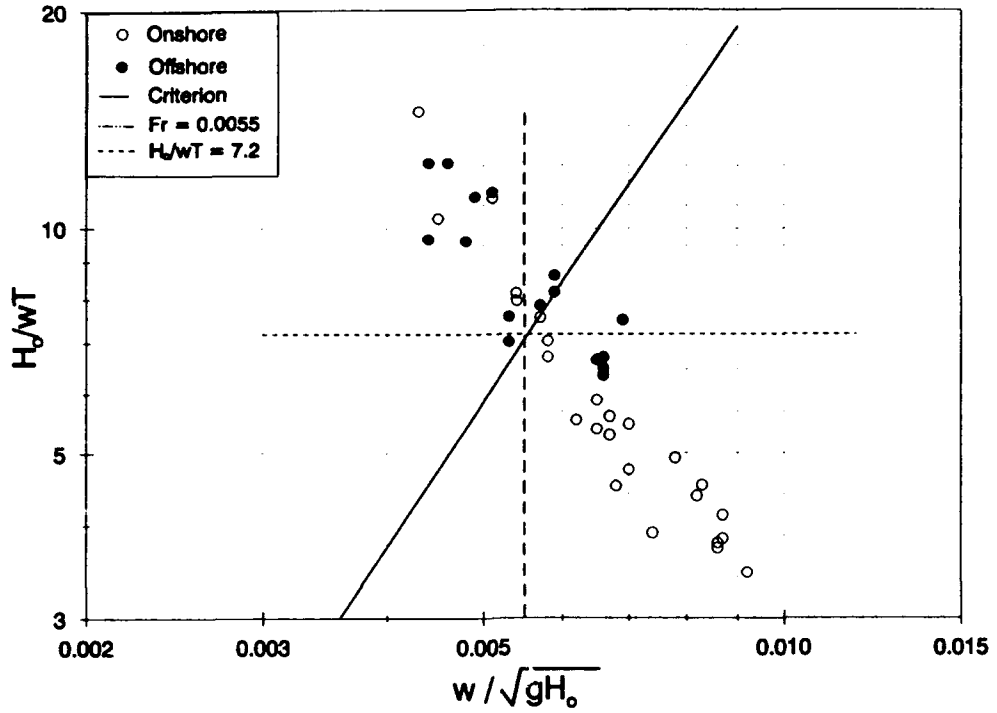

Figure 39. Prediction of cross-shore movement of inner bar using $w/(gH_o)^{1/2}$ and H_o/wT

The two parameters in this criterion may be obtained from the parameters in Equation 4 (Kraus, Larson, and Kriebel 1991). However, the form of Equation 6 is somewhat more convenient because the wave height appears inversely in the respective parameters, implying that a more distinct separation of accretionary and erosional events might be achieved. As in the case of Equation 4, a reasonable separation is given by $H_o/wT = 7.2$ and, similarly, $w/(gH_o)^{1/2} = 0.0055$ provides a simple criterion.

107. The above-discussed criteria approximately distinguished accretionary and erosional events, although several points fell on the wrong side of the dividing line, in particular one event with the largest value on H_o/wT. However, closer inspection of the conditions during this event showed that in this case (861125 to 861205, see Appendix A), the inner bar prior to the storm event extended far offshore, but after the storm the seaward portion of the inner bar formed an outer bar. In this situation, the presently used definition of a bar from the crossings between a specific survey and the reference profile produces a long bar. The length of the bar for the survey prior to the storm causes the center of mass and volume to decrease during the storm. If instead, the inner bar crest is taken as indicator of the direction of bar movement, this event

would be classified as erosional, and thus fall on the correct (right) side of the dividing line. This example clearly illustrates the difficulties in selecting an unambiguous definition of a bar that is objective and may be efficiently implemented for automated analysis of large amounts of data.

Outer bar

108. In total, 45 occurrences of onshore or offshore movement of the outer bar were identified after the above-described data censoring had been employed, involving applying a threshold and only incorporating significant events (bar volume change and mass center movement having the same sign). Figures 40 to 42 illustrate the degree to which accretionary and erosional events are distinguished by different combinations of the dimensionless parameters for the outer bar. Also, the different criteria for predicting on- and offshore transport are displayed in the figures.

109. The same parameter combinations used in predicting the movement of the inner bar were found to provide a satisfactory distinction between accretionary and erosional events for the outer bar. Furthermore, the criterion derived for the inner bar also proved to give acceptable results for the outer bar; that is, Equations 4 to 6 are also applicable for determining the direction of movement of the outer bar.

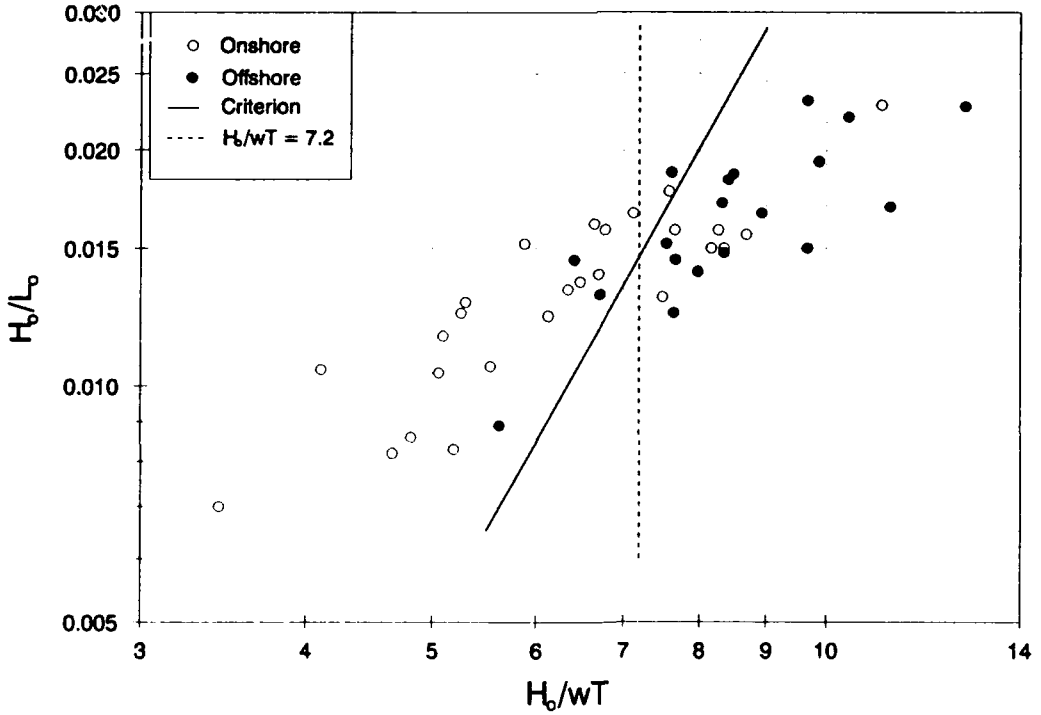

Figure 40. Prediction of cross-shore movement of outer bar using H_o/wT and H_o/L_o

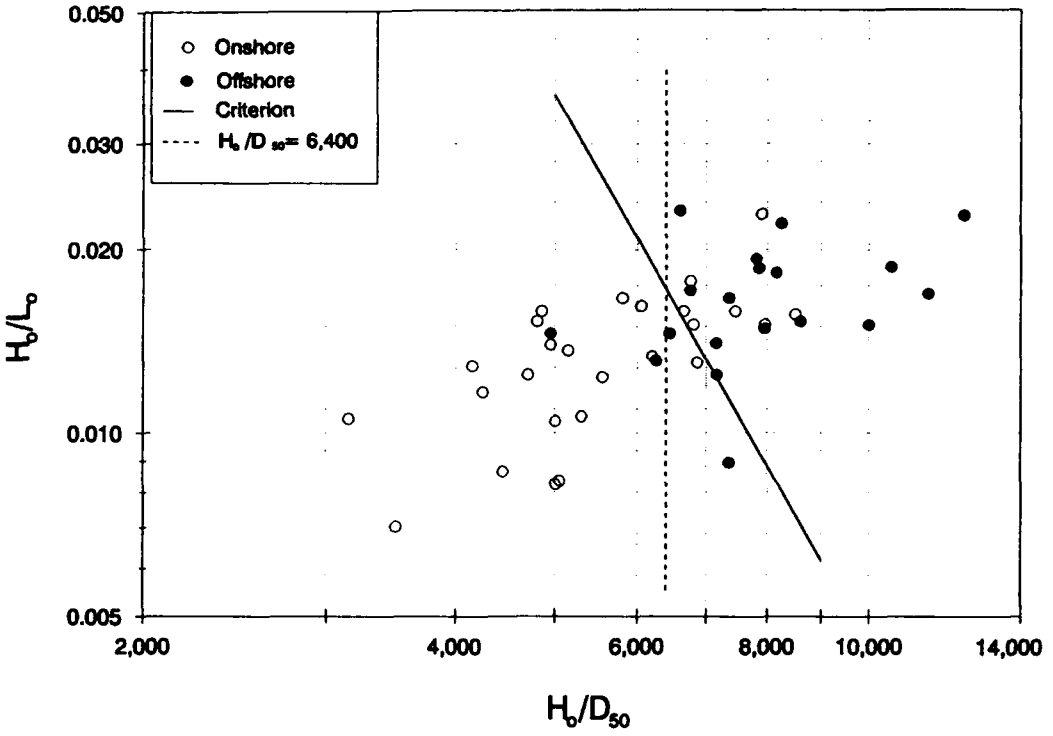

Figure 41. Prediction of cross-shore movement of outer bar using H_o/D_{50} and H_o/L_o

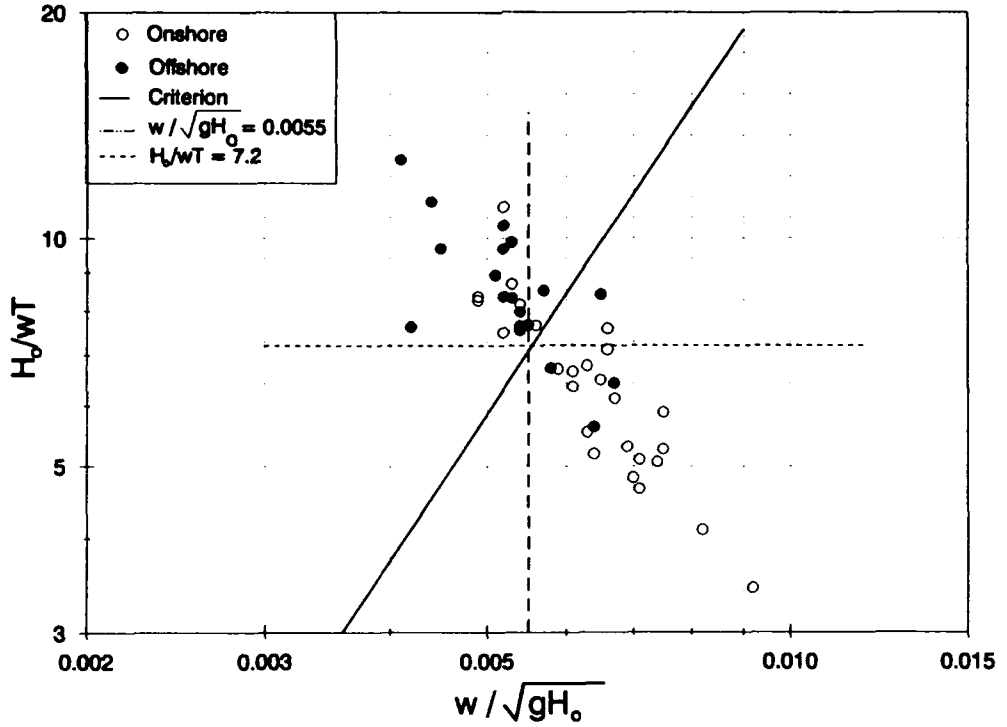

Figure 42. Prediction of cross-shore movement of outer bar using $w/(gH_o)^{1/2}$ and H_o/wT

110. As previously mentioned, the non-dimensional parameters appearing in the criteria are the same as those used in other studies by the authors focusing on the direction of cross-shore transport. Larson and Kraus (1989) and Kraus, Larson, and Kriebel (1991) developed criteria to predict whether a beach eroded or accreted under the action of incident short-period waves. These criteria were directed towards determining the overall response of the beach nearshore, with focus on the response of the foreshore. However, these types of criteria are intimately linked to bar response criteria because the bar typically moves offshore during storms when the foreshore is eroded.

111. The parameters and their exponents in the predictive equations derived in this study were the same as in previous studies examining beach change, with only the values of the empirical multipliers being different. The multipliers in Equations 4 to 6 differed significantly from the corresponding values reported by Larson and Kraus (1989) and Kraus, Larson, and Kriebel (1991), and instead of 0.00027, $3.22 \cdot 10^{8}$, and 29,900, the values of $3.92 \cdot 10^{-5}$, $4.5 \cdot 10^{9}$, and $2.34 \cdot 10^{5}$ were determined, respectively. The change in coefficient values shifts the dividing line(s) toward the erosion side of the diagrams, implying that a bar or mound will move onshore under wave conditions that would be predicted to be erosional using previously developed criteria. There are several possible explanations for the difference in the values of the empirical multiplier:

a. Use of characteristic wave quantities. The previously developed criteria typically used wave quantities based on a specific event and not an average over a significant period of time between profile surveys. The averaging was done with respect to all measurements performed between surveys, with a possible bias towards larger waves, underestimating the influence of the large number of small waves present. All these smaller waves occurring in between the surveys would tend to build up the beach, and thus cause the beach to accrete for a mean wave height that is larger than in the case of a single event.

b. Effect of non-breaking waves. In the criteria for bar movement, events are included where the bar was not exposed to wave breaking; non-breaking waves acted across the bar, and the incident waves broke closer to shore. Criteria developed for the overall response of the beach typically focus on beach evolution in the surf zone, where wave breaking prevails. The tendency for material to be transported onshore is much greater under the action of non-breaking waves in comparison with breaking waves. Thus, in the present analysis the bar may move onshore under waves that were erosive closer to shore but produced onshore transport in deeper water seaward of the break point.

PART VII: NEARSHORE BERM AT SILVER STRAND, CALIFORNIA

Nearshore Placement Berm

112. During December 1988, material dredged from the entrance channel to San Diego Harbor was placed in the form of a rectangular berm off Silver Strand State Park as a means of nourishing the beach (Juhnke, Mitchell, and Piszker 1989; Andrassy 1991). Figure 43 displays the location of the entrance channel and the placement site, which was situated about 7.5 km southwest of the dredging area. The dimensions of the berm were approximately 360 m alongshore and 180 m across shore, with an average relief of about 2 m. Approximately 110,000 cu m of dredged material were placed between a water depth of 3 and 9 m (Andrassy 1991). This amount includes material from suppiementary dredging carried out in the beginning of January to clear selected small areas within the entrance channel.

113. The native material at the placement site consisted primarily of well-sorted fine to medium sand down to a water depth of about 5.5 m Mean Lower Low Water (MLLW), and seaward of this depth fine-grained silty sand dominated (US Army Corps of Engineers (USACE) 1990). The median grain size for the fill was about 0.2 mm (Andrassy 1991), which was somewhat finer than the native material (0.25 mm according to Juhnke, Mitchell, and Piszker 1989) along the portion of the profile where the dredged material was placed.

114. The response of the berm was monitored through periodic surveying along eight profile lines, of which five lines covered the initial location of the berm, and three lines were located alongshore beyond this location (see Figure 43). Nine bathymetric surveys were carried out along these lines except for the profile line located north of the berm for which only three surveys were made (this line was added later to the original survey program). The profile lines were surveyed before and after the placement of the dredged material and then on seven different occasions (another survey was conducted in the beginning of November 1990 that was not available at the time of the present analysis). The time interval between post-construction surveys ranged from 1 and 3 months. All depths given in this report regarding the surveys at Silver Strand are referenced with respect to MLLW, and the difference between MSL and MLLW at Silver Strand is 0.85 m.

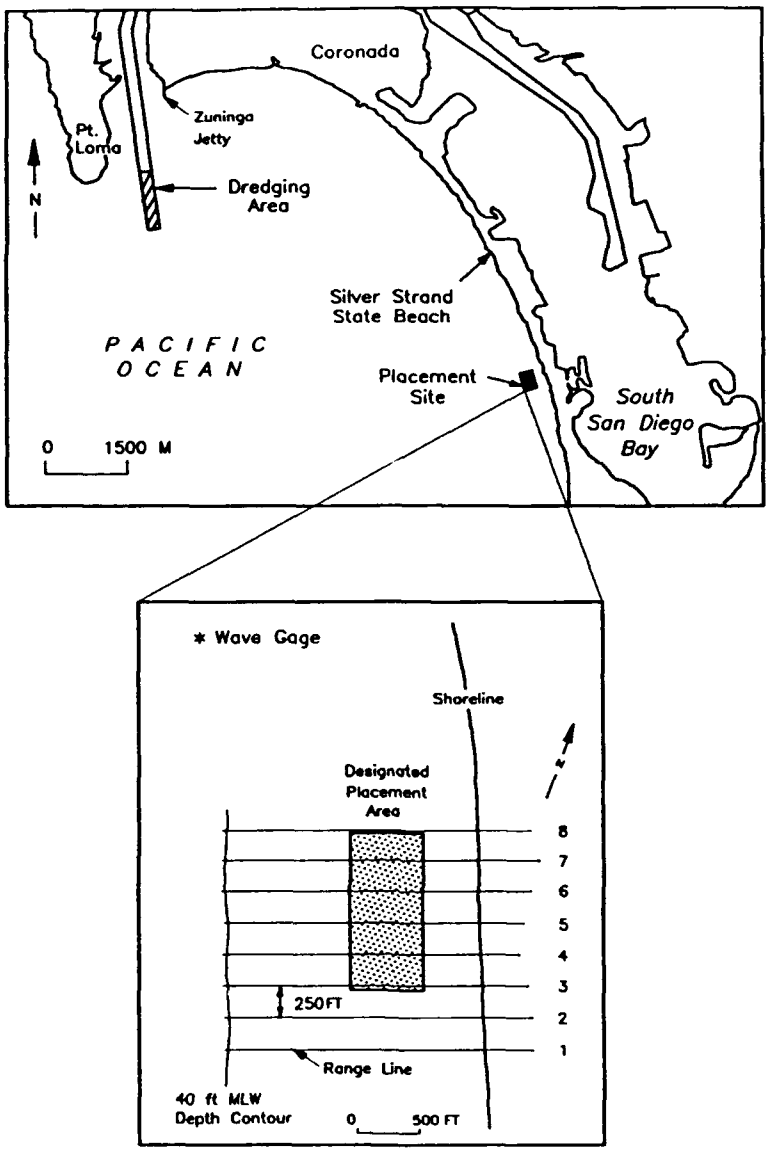

Figure 43. Location map for the Silver Strand, California, site

115. Waves were recorded by means of a pressure-current-type directional wave gage - located in about the 10-m water depth (MLLW), located less than 500 m north northeast of the placement site. Wave measurements were taken between January and May 1989, covering a time period for which four of the post-construction surveys were made. The wave spectrum was recorded every 3 hr, and the energy-based significant wave height and peak spectral period were determined from the spectrum.

Profile Response

116. In order to quantify the effects of the placed berm on the profile evolution at Silver Strand, it was necessary to derive a representative profile to which profile change could be referred. The analysis of nearshore bar movement at Duck described in Parts IV and V was carried out with respect to a modified equilibrium profile that was least-square fitted through an average profile based on all conducted surveys. The same method was employed for the profile data from Silver Strand; however, in this case the representative profile had to be determined from only the pre-construction survey. Thus, special care was taken in the least-square fitting process because the single profile used for obtaining a representative profile contained short-term features that were functions of the wave climate preceding the survey. Furthermore, the pre-construction surveys along the profile lines covering the initial location of the placement site did not record purely natural conditions in that some dredged material had been placed prior to these surveys.

117. Figure 44 plots the fit of the modified equilibrium profile to the pre-construction profile surveyed along Line 5, which was located approximately in the middle of the berm (see Figure 43). A clear berm is already apparent, partly formed by early placement of dredged material, but also because a nearshore bar-type feature existed in this region prior to construction of the berm. This nearshore feature is more easily visualized by examining the pre-construction survey for profile Line 1 located south of the placement site. Figure 45 shows this survey together with the modified equilibrium profile. Note that Figures 44 and 45 display different locations of the shoreline, the shift primarily caused by different origins for the cross-shore distance in the surveying (about a 30-m difference between Lines 1 and 5).

118. The parameter values in the modified equilibrium profile equation (Equation 3) were determined by fitting the equation to the surveyed points shoreward and seaward of the nearshore feature. The obtained values were $A_* = 0.067$ m$^{1/3}$, $D_o/D_\infty = 7.5$, and $\lambda = 0.003$ m^{-1}, which give a median grain size at the shoreline of 1.3 mm and in the offshore of 0.15 mm according to Moore (1982) (see also Kriebel, Kraus, and Larson 1991). The grain size near the shoreline seems to be somewhat high, but is needed to replicate the steep profile observed in the nearshore, whereas in the offshore the predicted grain size is more in agreement with the field measurements.

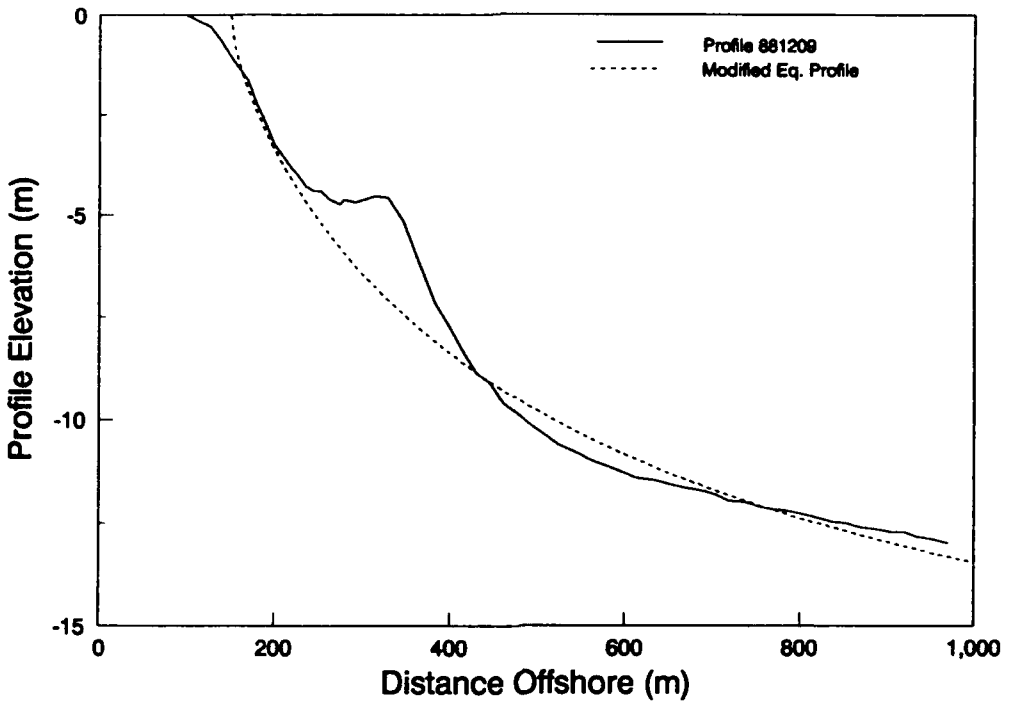

Figure 44. Modified equilibrium profile and post-placement profile survey Line 5

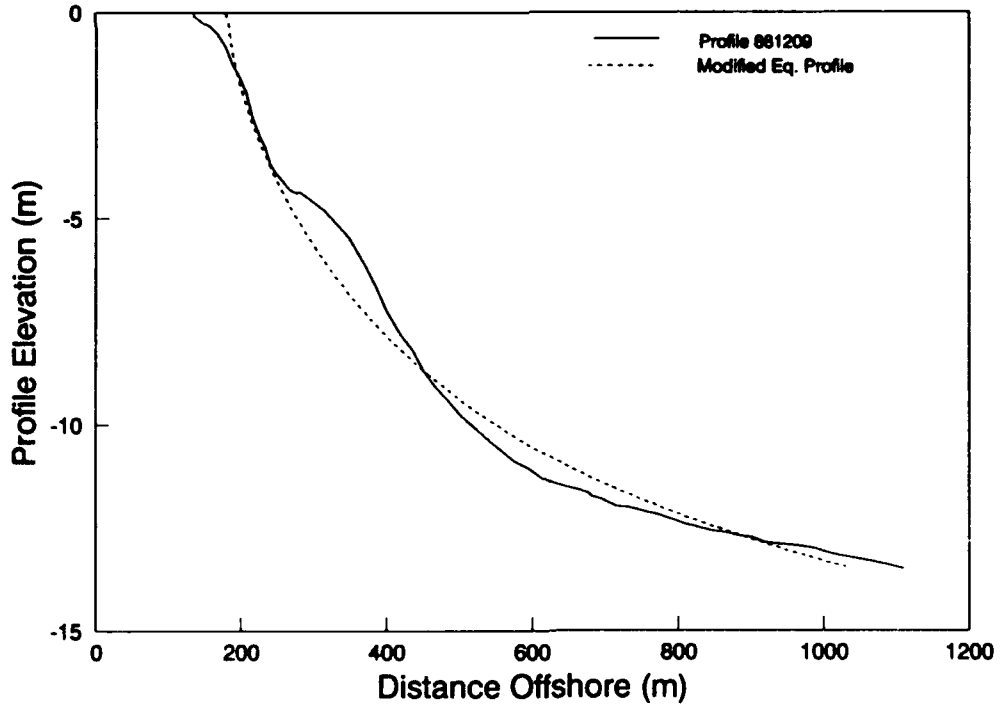

Figure 45. Modified equilibrium profile and pre-placement profile survey Line 1

119. The properties of the nearshore berm were determined in the same manner as for the inner and outer bars at Duck. The extent of the berm was defined with respect to the derived modified equilibrium profile, and the berm properties calculated for the different surveys were volume, maximum height, length, and mass center location. Only results from the analysis of profile Line 5 are shown here because all survey lines located across the berm displayed similar behavior (USACE 1990). Also, Line 5 was located approximately in the middle of the berm where end effects caused by longshore transport should have been minimal (compare Andrassy 1991). The analysis of profile change was made under the assumption that cross-shore transport dominated for the time period investigated and that longshore transport was negligible.

120. The calculated volume and maximum height of the berm with respect to the reference profile are shown in Figure 46 for the different surveys along profile Line 5, where time is given in days after the pre-construction survey carried out on 881209. Initially, the berm grew rapidly because the placement of dredged material continued until the beginning of January

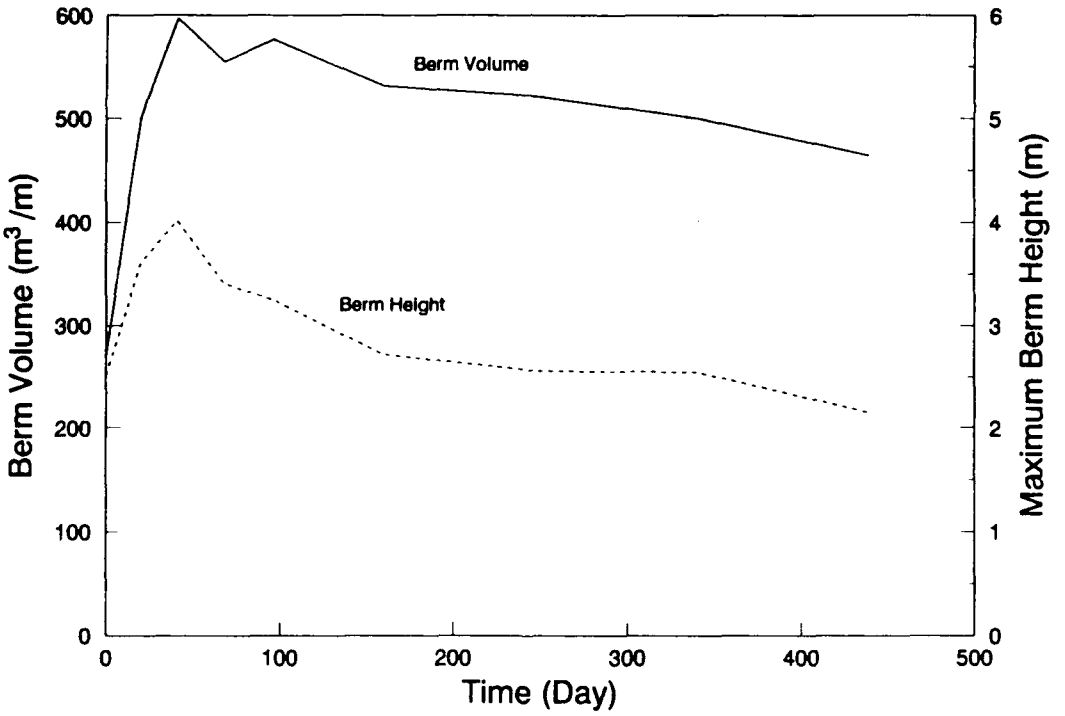

Figure 46. Berm volume and height with respect to reference profile

1989, but thereafter the volume and the maximum height decreased as the berm flattened out and material was transported onshore. Simultaneously, the center of mass was displaced shoreward, whereas the length of the berm showed an increase at first followed by a slight decrease. However, the onshore center of mass movement was less marked than, for example, the decrease in maximum height, especially in the beginning of the survey period, indicating that the berm was primarily flattened out during this period. During the period when wave measurements were made (January to May 1989), the mass center moved about 10 m onshore, and the maximum berm height decreased almost 1 m, more than 25 percent of its height. The maximum calculated berm volume with respect to the reference profile was about 600 m^3/m along Line 5, which includes the volume of the nearshore feature that was present along the profile before placement of the dredged material occurred.

121. Andrassy (1991) computed the volume of sand in three different depth zones (+3 to 0 m, 0 to -3 m, and -3 to -10 m MLLW) with respect to the pre-construction profiles and noted a distinct shoreward transport of material from the most seaward zone to the two more shoreward zones. Thus, it is evident that the flattening and onshore movement of the berm contributed to the accumulation of material along the inner portion of the profile. The dredged material was placed in a profile region where a natural nearshore feature already existed, thus increasing the possibility for onshore transport and profile nourishment for material placed under favorable wave conditions.

Relationship Between Wave and Bar Properties

122. Wave measurements were made in the vicinity of the berm between January and May 1989, as previously discussed. This time period encompassed four profile surveys, giving only a limited number of cases for relating the profile response to the wave characteristics. The same wave properties were calculated as for the data from Duck, including mean and maximum significant wave height, mean and maximum peak spectral wave period, mean and maximum wave steepness, and mean fall speed. Unrefracted deepwater quantities were computed in order to compare them with the results of the analysis from Duck, and all wave properties referred to here pertain to deep water.

123. The mean significant wave height for the measurement period was 0.62 m, the corresponding mean spectral peak period was 13.1 sec, and the maximum significant wave height recorded was 1.67 m. Thus, the wave climate was quite mild during the measurement period, which tended to promote the onshore transport of material on the berm. The dimensionless quantities calculated also indicated low-energy wave conditions with $(H_o/L_o)_{mean} = 0.0035$, $(H_o/wT)_{mean} = 2.3$, and $(H_o/L_o)_{max} = 0.026$. The fall speed was calculated based on a grain size of 0.2 mm for an estimated mean monthly water temperature of 15 °C.

124. Based on the results of the Duck data analysis of direction of cross-shore sand transport (Part VI) by natural waves, the value of the mean fall speed parameter during the measurement period predicts onshore transport. The nearshore berm constructed at Silver Strand exhibited this response by flattening and moving onshore simultaneously as material accumulated on the foreshore. Figure 47 shows the four profile surveys carried out during the period when wave measurements were taken, together with the modified equilibrium profile to which the berm response was referred. A distinct onshore transport of material between the surveys is noted through the lowering of the maximum berm height and the increase of material in the inshore portion of the profile.

125. The mean fall speed parameter, based on the measured wave properties preceding a specific survey, took on the values 2.6, 2.3, and 2.2 for the three intermediate time periods shown in Figure 47, respectively. These values are considerably less than 7.2 determined from the Duck data as a value distinguishing conditions favorable to onshore and offshore transport. Thus, the criteria developed from the analysis of the response of nearshore bars at Duck would predict onshore movement of the berm in agreement with the measurements from Silver Strand, indicating consistency of results between both coasts for the particular data sets.

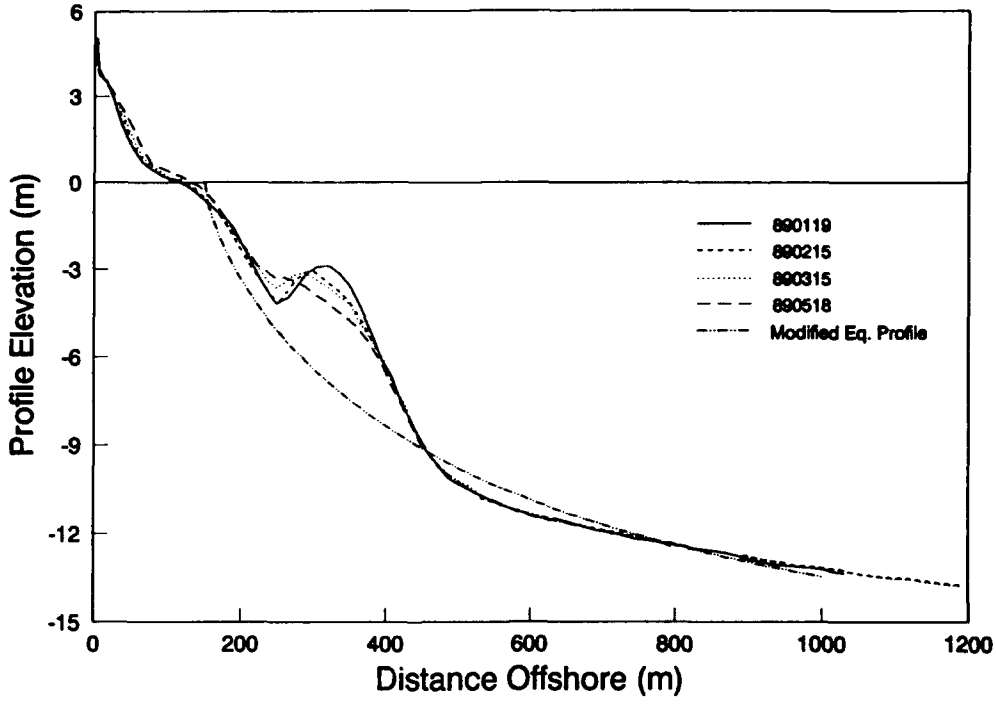

Figure 47. Onshore translation of the placed berm

PART VIII: SUMMARY AND CONCLUSIONS

126. Repetitive, high-accuracy beach profile surveys made at the FRF located at Duck, North Carolina, were analyzed to determine the properties of natural longshore bars and their response to the wave climate. Profiles were surveyed along four shore-normal lines at approximately bi-weekly intervals from 1981 to 1989, and the associated waves were recorded with a time resolution of at least 6 hr. In total, between 200 and 300 measured profiles were available from the survey lines. By determining the properties of natural longshore bars and how they interact with the prevailing wave climate, the reliability of predicting the behavior of artificial bars or nearshore berms created by placing dredged material in the nearshore should increase. Beach nourishment through nearshore placement of dredged material is a desirable technique, but presently available engineering methods are limited for predicting the response of such berms to nearshore waves and where the material is transported by the waves.

127. To investigate if the surveyed profiles at the FRF exhibited long-term trends, the time variation of subaerial and subaqueous sand volumes above specific contours was evaluated. The movement of contours with time was calculated for the same purpose. The subaerial volume calculations showed a net long-term increase in the volume above NGVD, particularly for the survey lines north of the pier, indicating accretion of sand in the dune region. However, the subaqueous volume was approximately constant over the measurement period, although considerable short-term fluctuations were encountered. The calculated average profile shapes for the different survey lines were very similar, but the two survey lines south of the FRF pier had a shoreline position somewhat closer to the FRF baseline. In summary, the analysis of long-term variation in volume and contour location indicated that the beach at the FRF accreted slightly above NGVD, with little systematic change below NGVD.

128. Because of the similar behavior of the profile on the four survey lines, and to decrease the great amount of effort involved in the analysis, only one line was used in the analysis of bar properties (Line 62). The chosen line encompassed the largest number of individual surveys and displayed the closest response in bar evolution. To determine the bar properties, a reference profile was developed by fitting a modified equilibrium profile to the average profile taking into account a varying grain size across shore. The studied bar properties were:

a. Depth to bar crest.

b. Maximum bar height.

c. Bar volume.

d. Bar length.

e. Location of bar mass center.

f. Speed of bar movement.

Also, the characteristic time scales of bar movement were established using the box-counting method.

129. For the nearshore profile at the FRF, two bars were typically present, one located about 100 m from the mean shoreline (inner bar) and the other located about 300 m from the shoreline (outer bar). These two bar features were analyzed separately because they displayed different behavior with respect to the time evolution and response to the waves. The inner bar was often exposed to breaking waves, and thus large cross-shore sand transport, whereas the outer bar only experienced wave breaking during severe storms.

130. The average depth to crest for the inner bar was 1.6 m, the average maximum bar height was 0.9 m, and the average bar volume was 42 m^3/m. Comparison between inner bar properties from the surveys at the FRF and results from experiments carried out in large wave tanks indicated similar behavior of the bar in the laboratory and in the field. Thus, data from large wave tanks should be of considerable value for investigating the fundamentals of cross-shore transport and bar movement. The average speed of the inner bar was 1.5 m/day for onshore movement and 2.9 m/day for offshore movement, with maximum recorded speeds of 8.7 m/day and 18 m/day, respectively. Box-counting analysis showed that the typical maximum duration between wave conditions that moved the inner bar offshore was about 2 months.

131. The average depth to crest for the outer bar was 3.8 m, the average maximum bar height was 0.4 m, and the average bar volume was 45 m^3/m. Although the outer bar on the average had a volume similar to the inner bar, the maximum height was considerably lower, producing a much more gentle bar shape. The average speed of the outer bar was 0.6 m/day for onshore and 1.1 m/day for offshore movement, with maximum recorded speeds of 6.1 m/day and 15.2 m/day, respectively. Box-counting analysis showed that the typical maximum duration between wave conditions that moved the outer bar offshore was about 4 months.

132. Extensive correlation analysis between bar and wave properties was carried out to determine the linear dependence between the properties, and possibly establish simple predictive relationships for engineering applications. Mean wave properties were employed and different non-dimensional parameters such as wave steepness and dimensionless fall speed were formed to achieve greater generality in the obtained results. In most of the analysis, deepwater quantities were used, derived by shoaling waves to deep water from the measurement depth, neglecting refraction. The grand average of the significant wave height at the FRF was 1.1 m, and the average peak spectral period was 8.4 sec at the gage depth of 18 m.

133. As expected, significant correlation was found between several of the geometric bar properties such as volume versus height, volume versus length, and depth to crest versus distance to mass center, both for the inner and outer bar. The correlation is a consequence of the fact that as a bar moves offshore its size increases with a corresponding increase in volume, height, and length. To arrive at significant correlation between bar and wave properties, threshold values had to be employed to only include events with marked profile change. After this data screening, correlations could be obtained, for example, between $h_c / (H_o)_{max}$ and $(H_o / L_o)_{mean}$, and change in volume $\Delta V_b / H_o^2$ and $(H_o / wT)_{mean}$ for the inner bar, and similar results could be derived for the outer bar.

134. The typical time interval of 10 days between surveys made it difficult to determine appropriate wave properties for use in the analysis. In the present study, mean quantities were employed as the characteristic measure, although considerable variability in the wave conditions occurred between profile surveys. Regression relationships were derived for some combinations of bar and wave properties but the coefficient of determination was too low to be significant. Thus, the results of the correlation and regression analysis were mostly of a qualitative nature.

135. Several different criteria were derived to determine onshore and offshore movement of the inner and outer bar. To determine the direction of bar movement, and thus the net direction of the sand transport across the bar, both change in bar volume and change in the location of bar mass center were employed. Furthermore, a threshold value was applied to include only events with a marked profile change. The criteria were expressed in terms of non-dimensional parameters characterizing wave and profile properties, where the wave properties referred to deepwater conditions.

136. The following non-dimensional parameter combinations were evaluated with respect to separating onshore and offshore bar movement:

a. H_o/L_o versus H_o/wT.

b. H_o/L_o versus H_o/D_{50}.

c. H_o/wT versus $w(gH_o)^{1/2}$.

The dividing line that best separated points corresponding to onshore and offshore bar movement was subjectively drawn in the respective diagrams for the parameter-pair combinations, and empirical coefficient values were established. Similar relationships were obtained as previously derived for beach erosion and accretion predictors, but the empirical multiplier was different. The dividing lines were displaced towards erosion for the criteria describing onshore and offshore bar movement in comparison with the criteria for beach erosion or accretion.

137. The criteria summarized above that were developed through analysis of natural longshore bars on an east-coast beach were applied to predict the movement of a longshore bar-like feature or "nearshore berm" constructed of mainly littoral material dredged from the entrance to San Diego Harbor, California. Bathymetric surveys of the berm made during a 5-month period when a wave gage operated at the site indicated onshore movement of the berm, in agreement with unambiguous predictions of the criterion. Although not serving as conclusive validation, the agreement suggests that the criteria for predicting the direction of cross-shore movement of bars and placed berms based on readily available or estimated information in coastal studies may have generality for all coasts exposed to energetic waves.

REFERENCES

Andrassy, C. J. 1991. "Monitoring of a Nearshore Disposal Mound at Silver Strand State Park," *Proceedings Coastal Sediments '91*, American Society of Civil Engineers, pp 1970-1984.

Birkemeier, W. A. 1985. "Field Data on the Seaward Limit of Profile Change," *Journal of Waterway, Port, Coastal, and Ocean Engineering*, Vol 111, No. 3, pp 598-602.

Birkemeier, W. A., and Mason, C. 1984. "The CRAB: A Unique Nearshore Research Vehicle," *Journal of Surveying Engineering*, Vol 110, No. 1, pp 1-7.

Birkemeier, W. A., Miller, H. C., Wilhelm, S. D., DeWall, A. E., and Gorbics, C. S. 1985. "A User's Guide to the Coastal Engineering Research Center's (CERC's) Field Research Facility," Instruction Report CERC-85-1, Coastal Engineering Research Center, US Army Engineer Waterways Experiment Station, Vicksburg, MS.

Bruun, P. 1954. "Coast Erosion and the Developments of Beach Profiles," Technical Memorandum No. 44, Beach Erosion Board, Coastal Engineering Research Center, US Army Engineer Waterways Experiment Station, Vicksburg, MS.

Dean, R. G. 1977. "Equilibrium Beach Profiles: U.S. Atlantic and the Gulf Coasts," Ocean Engineering Report No. 12, Department of Civil Engineering, University of Delaware, Newark, DE.

_____. 1987. "Coastal Sediment Processes: Toward Engineering Solutions," *Proceedings of Coastal Sediments '87*, American Society of Civil Engineers, pp 1-24.

Foster, G. A., Healy, T. R., and de Lange, W. P. 1991. "Predictions of Sediment Movement From a Spoil Dump at Mount Maunaganui Beach," Proceedings of 10th Australasian Conference on Coastal and Ocean Engineering, Water Quality Publication No. 21, Hamilton, New Zealand, pp 505-510.

Gravens, M. B., Kraus, N. C., and Hanson, H. 1991. "GENESIS: Generalized Model for Simulating Shoreline Change," Report 2: Workbook and System User's Manual, Technical Report CERC-89-19, Coastal Engineering Research Center, US Army Engineer Waterways Experiment Station, Vicksburg, MS.

Hallermeier, R. J. 1978. "Uses for a Calculated Limit Depth to Beach Erosion," *Proceedings of the 16th Conference on Coastal Engineering*, American Society of Civil Engineers, pp 1493-1512.

Hands, E. B., and Allison, M. C. 1991. "Mound Migration in Deeper Water and Methods of Categorizing Active and Stable Berms," *Proceedings of Coastal Sediments '91*, American Society of Civil Engineers, pp 1985-1999.

Hanson, H., and Kraus, N. C. 1989. "GENESIS: Generalized Model for Simulating Shoreline Change," Report 1: Technical Reference, Technical Report CERC-89-19, Coastal Engineering Research Center, US Army Engineer Waterways Experiment Station, Vicksburg, MS.

Hentschel, H. G. E., and Procaccia, I. 1983. "Relative Diffusion in Turbulent Media: The Fractal Dimension of Clouds," *Physics Review*, Vol A29, pp 1461-1470.

Hom-ma, M., and Sonu, C. J. 1962. "Rhythmic Pattern of Longshore Bars Related with Sediment Characteristics," *Proceedings 8th Coastal Engineering Conference*, American Society of Civil Engineers, pp 248-278.

Howd, P. A., and Birkemeier, W. A. 1987a. "Beach and Nearshore Survey Data: 1981-1984 CERC Field Research Facility," Technical Report CERC-87-9, Coastal Engineering Research Center, US Army Engineer Waterways Experiment Station, Vicksburg, MS.

_____. 1987b. "Storm-Induced Morphology Changes During DUCK85," *Proceedings Coastal Sediments '87*, American Society of Civil Engineers, pp 834-847.

Juhnke, L., Mitchell, T., and Piszker, M. J. 1989. "Construction and Monitoring of Nearshore Disposal of Dredged Material at Silver Strand State Park, San Diego, California," *Proceedings of the 22nd Dredging Seminar*, Texas Engineering Experiment Station, CDS Report No. 317, pp 203-217.

Kajima, R., Shimizu, T., Maruyama, K., and Saito, S. 1982. "Experiments of Beach Profile Change with a Large Wave Flume," *Proceedings of the 18th Coastal Engineering Conference*, American Society of Civil Engineers, pp 1385-1404.

Keulegan, G. H. 1945. "Depths of Offshore Bars," Engineering Notes No. 8, Beach Erosion Board, Coastal Engineering Research Center, US Army Engineer Waterways Experiment Station, Vicksburg, MS.

_____. 1948. "An Experimental Study of Submarine Sand Bars," Technical Report No. 8, Beach Erosion Board, Coastal Engineering Research Center, US Army Engineer Waterways Experiment Station, Vicksburg, MS.

Kraus, N. C., and Larson, M. 1988. "Beach Profile Change Measured in the Tank for Large Waves, 1956-1957 and 1962," Technical Report CERC-88-6, Coastal Engineering Research Center, US Army Engineer Waterways Experiment Station, Vicksburg, MS.

Kraus, N. C., Gingerich, K. J., and Rosati, J. D. 1989. "Duck85 Surf Zone Sand Transport Experiment," Technical Report CERC-89-5, Coastal Engineering Research Center, US Army Engineer Waterways Experiment Station, Vicksburg, MS.

Kraus, N. C., Larson, M., and Kriebel, D. L. 1991. "Evaluation of Beach Erosion and Accretion Predictors," *Proceedings of Coastal Sediments '91*, American Society of Civil Engineers, pp 572-587.

Kriebel, D. L., Kraus, N. C., and Larson, M. 1991. "Engineering Methods for Predicting Beach Profile Response," *Proceedings of Coastal Sediments '91*, American Society of Civil Engineers, pp 557-571.

Larson, M. 1991. "Equilibrium Profile of a Beach with Varying Grain Size," *Proceedings of Coastal Sediments '91*, American Society of Civil Engineers, pp 905-919.

Larson, M., and Kraus, N. C. 1989. "SBEACH: Numerical Model for Simulating Storm-Induced Beach Change, Report 1: Theory and Model Foundation," Technical Report CERC-89-9, Coastal Engineering Research Center, US Army Engineer Waterways Experiment Station, Vicksburg, MS.

Larson, M., Kraus, N. C., and Sunamura, T. 1988. "Beach Profile Change: Morphology, Transport Rate, and Numerical Simulation," *Proceedings of the 21st Coastal Engineering Conference*, American Society of Civil Engineers, pp 1295-1309.

Lippman, T. C., and Holman, R. A. 1990. "The Spatial and Temporal Variability of Sand Bar Morphology," *Journal of Geophysical Research*, Vol. 95, No. C7, pp 11,575-11,590.

Mason, C., Birkemeier, W. A., and Howd, P. A. 1987. "Overview of Duck85 Nearshore Processes Experiment," *Proceedings of Coastal Sediments '87, American Society of Civil Engineers*, pp 818-833.

McLellan, T. N. 1990. "Nearshore Mound Construction Using Dredged Material," *Journal of Coastal Research*, Vol 7, pp 99-107.

McLellan, T. N., and Kraus, N. C. 1991. "Design Guidance for Nearshore Berm Construction," *Proceedings of Coastal Sediments '91*, American Society of Civil Engineers, pp 2000-2011.

Moore, B. D. 1982. "Beach Profile Evolution in Response to Changes in Water Level and Wave Height," unpublished M.S. thesis, Department of Civil Engineering, University of Delaware, Newark, DE.

Sallenger, A. S., Holman, R. A., and Birkemeier, W. A. 1985. "Storm-Induced Response of a Nearshore-Bar System," *Marine Geology*, Vol 64, pp 237-257.

Saville, T. 1957. "Scale Effects in Two Dimensional Beach Studies," *Transactions from the 7th General Meeting of the International Association of Hydraulic Research*, Vol 1, pp A3.1-A3.10.

Smith, A. W., and Jackson, L. A. 1990. "The Siting of Beach Nourishment Placements," *Shore and Beach*, Vol 58, No. 1, pp 17-24.

Sunamura, T., and Maruyama, K. 1987. "Wave-Induced Geomorphic Response of Eroding Beaches - With Special Reference to Seaward Migrating Bars -," *Proceedings of Coastal Sediments '87*, American Society of Civil Engineers, pp 788-801.

USACE. 1990. "Monitoring of a Nearshore Dredged Material Disposal Berm at Silver Strand State Park, San Diego, California," US Army Corps of Engineers, Los Angeles District, Los Angeles, California.

Wright, L. D., Boon, J. D., Kim, S. C., and List, J. H. 1991. "Modes of Cross-Shore Sediment Transport on the Shoreface of the Middle Atlantic Bight," *Marine Geology*, Vol 96, pp 19-51.

APPENDIX A: CALCULATED INNER BAR PROPERTIES

Date	Time	x_{start} m	x_{end} m	h_c m	z_m m	V_b m^3/m	l_b m	x_{cg} m
810126	850	191.0	270.4	1.58	1.00	49.2	79.4	224.1
810210	900	186.9	279.1	2.10	0.65	36.4	92.1	231.1
810224	1540	225.3	299.4	2.35	0.62	28.3	74.1	256.3
810310	1440	246.5	329.1	2.29	1.12	55.4	82.6	287.0
810325	1555	242.0	340.7	2.19	1.20	63.1	98.7	286.9
810406	1030	239.8	322.5	2.04	1.12	41.3	82.6	272.8
810415	1245	230.6	330.5	2.26	0.86	48.0	99.9	273.1
810427	1400	231.1	325.9	2.01	1.08	52.2	94.8	266.3
810511	1300	223.3	325.7	1.65	1.28	69.8	102.4	260.9
810526	1400	207.1	309.8	1.43	1.32	69.8	102.7	243.0
810609	1245	202.7	293.9	1.74	0.88	45.8	91.2	237.0
810622	1300	196.9	293.0	1.77	0.82	45.4	96.1	233.3
810701	1200	195.5	297.2	2.04	0.82	48.1	101.7	239.8
810717	1200	197.9	292.6	1.95	0.82	40.8	94.7	237.8
810727	1100	195.3	287.0	1.86	0.77	37.7	91.6	231.7
810804	1200	190.0	284.5	1.71	0.83	43.8	94.4	226.7
810818	1400	182.8	286.2	1.65	0.73	45.8	103.4	223.1
810821	1500	180.0	287.0	2.07	0.90	49.4	107.0	242.7
810823	1100	193.1	317.6	2.13	0.95	58.9	124.5	253.4
810831	1500	195.7	309.4	1.65	1.01	60.5	113.7	240.8
810908	1200	216.3	327.5	1.83	1.11	56.7	111.1	260.1
810914	1145	211.7	313.9	1.58	1.27	57.4	102.2	249.2
810919	630	205.6	308.9	1.98	0.96	46.6	103.3	247.2
810928	1115	190.5	305.3	1.80	1.00	60.6	114.7	238.3
821007	1505	122.9	183.2	0.66	0.53	20.6	60.4	148.9
821013	1110	162.5	204.9	1.55	0.73	17.9	42.4	186.2
821014	1500	159.3	208.8	1.41	0.71	23.0	49.6	181.6
821015	1140	151.6	207.4	1.33	0.67	22.6	55.8	175.4
821016	1550	150.5	207.4	1.44	0.69	21.6	56.8	175.9
821017	1040	145.4	207.7	1.52	0.65	22.1	62.3	176.5
821019	1230	148.5	207.8	1.55	0.62	17.5	59.2	180.3
821022	1150	140.9	207.1	1.44	0.68	27.5	66.2	175.8
821027	1500	148.7	220.1	1.30	0.96	44.8	71.4	184.0
821108	1550	124.7	198.6	0.87	0.61	28.7	73.9	159.4
821206	1430	172.4	230.0	1.64	0.73	22.5	57.6	201.7
821214	1525	174.6	231.0	1.90	0.56	20.7	56.4	204.1
821222	1300	134.1	218.9	0.82	0.94	50.5	84.7	169.9
830113	1310	163.6	227.8	1.23	1.12	44.0	64.2	194.4
830124	1220	175.4	230.3	1.66	0.82	27.1	54.9	201.2
830208	1250	157.7	210.2	1.43	0.58	19.3	52.4	180.7
830224	1500	149.9	233.3	1.25	0.79	47.0	83.4	187.7
830322	1245	157.9	234.1	1.58	0.83	30.2	76.2	200.9
830328	1300	163.7	228.1	1.83	0.63	23.3	64.4	198.5
830412	1130	134.4	205.9	1.02	0.70	37.1	71.5	169.1
830505	845	156.1	204.1	1.52	0.51	14.1	47.9	177.7
830525	930	146.2	197.0	1.54	0.54	15.3	50.8	171.8
830614	900	131.8	196.8	1.00	0.75	30.7	65.0	162.2
830630	1245	132.6	193.5	1.14	0.53	22.2	60.9	162.5
830712	1610	130.3	191.0	1.05	0.66	23.2	60.8	159.2
830725	1155	119.5	187.0	0.57	0.55	27.6	67.5	149.4
830826	1230	161.4	196.3	1.90	0.35	6.0	34.9	180.8
830906	1410	163.3	197.3	1.89	0.36	6.2	34.0	181.3
830918	1240	144.3	204.8	1.14	0.80	28.4	60.5	172.8
831001	1130	178.8	223.1	1.91	0.60	15.3	44.3	202.4
831014	850	146.1	214.9	0.94	1.05	42.1	68.8	177.9
831024	1415	126.6	214.5	0.66	0.93	53.1	87.9	165.4

831107	1300	132.5	214.0	1.13	0.93	41.7	81.5	172.6
831121	836	140.7	204.5	1.12	0.82	33.7	63.8	173.2
831202	1000	132.8	202.6	0.91	0.72	35.1	69.9	164.9
831227	1415	165.6	225.4	1.49	0.71	28.9	59.9	192.4
840105	900	212.9	253.0	2.35	0.52	10.4	40.1	233.7
840117	1050	147.7	264.1	1.40	0.88	66.1	116.4	203.1
840202	1300	170.8	248.9	1.74	0.88	37.5	78.1	209.3
840209	850	165.5	241.6	1.14	1.19	49.1	76.1	200.2
840216	1145	186.5	251.2	1.77	0.75	30.4	64.8	215.3
840224	1015	183.9	246.7	1.91	0.73	24.8	62.8	214.3
840308	1025	195.0	251.9	1.80	0.96	30.7	57.0	222.5
840320	1200	210.5	273.0	2.28	0.60	27.1	62.4	242.3
840402	1405	181.5	256.7	1.97	0.65	29.0	75.2	217.8
840406	915	196.0	259.0	2.18	0.57	19.5	63.0	226.9
840413	845	200.4	262.5	2.14	0.63	21.4	62.2	231.9
840425	1330	181.6	244.2	1.87	0.49	21.0	62.6	209.5
840509	1230	179.0	235.7	1.72	0.60	20.4	56.7	201.8
840514	850	176.9	235.7	1.94	0.50	15.9	58.8	203.4
840524	1125	165.8	234.5	1.85	0.49	20.8	68.7	200.8
840601	1040	170.7	237.7	1.72	0.78	25.0	67.0	204.6
840613	1040	163.6	233.0	1.51	0.82	29.2	69.4	196.6
840628	800	164.0	225.1	1.50	0.80	23.9	61.1	193.1
840709	820	158.1	218.1	1.55	0.63	18.4	60.1	184.7
840721	1200	147.8	207.9	1.39	0.60	20.6	60.1	173.7
840727	1150	146.3	202.1	1.14	0.61	17.9	55.8	167.6
840811	800	140.9	194.8	1.11	0.54	15.2	53.8	160.9
840906	1310	118.7	183.2	0.80	0.81	23.7	64.5	153.9
840910	900	145.8	213.2	1.25	0.86	33.1	67.5	178.8
840920	1030	129.6	216.8	0.78	0.87	49.6	87.2	167.7
841002	1300	176.4	241.9	1.21	1.18	47.1	65.5	207.1
841007	1000	174.1	240.9	1.41	1.07	47.9	66.7	205.8
841016	1230	194.4	264.7	1.92	1.04	35.1	70.3	235.9
841029	1450	149.7	246.9	0.99	0.95	54.6	97.2	186.0
841127	1320	160.6	266.1	0.85	1.27	67.2	105.6	198.9
841213	1508	138.7	271.8	0.91	0.64	53.7	133.0	192.1
850105	1125	186.5	258.0	1.62	0.94	39.0	71.6	220.4
850125	1200	181.4	263.6	1.50	1.01	48.7	82.3	214.6
850214	1430	176.0	261.2	1.98	0.58	28.4	85.2	215.3
850301	1054	171.5	251.5	1.64	0.66	31.4	80.0	204.1
850315	1210	173.3	252.0	1.80	0.72	34.1	78.7	211.6
850326	1430	167.3	259.1	1.43	0.78	45.1	91.8	205.1
850423	1005	157.7	247.8	1.85	0.37	20.2	90.0	200.4
850509	1138	175.1	258.1	1.51	0.94	48.7	83.0	213.5
850531	930	166.9	247.3	1.24	1.16	51.4	80.3	203.1
850620	1059	169.7	249.9	1.78	0.96	39.7	80.2	213.4
850715	945	152.1	246.2	0.88	1.18	67.4	94.1	193.1
850719	1125	159.0	242.9	1.64	0.97	46.4	83.9	203.4
850724	1710	157.9	242.4	1.48	0.98	47.7	84.5	198.6
850807	1000	163.4	253.9	1.69	0.83	44.2	90.5	211.0
850821	735	147.8	240.4	1.61	0.83	32.3	92.6	198.5
850913	1640	142.5	229.4	1.23	1.12	54.8	86.9	190.4
850914	0	144.3	232.1	1.25	1.15	56.9	87.8	193.0
850914	730	150.8	238.8	1.18	1.23	58.5	88.0	197.4
850914	930	152.3	237.1	1.19	1.15	57.4	84.8	198.6
850914	1248	154.9	236.7	1.31	1.17	54.9	81.8	199.8
850914	1905	156.7	237.5	1.25	1.21	55.7	80.8	200.1
850915	55	156.1	239.2	1.19	1.24	57.5	83.2	199.9
850915	703	155.7	239.6	1.26	1.23	57.0	83.9	200.7
850915	1018	155.9	239.6	1.25	1.20	56.9	83.6	200.6
850915	1350	155.5	242.1	1.36	1.04	54.8	86.6	202.4
850916	915	153.2	248.1	1.40	0.98	57.3	94.9	204.2
850916	2015	150.0	257.3	1.55	0.88	58.4	107.3	207.1

850917	845	155.0	261.0	1.45	0.92	63.0	106.0	208.2
850917	1510	156.4	273.0	1.46	0.77	55.5	116.7	212.0
850918	735	167.7	262.8	1.92	0.88	40.2	95.1	223.8
850919	1250	153.4	264.0	1.74	0.71	44.0	110.7	214.8
850920	945	148.1	261.8	1.58	0.79	50.2	113.7	208.2
850925	1045	138.4	252.5	0.86	1.19	81.9	114.1	187.8
850927	1600	137.7	251.4	1.32	0.83	46.6	113.7	204.3
851015	1355	178.8	249.1	1.84	0.59	29.7	70.3	213.3
851019	945	180.2	252.7	1.77	0.81	29.5	72.5	217.3
851020	835	180.6	250.8	1.83	0.83	31.4	70.3	217.4
851021	1640	177.7	252.3	1.83	0.90	33.5	74.7	220.0
851022	1522	192.9	257.9	1.94	0.81	30.5	65.0	224.7
851023	1024	196.4	256.8	1.90	0.82	29.4	60.4	223.8
851024	1491	196.4	252.0	1.82	0.80	25.0	55.6	221.2
851106	1030	209.3	282.5	1.87	0.94	35.7	73.2	238.2
851121	820	185.1	267.7	1.70	0.74	29.0	82.6	216.7
851209	1320	225.1	483.5	2.02	1.00	88.8	258.5	311.6
851219	1330	223.2	486.0	1.80	1.37	97.8	262.8	307.2
851231	1345	220.7	492.0	1.57	1.40	96.4	271.4	302.4
860122	845	219.9	488.8	1.70	1.26	89.7	268.9	301.2
860129	1550	220.7	477.9	1.67	1.27	88.7	257.3	293.7
860210	1400	210.4	475.7	1.67	1.21	91.8	265.3	282.4
860228	1215	223.9	472.3	1.79	1.29	86.3	248.4	286.0
860311	1015	217.7	476.7	1.87	1.17	82.0	259.0	289.2
860330	1520	204.3	468.8	1.78	1.01	80.4	264.6	275.9
860416	1200	188.1	452.4	1.74	0.85	63.1	264.3	252.1
860422	1645	221.2	502.4	2.40	0.63	63.3	281.2	331.4
860516	1224	157.2	278.1	1.50	0.84	63.4	120.9	212.6
860602	1430	130.4	269.8	1.24	0.71	50.8	139.4	196.6
860818	1115	160.0	241.0	2.13	0.25	10.6	81.0	202.9
860903	1500	164.9	241.2	1.32	1.02	38.5	76.3	198.6
860912	1235	175.0	235.4	1.45	0.97	26.9	60.4	200.6
861011	840	157.2	245.1	1.41	1.03	47.9	87.9	200.6
861012	938	160.7	246.2	1.35	1.07	54.1	85.5	202.1
861013	1300	158.5	262.5	1.55	0.82	49.9	103.9	208.2
861014	1000	159.8	276.5	1.82	0.71	47.9	116.7	218.4
861015	900	150.6	267.3	1.63	0.71	56.1	116.6	210.2
861016	1120	164.6	270.4	1.54	0.87	58.0	105.8	212.2
861017	1010	167.0	263.5	1.46	0.87	57.2	96.5	210.2
861018	1204	165.6	261.0	1.30	0.93	57.5	95.4	205.9
861020	1212	159.6	266.4	1.41	1.17	71.0	106.8	211.6
861021	1650	160.0	274.8	1.32	1.17	69.9	114.8	207.7
861022	1150	157.3	262.5	1.06	1.15	72.0	105.2	200.7
861125	1440	173.8	451.2	1.08	1.39	78.5	277.5	243.2
861205	931	181.2	269.4	1.61	1.00	44.9	88.2	221.9
861218	1002	169.8	272.0	1.60	1.17	48.3	102.2	229.5
870106	1020	221.0	300.5	2.09	1.02	40.8	79.6	259.3
870121	1150	203.2	301.7	2.21	0.72	41.8	98.4	251.7
870123	1144	197.1	301.3	2.30	0.77	45.5	104.1	250.6
870213	1345	159.4	291.1	1.77	0.97	58.0	131.7	234.4
870219	1155	206.4	295.2	1.95	1.01	47.0	88.8	248.8
870303	929	202.1	279.6	1.99	0.88	38.3	77.6	239.0
870318	1025	228.5	282.5	2.40	0.74	18.3	54.0	258.5
870326	1300	181.5	273.8	2.00	0.79	37.9	92.3	227.7
870402	1511	142.0	256.9	1.36	0.96	62.5	114.9	195.1
870430	1120	153.7	245.6	1.31	0.94	53.4	91.9	200.1
870511	916	150.0	238.9	1.23	1.17	45.3	88.9	197.9
870901	605	143.6	216.5	1.26	0.83	35.1	72.9	176.6
870908	1357	156.9	219.9	1.40	0.79	30.7	63.0	188.6
870929	730	127.2	202.1	0.94	0.68	31.3	74.9	160.6
871105	1350	136.6	223.7	1.01	1.03	51.6	87.1	176.5
871113	1155	165.2	232.7	1.28	1.14	42.2	67.5	198.5

871125	1138	149.7	235.4	1.66	0.89	30.8	85.7	205.4
871202	1148	141.9	238.4	0.85	0.96	59.1	96.5	180.1
871209	800	126.3	245.7	0.98	0.99	52.7	119.4	190.5
871223	1104	163.7	244.1	1.80	0.71	29.3	80.4	208.7
880104	1348	170.9	245.0	0.99	1.26	56.2	74.1	200.3
880112	1140	151.3	231.0	1.47	0.91	40.2	79.7	190.2
880202	824	164.1	241.1	1.93	0.44	20.1	77.0	202.6
880218	1302	195.1	271.9	2.40	0.42	17.8	76.8	234.7
880303	1107	208.7	273.9	2.18	0.55	21.7	65.2	236.6
880321	1016	206.4	272.4	2.41	0.36	15.5	66.0	238.5
880401	858	190.5	279.2	1.88	0.79	29.0	88.7	224.5
880415	1025	182.4	269.3	1.70	0.89	45.5	86.9	224.0
880421	800	178.9	268.7	1.96	0.77	32.8	89.8	227.4
880518	1005	180.1	267.3	2.02	0.56	25.2	87.2	219.6
880602	1012	171.9	264.6	2.19	0.22	11.4	92.7	212.7
880607	837	188.7	316.9	2.30	0.63	23.9	128.2	253.7
880621	935	199.3	305.0	2.51	0.38	18.8	105.7	246.5
880708	700	162.5	293.3	2.16	0.45	25.3	130.8	225.5
880720	913	147.5	277.7	1.95	0.37	19.7	130.2	220.1
880909	1015	160.5	263.5	1.29	0.97	43.9	103.0	198.4

APPENDIX B: CALCULATED OUTER BAR PROPERTIES

Date	Time	x_{start} m	x_{end} m	h_c m	z_m m	V_b m^3/m	l_b m	x_{cg} m
810126	850	452.7	601.7	4.88	0.16	16.2	149.1	523.4
810210	900	459.9	573.8	5.00	0.15	11.1	113.9	515.5
810224	1540	441.4	599.1	4.85	0.15	15.9	157.7	518.3
810310	1440	422.8	582.0	4.66	0.14	10.5	159.2	497.8
810325	1555	420.3	602.4	4.72	0.17	15.0	182.1	503.5
810406	1030	435.5	561.6	4.75	0.10	7.1	126.1	501.9
810415	1245	426.4	480.5	4.72	0.04	1.0	54.1	446.7
810427	1400	414.1	554.4	4.66	0.12	9.7	140.2	488.0
810511	1300	412.8	559.6	4.75	0.08	7.3	146.9	481.9
810526	1400	409.8	564.6	4.72	0.07	6.8	154.9	478.3
810609	1245	454.6	490.7	5.06	0.02	0.3	36.1	474.4
810622	1300	422.6	521.0	4.66	0.04	2.5	98.5	468.9
810701	1200	399.9	653.2	4.48	0.08	11.4	253.3	498.9
810717	1200	406.4	604.1	4.57	0.08	9.0	197.7	494.2
810928	1115	190.5	305.3	1.80	1.00	60.6	114.7	238.3
811016	1700	242.9	352.5	2.38	1.04	51.0	109.7	291.1
811026	1530	235.8	354.9	2.23	1.09	59.7	119.1	286.2
811104	1500	252.8	406.5	2.44	1.14	77.8	153.7	317.8
811117	1415	274.8	498.4	2.65	1.13	103.3	223.6	354.9
811130	1200	292.7	504.5	2.65	1.27	121.4	211.8	370.2
811216	1100	291.7	499.7	2.72	1.15	108.4	208.1	368.5
820105	1300	294.4	524.9	3.18	0.75	103.1	230.5	389.1
820120	59	290.1	521.4	3.18	0.77	101.5	231.3	385.5
820128	1210	298.6	519.6	3.22	0.80	98.0	221.0	391.0
820209	845	289.9	525.8	3.19	0.73	97.0	235.9	387.1
820216	1430	286.4	532.5	3.17	0.76	97.7	246.1	384.5
820302	1045	304.6	528.8	3.36	0.74	94.1	224.1	398.3
820317	1435	300.0	536.2	3.36	0.73	90.6	236.2	395.7
820324	1130	295.8	541.1	3.31	0.71	91.6	245.3	393.1
820414	1115	291.4	518.3	3.35	0.64	80.9	226.9	388.1
820503	1430	288.5	521.2	3.34	0.54	70.5	232.6	383.0
820517	1515	281.5	508.7	3.27	0.49	63.4	227.2	373.5
820602	75	281.8	501.7	3.23	0.48	61.2	219.9	371.2
820616	1200	273.4	478.1	3.23	0.37	45.4	204.7	360.9
820701	1245	269.8	490.7	3.19	0.36	47.9	220.9	362.0
820714	1630	270.6	509.4	3.23	0.32	45.9	238.8	366.5
820726	1230	274.4	488.7	3.20	0.31	42.6	214.3	362.7
820810	1100	270.5	483.2	3.28	0.31	38.9	212.7	359.7
820824	1340	271.4	476.4	3.23	0.30	37.8	205.0	356.0
820901	1600	271.3	471.3	3.24	0.30	37.5	200.0	360.5
820913	1505	272.5	467.8	3.29	0.23	28.5	195.3	358.3
821007	1505	277.3	442.6	3.45	0.12	13.1	165.4	358.7
821014	1500	287.0	466.0	3.44	0.27	28.4	179.1	366.7
821015	1140	283.4	460.4	3.43	0.25	27.6	177.0	363.7
821016	1550	282.4	464.5	3.37	0.26	28.4	182.0	365.9
821017	1040	287.4	458.8	3.50	0.26	24.8	171.4	364.4
821027	1500	312.4	495.6	3.64	0.35	37.0	183.2	391.3
821108	1550	311.3	488.5	3.63	0.32	32.2	177.2	386.2
821206	1430	320.6	497.9	3.67	0.42	43.2	177.3	395.2
821214	1525	342.1	545.2	3.71	0.59	67.0	203.0	425.0
821222	1300	337.8	536.4	3.73	0.55	61.0	198.7	417.0
830113	1310	335.3	539.0	3.72	0.56	65.3	203.7	419.5
830124	1220	333.1	518.6	3.72	0.48	52.0	185.5	412.3
830208	1250	342.7	566.4	3.78	0.55	69.6	223.7	433.9
830224	1500	353.5	602.2	3.89	0.64	87.2	248.7	455.9
830322	1245	364.5	604.8	3.99	0.68	93.8	240.3	470.9
830328	1300	396.4	609.6	4.08	0.80	93.3	213.2	486.9

830412	1130	387.1	599.8	3.96	0.75	92.4	212.7	476.7
830505	845	376.3	605.9	3.99	0.69	92.4	229.6	474.7
830525	930	372.4	604.7	4.06	0.65	89.3	232.3	475.3
830614	900	374.2	602.4	4.00	0.66	86.8	228.2	471.4
830630	1245	374.9	607.0	4.02	0.65	82.3	232.1	469.6
830712	1610	369.9	593.3	4.03	0.65	80.5	223.4	466.0
830725	1155	372.2	599.6	4.05	0.64	80.8	227.4	467.9
830808	1245	371.3	594.5	4.08	0.60	78.3	223.2	469.1
830826	1230	367.3	592.9	4.08	0.65	80.9	225.6	467.2
830906	1410	366.5	585.5	4.03	0.58	77.7	219.0	464.9
830918	1240	369.6	583.4	4.06	0.56	72.9	213.8	465.0
831001	1130	383.6	582.0	4.13	0.65	73.0	198.4	470.1
831014	850	376.7	582.9	4.08	0.61	70.1	206.1	462.7
831024	1415	372.3	568.2	4.07	0.56	63.4	195.9	454.8
831107	1300	364.8	561.3	4.06	0.47	53.7	196.5	450.4
831121	836	365.4	546.2	4.06	0.41	46.3	180.9	446.3
831202	1000	365.3	554.1	4.04	0.43	49.1	188.9	446.8
831227	1415	368.6	553.3	4.06	0.42	46.0	184.7	446.0
840105	900	366.4	549.7	4.06	0.42	43.8	183.2	443.8
840117	1050	370.4	555.3	4.06	0.51	55.7	184.9	449.2
840202	1300	369.9	547.1	4.04	0.44	46.1	177.2	445.5
840209	850	369.1	544.7	4.05	0.45	45.9	175.6	445.1
840216	1145	373.7	551.1	4.13	0.49	48.6	177.4	448.9
840224	1015	371.2	547.9	4.08	0.47	45.9	176.7	447.0
840308	1025	375.1	552.0	4.11	0.43	44.4	176.9	449.3
840320	1200	367.9	543.0	4.09	0.36	36.9	175.0	439.9
840402	1405	363.6	522.6	4.18	0.27	25.6	159.0	434.4
840406	915	361.2	512.3	4.08	0.22	22.8	151.1	432.4
840413	845	355.8	521.8	4.11	0.26	25.5	166.1	428.6
840425	1330	354.9	507.2	4.20	0.21	20.0	152.3	425.5
840509	1230	351.6	511.0	4.01	0.20	21.0	159.4	423.5
840514	850	356.0	513.9	4.14	0.20	22.2	157.9	429.6
840524	1125	348.6	501.0	3.98	0.18	17.2	152.3	415.7
840601	1040	352.3	487.3	4.02	0.17	14.8	135.0	416.7
840613	1040	351.0	512.8	4.48	0.18	14.0	161.8	428.1
840628	800	348.7	508.1	3.99	0.21	18.7	159.5	420.1
840709	820	349.6	495.4	4.02	0.16	15.4	145.7	416.7
840721	1200	356.3	501.0	4.05	0.15	12.9	144.7	419.5
840727	1150	350.8	492.9	4.00	0.19	15.0	142.1	415.3
840811	800	356.1	505.2	4.11	0.17	14.1	149.0	420.7
840830	1330	349.6	492.8	4.00	0.23	17.7	143.1	416.3
840906	1310	351.5	496.2	4.01	0.16	15.4	144.7	416.5
840910	900	352.5	477.1	4.16	0.17	12.9	124.6	413.6
840920	1030	363.6	469.8	4.18	0.08	4.8	106.2	412.6
850125	1200	377.8	421.5	4.28	0.02	0.5	43.8	400.9
850214	1430	354.2	484.4	4.05	0.22	17.6	130.2	417.6
850301	1054	354.0	483.2	4.06	0.20	17.3	129.1	415.1
850315	1210	351.9	482.4	4.10	0.18	14.4	130.5	413.5
850326	1430	345.0	481.4	3.98	0.22	18.1	136.4	406.7
850423	1005	353.0	522.2	4.01	0.38	40.4	169.2	432.7
850509	1138	347.3	520.6	3.97	0.36	41.2	173.3	429.7
850531	930	342.3	521.5	3.92	0.33	38.9	179.2	427.1
850620	1059	343.0	522.5	3.93	0.31	35.2	179.5	426.1
850715	945	345.6	514.8	4.01	0.29	30.4	169.2	425.7
850724	1710	344.0	505.2	3.95	0.25	25.5	161.2	419.7
850807	1000	348.1	507.0	4.00	0.26	24.3	158.9	421.3
850821	735	348.2	501.5	3.97	0.22	20.5	153.3	420.0
850903	1150	349.5	499.4	4.04	0.23	20.0	150.0	419.7
850906	1500	351.6	492.3	4.01	0.23	18.3	140.7	417.2
850909	1030	356.6	488.8	4.12	0.23	17.4	132.2	417.8
850911	1330	345.5	496.5	3.96	0.22	18.9	151.0	418.8
850911	1400	354.4	496.5	4.09	0.22	17.6	142.1	422.6

850911	1600	353.0	490.2	4.03	0.21	17.5	137.1	415.8
850912	1408	352.7	489.1	4.03	0.20	16.9	136.4	416.7
850912	1705	354.6	490.3	4.06	0.18	16.3	135.8	418.1
850915	1350	352.4	492.3	4.02	0.20	15.7	139.9	416.3
850918	735	350.0	488.0	4.04	0.16	14.0	138.1	413.8
850927	1600	361.8	505.8	4.10	0.22	17.9	143.9	429.9
851015	1355	365.3	500.0	4.26	0.17	14.7	134.7	430.0
851019	945	364.3	499.6	4.20	0.16	14.0	135.3	429.0
851020	835	361.0	501.4	4.14	0.18	15.4	140.4	427.0
851023	1024	356.0	510.3	4.04	0.26	24.5	154.3	426.2
851106	1030	324.7	508.2	3.72	0.45	49.3	183.5	407.6
851121	820	316.5	504.6	3.71	0.37	42.8	188.1	403.0
860516	1224	337.9	491.0	3.86	0.35	32.3	153.1	409.4
860602	1430	336.7	486.3	3.87	0.31	28.7	149.6	406.4
860611	1700	333.4	488.9	3.85	0.32	29.5	155.5	407.4
860623	1145	331.7	480.8	3.85	0.29	26.9	149.1	402.8
860709	1145	330.6	479.0	3.83	0.26	23.0	148.4	401.4
860723	1345	332.9	484.6	3.85	0.28	22.0	151.7	402.5
860813	920	331.3	483.5	3.88	0.24	22.3	152.2	401.3
860818	1115	328.3	489.5	3.81	0.33	34.2	161.2	407.9
860903	1500	322.5	479.8	3.78	0.29	27.7	157.3	395.4
860912	1235	325.9	475.6	3.78	0.27	21.9	149.7	399.2
860918	1115	322.5	466.0	3.74	0.24	20.6	143.5	390.0
860926	1130	322.3	466.5	3.74	0.26	22.1	144.3	390.7
861006	1405	319.3	473.7	3.71	0.24	24.9	154.4	395.1
861013	1300	327.5	464.4	3.79	0.27	24.2	136.9	390.5
861014	1000	323.8	472.2	3.75	0.30	26.8	148.5	391.3
861017	1010	321.2	477.3	3.72	0.28	27.8	156.1	391.0
861205	931	355.4	505.1	4.03	0.34	32.6	149.7	425.2
861218	1002	350.0	507.9	4.04	0.35	32.4	157.9	424.2
870106	1020	358.9	511.4	4.06	0.39	36.4	152.5	431.3
870121	1150	350.0	522.3	3.99	0.38	40.0	172.3	430.4
870123	1144	348.0	517.3	3.98	0.40	39.2	169.2	428.4
870213	1345	349.1	532.0	3.94	0.50	54.3	182.9	433.8
870219	1155	364.1	536.8	4.08	0.45	49.6	172.7	444.7
870303	929	358.0	528.2	4.00	0.44	44.6	170.2	433.2
870318	1025	375.6	565.1	4.05	0.50	54.4	189.5	452.5
870326	1300	369.5	558.5	4.04	0.49	54.9	189.0	449.8
870402	1511	367.3	561.3	4.04	0.45	51.7	194.0	448.8
870430	1120	374.7	587.1	4.07	0.47	61.4	212.4	464.6
870511	916	372.6	574.4	4.05	0.47	60.4	201.8	460.4
870529	1053	365.3	559.6	4.07	0.39	50.1	194.3	452.0
870617	1033	367.1	564.1	4.07	0.41	51.2	197.0	454.6
870706	1325	366.4	549.6	4.09	0.40	47.2	183.2	449.0
870722	723	366.3	560.2	4.08	0.42	47.4	193.9	451.6
870731	920	367.3	561.1	4.08	0.40	47.4	193.8	451.6
870812	1100	366.5	556.2	4.09	0.42	46.9	189.6	451.7
870901	605	366.0	561.0	4.09	0.41	45.2	194.9	450.6
870908	1357	358.4	546.9	4.04	0.35	45.0	188.5	443.1
870929	730	363.3	544.3	4.09	0.32	36.1	181.0	443.8
871105	1350	356.5	542.5	4.03	0.35	40.8	186.0	439.7
871113	1155	363.3	521.1	4.09	0.28	29.2	157.8	438.2
871125	1138	361.7	529.8	4.09	0.28	29.4	168.1	437.4
871202	1148	358.0	509.1	4.08	0.23	22.5	151.1	426.5
871209	800	363.9	509.3	4.17	0.23	21.1	145.5	429.8
871223	1104	361.4	502.5	4.10	0.17	16.7	141.1	427.1
880104	1348	358.2	513.5	4.08	0.22	22.1	155.2	427.3
880112	1140	358.7	507.3	4.07	0.18	16.4	148.5	424.4
880202	824	355.8	483.8	4.12	0.18	13.9	128.0	414.0
880218	1302	350.1	495.6	4.06	0.15	12.3	145.5	409.1
880303	1107	339.5	463.4	3.91	0.13	9.3	123.8	398.2
880321	1016	337.3	451.4	3.92	0.07	5.1	114.1	391.4

880401	858	331.9	463.3	3.90	0.06	4.7	131.3	394.8
880415	1025	337.3	425.9	4.06	0.06	3.4	88.5	380.1
880421	800	345.3	453.4	3.99	0.07	5.0	108.1	396.0
880518	1005	335.2	388.8	4.09	0.04	1.1	53.6	363.5
880602	1012	366.8	391.3	4.29	0.01	0.1	24.5	380.1
880909	1015	160.5	263.5	1.29	0.97	43.9	103.0	198.4
881011	1028	206.2	308.4	1.52	1.37	72.7	102.2	248.5
881109	926	196.1	303.6	1.67	1.19	69.7	107.5	242.3
881121	1445	197.5	315.9	1.79	0.92	63.1	118.4	244.9
881205	952	213.7	336.2	1.91	1.06	55.0	122.5	259.8
881219	1135	215.2	325.1	1.87	1.19	59.1	109.9	262.1
890117	1222	220.8	344.3	1.80	1.20	61.7	123.5	265.2
890125	1226	224.4	371.1	2.42	0.90	63.5	146.6	286.4
890202	1347	221.8	390.1	2.70	0.33	35.4	168.3	299.0
890216	1343	229.7	382.5	2.29	0.73	61.7	152.8	285.9
890221	1130	236.1	374.5	2.34	1.12	75.9	138.5	296.7
890227	1210	287.5	519.4	3.41	0.65	79.5	231.9	387.9
890312	1300	354.3	590.0	3.40	0.80	91.1	235.7	433.6
890328	1348	331.8	500.0	3.29	0.99	94.0	168.2	411.5
890426	942	312.0	515.0	3.40	0.87	99.8	203.0	406.7
890508	1336	312.4	490.0	3.22	0.80	97.0	177.6	398.6
890516	1000	311.7	500.0	3.24	0.87	101.6	188.3	400.0
890517	1030	309.9	490.0	3.25	0.83	99.6	180.1	398.4
890524	938	309.6	510.0	3.24	0.70	97.9	200.4	402.2
890615	859	308.8	480.0	3.26	0.81	91.8	171.2	388.8
890629	1034	302.4	520.0	3.35	0.73	90.1	217.6	400.4
890719	1025	298.9	520.0	3.30	0.65	96.0	221.1	398.6
890726	840	304.5	520.0	3.25	0.67	103.1	215.5	405.9
890815	1620	301.0	510.0	3.27	0.59	86.5	209.0	397.4
890824	1620	297.8	580.0	3.39	0.60	97.1	282.2	423.4
890912	1010	310.7	570.0	3.33	0.60	95.4	259.3	420.1
891003	1342	311.1	500.0	3.33	0.72	78.0	188.9	396.7
891010	1350	311.7	510.0	3.27	0.61	89.5	198.3	402.9
891101	1326	297.8	510.0	3.38	0.49	73.4	212.2	404.2
891117	1130	299.1	530.0	3.34	0.39	66.6	230.9	405.0
891128	1540	301.5	520.0	3.33	0.51	75.3	218.5	400.0
891207	1050	299.7	550.0	3.36	0.50	73.5	250.3	408.7
891212	1025	319.2	450.0	3.59	0.56	48.0	130.8	389.0
891221	1220	305.9	510.0	3.42	0.50	66.9	204.1	401.0
891228	1550	302.6	410.0	3.47	0.43	33.8	107.4	362.5

APPENDIX C: CALCULATED WAVE CHARACTERISTICS FOR THE INNER BAR

Date	Time	Values	$(H_o)_{mean}$ m	$(H_o)_{max}$ m	T_{mean} sec	T_{max} sec	$(H_o/L_o)_{mean}$	$(H_o/L_o)_{max}$	$(H_o/wT)_{mean}$
810126	850	23	0.9	2.7	7.9	11.9	0.0119	0.0400	5.7
810210	900	57	0.9	2.0	8.3	12.8	0.0126	0.0600	6.1
810224	1540	57	1.6	2.9	9.6	16.0	0.0136	0.0466	8.3
810310	1440	55	1.3	2.3	9.7	14.8	0.0122	0.0486	7.0
810325	1555	57	1.3	3.9	9.9	15.3	0.0128	0.0413	7.4
810406	1030	38	0.8	1.3	8.5	14.8	0.0096	0.0463	4.7
810415	1245	28	1.1	2.4	7.6	11.0	0.0149	0.0350	6.7
810427	1400	39	0.9	2.2	9.0	16.3	0.0123	0.0572	5.5
810511	1300	54	1.3	2.7	7.5	12.2	0.0193	0.0717	8.2
810526	1400	57	1.0	2.2	8.2	12.8	0.0133	0.0396	6.1
810609	1245	52	0.7	1.1	7.9	10.1	0.0080	0.0232	3.8
810622	1300	51	0.6	1.1	8.2	11.4	0.0074	0.0335	3.4
810701	1200	31	1.0	2.4	7.1	12.2	0.0156	0.0295	6.0
810717	1200	57	0.7	1.3	8.1	10.8	0.0093	0.0438	3.7
810727	1100	39	0.7	1.1	7.4	14.2	0.0126	0.0575	4.5
810804	1200	30	0.9	1.5	6.7	9.1	0.0156	0.0338	5.7
810818	1400	43	0.6	1.6	8.5	12.2	0.0079	0.0356	3.3
810821	1500	12	2.4	3.8	8.3	12.3	0.0258	0.0401	12.0
810823	1100	7	1.9	2.3	11.1	13.8	0.0130	0.0298	7.6
810831	1500	23	1.0	1.5	7.8	12.2	0.0135	0.0305	5.6
810908	1200	24	1.6	2.4	11.0	13.5	0.0090	0.0142	5.9
810914	1145	24	0.8	1.5	11.1	12.5	0.0042	0.0079	2.9
810919	630	18	1.0	1.4	11.3	14.2	0.0063	0.0242	3.9
810928	1115	37	0.8	2.1	7.4	14.2	0.0126	0.0372	4.9
821007	1505								
821013	1110	23	1.5	2.5	10.2	17.0	0.0095	0.0335	5.9
821014	1500	4	1.4	1.6	13.5	14.0	0.0049	0.0070	4.3
821015	1140	3	0.9	1.1	12.7	14.0	0.0037	0.0042	3.0
821016	1550	5	0.7	0.9	10.6	12.0	0.0056	0.0168	3.0
821017	1040	3	1.3	1.5	6.3	7.0	0.0221	0.0312	8.7
821019	1230	8	0.9	1.5	9.0	14.0	0.0124	0.0261	5.0
821022	1150	12	1.1	1.7	7.7	12.0	0.0147	0.0321	6.5
821027	1500	19	2.1	4.6	8.3	12.0	0.0236	0.0416	11.2
821108	1550	48	0.9	1.8	9.8	17.0	0.0092	0.0361	4.5
821206	1430	64	1.0	2.3	7.3	12.0	0.0145	0.0361	6.4
821214	1525	28	1.7	4.3	7.6	12.0	0.0220	0.0416	10.4
821222	1300	31	1.6	2.6	9.8	14.0	0.0150	0.0468	8.4
830113	1310	88	1.3	3.4	8.6	17.0	0.0176	0.0427	8.5
830124	1220	39	1.3	2.5	9.1	14.0	0.0158	0.0481	8.3
830208	1250	59	1.4	4.8	8.9	12.0	0.0140	0.0481	8.0
830224	1500	65	2.0	4.6	10.5	15.0	0.0150	0.0598	9.7
830322	1245	102	1.4	3.6	9.3	13.0	0.0124	0.0468	7.6
830328	1300	25	2.0	5.1	9.7	15.0	0.0174	0.0466	10.3
830412	1130	59	1.0	3.1	8.8	13.0	0.0113	0.0640	5.9
830505	845	84	0.9	3.2	8.7	14.0	0.0145	0.1441	5.7
830525	930	78	0.8	2.3	7.5	11.0	0.0122	0.0498	5.2
830614	900	79	0.8	2.2	8.0	14.0	0.0105	0.0391	4.8
830630	1245	62	0.8	1.8	7.8	14.0	0.0107	0.0361	4.5
830712	1610	46	0.7	1.3	8.1	17.0	0.0104	0.0569	4.1
830725	1155	51	0.5	1.4	8.9	17.0	0.0050	0.0280	2.4
830826	1230								
830906	1410	45	0.8	1.4	8.1	14.0	0.0105	0.0364	4.3
830918	1240	46	0.9	3.2	9.0	14.0	0.0119	0.0520	5.0
831001	1130	52	1.5	4.1	8.4	12.0	0.0163	0.0481	7.2
831014	850	52	1.2	2.7	9.2	14.0	0.0145	0.0561	6.6
831024	1415	41	1.5	3.2	9.0	14.0	0.0158	0.0442	7.7

831107	1300	54	1.2	2.7	9.1	12.0	0.0133	0.0480	6.4
831121	836	53	0.8	2.3	7.9	17.0	0.0128	0.0361	5.3
831202	1000	43	0.6	1.7	8.4	14.0	0.0091	0.0442	3.7
831227	1415	94	1.2	3.6	8.6	14.0	0.0157	0.0428	7.6
840105	900	35	1.5	2.5	8.9	14.0	0.0164	0.0447	8.7
840117	1050	48	1.5	3.3	8.5	12.0	0.0166	0.0494	8.9
840202	1300	60	1.0	1.8	8.0	12.0	0.0139	0.0390	6.7
840209	850	27	1.0	2.1	8.2	11.0	0.0125	0.0372	6.6
840216	1145	26	1.0	3.4	9.2	11.0	0.0087	0.0240	5.5
840224	1015	16	1.0	3.1	7.9	12.0	0.0169	0.0569	7.0
840308	1025	33	1.1	2.1	6.5	12.0	0.0209	0.0468	8.6
840320	1200	39	1.4	2.4	9.5	14.0	0.0130	0.0442	7.5
840402	1405	51	1.0	1.7	9.7	12.0	0.0083	0.0442	5.2
840406	915	15	1.2	2.0	9.9	12.0	0.0096	0.0234	5.9
840413	845	28	1.1	1.7	9.8	12.0	0.0104	0.0481	5.6
840425	1330	47	0.9	1.7	8.9	12.0	0.0086	0.0280	4.8
840509	1230	51	0.7	1.6	8.6	12.0	0.0083	0.0321	4.1
840514	850	20	0.5	0.7	7.3	9.0	0.0074	0.0240	3.2
840524	1125	31	0.9	1.8	8.1	14.0	0.0116	0.0298	5.1
840601	1040	29	0.9	2.3	6.3	10.0	0.0155	0.0321	6.1
840613	1040	45	0.5	0.9	8.9	11.0	0.0043	0.0168	2.4
840628	800	60	0.7	1.2	7.1	11.0	0.0116	0.0361	4.5
840709	820	43	0.7	1.4	7.7	11.0	0.0093	0.0242	4.1
840721	1200	45	0.5	0.9	9.7	17.0	0.0045	0.0156	2.3
840727	1150	23	0.5	0.8	9.8	17.0	0.0085	0.0640	2.8
840811	800	59	0.5	1.0	8.3	12.0	0.0067	0.0361	2.6
840906	1310								
840910	900	15	1.3	1.8	7.0	9.0	0.0180	0.0298	7.5
840920	1030	39	1.3	2.0	7.4	10.0	0.0177	0.0354	7.6
841002	1300	49	1.2	3.1	8.3	12.0	0.0150	0.0442	6.6
841007	1000	19	0.8	1.7	9.0	11.0	0.0108	0.0441	4.6
841016	1230	36	1.9	3.7	9.8	14.0	0.0143	0.0390	8.2
841029	1450	52	0.9	1.9	11.1	17.0	0.0048	0.0149	3.4
841127	1320	61	1.3	2.5	8.2	17.0	0.0177	0.0520	7.9
841213	1508	28	0.9	2.6	7.8	12.0	0.0135	0.0441	5.9
850105	1125								
850125	1200	75	1.0	2.6	6.3	12.2	0.0241	0.0697	8.7
850214	1430	94	1.6	4.2	7.6	13.5	0.0193	0.0453	9.9
850301	1054	59	0.8	2.3	9.0	15.1	0.0100	0.0430	5.2
850315	1210	54	1.0	2.9	8.3	16.0	0.0137	0.0475	6.9
850326	1430	60	1.8	3.5	8.3	15.1	0.0200	0.0429	11.1
850423	1005	125	1.2	4.6	9.2	16.0	0.0131	0.0691	6.7
850509	1138	69	1.1	3.1	7.5	12.2	0.0153	0.0611	6.7
850531	930	88	1.0	2.0	7.2	9.8	0.0144	0.0411	6.4
850620	1059	78	0.6	1.0	7.2	11.1	0.0113	0.0709	4.2
850715	945	96	0.8	2.3	8.0	14.2	0.0107	0.0447	4.4
850719	1125	16	1.1	2.0	8.2	10.7	0.0154	0.0422	6.2
850724	1710	22	0.8	1.5	7.0	10.2	0.0163	0.0665	5.5
850807	1000	63	1.2	2.7	8.1	12.8	0.0146	0.0415	6.5
850821	735	52	0.9	1.5	7.6	9.8	0.0125	0.0480	4.9
850913	1640								
850914	0	8	2.2	2.3	6.7	7.3	0.0323	0.0489	13.2
850914	730	7	2.5	2.6	6.8	7.1	0.0343	0.0409	14.5
850914	930	2	2.3	2.3	6.4	6.7	0.0364	0.0397	14.5
850914	1248	2	2.3	2.3	6.5	6.6	0.0345	0.0355	14.0
850914	1905	7	2.0	2.2	7.2	10.2	0.0290	0.0382	11.8
850915	55	5	1.7	1.8	8.2	9.5	0.0169	0.0209	8.5
850915	703	7	1.6	1.7	7.5	9.5	0.0219	0.0390	9.2
850915	1018	2	1.4	1.5	8.3	8.3	0.0136	0.0137	7.0
850915	1350	3	1.3	1.3	8.5	9.1	0.0115	0.0142	6.0
850916	915	19	1.2	1.3	9.0	10.7	0.0115	0.0416	5.6
850916	2015	10	1.2	1.3	7.1	9.8	0.0215	0.0456	7.7

850917	845	12	1.1	1.2	8.3	9.1	0.0108	0.0143	5.5
850917	1510	6	1.2	1.3	8.4	9.1	0.0113	0.0134	5.9
850918	735	16	1.3	1.5	8.3	9.1	0.0126	0.0295	6.2
850919	1250	28	1.4	1.5	10.7	12.8	0.0082	0.0127	5.3
850920	945	20	1.3	1.5	10.6	12.2	0.0075	0.0112	4.9
850925	1045	54	1.4	2.2	11.5	23.3	0.0096	0.0240	5.6
850927	1600	34	3.1	6.5	14.9	23.3	0.0095	0.0194	8.5
851015	1355	57	1.1	1.7	7.8	13.5	0.0147	0.0383	6.2
851019	945	22	1.0	1.8	7.0	12.2	0.0164	0.0397	6.3
851020	835	8	0.7	0.8	7.0	7.3	0.0096	0.0107	4.3
851021	1640	32	1.7	2.6	6.7	7.5	0.0253	0.0490	10.7
851022	1522	23	2.9	3.4	7.8	9.8	0.0309	0.0438	15.4
851023	1024	19	1.8	2.1	8.2	9.8	0.0179	0.0224	9.4
851024	1491	23	1.5	1.6	7.7	8.8	0.0163	0.0184	8.1
851106	1030	111	2.6	4.2	9.0	12.8	0.0211	0.0416	12.3
851121	820	59	1.1	2.0	9.5	17.1	0.0106	0.0379	5.5
851209	1320	91	1.7	3.8	9.0	16.0	0.0190	0.0560	9.6
851219	1330	28	0.7	1.8	8.8	17.1	0.0110	0.0995	4.2
851231	1345	NO WAVE MEASUREMENTS							
860122	845	84	1.1	2.8	7.8	11.1	0.0157	0.0514	7.6
860129	1550	61	2.1	3.0	8.4	12.8	0.0233	0.0425	13.1
860210	1400	48	1.0	2.1	8.7	12.8	0.0105	0.0362	6.0
860228	1215	73	1.3	2.7	7.5	16.0	0.0186	0.0626	8.9
860311	1015	46	1.3	3.0	8.1	10.7	0.0156	0.0492	8.1
860330	1520	105	1.4	3.9	7.3	11.6	0.0196	0.0490	9.5
860416	1200	67	0.9	1.6	8.7	14.2	0.0105	0.0373	5.4
860422	1645	78	2.4	3.8	12.1	15.1	0.0122	0.0394	9.5
860516	1224	150	1.7	3.5	10.1	16.0	0.0132	0.0715	7.6
860602	1430	65	0.7	1.5	7.9	10.7	0.0082	0.0431	3.8
860818	1115								
860903	1500	61	1.2	2.3	8.6	14.2	0.0161	0.0473	6.7
860912	1235	40	0.9	1.6	7.4	23.3	0.0142	0.0399	5.3
861011	840								
861012	938	25	2.8	3.5	9.7	11.6	0.0204	0.0409	12.3
861013	1300	28	1.8	2.3	11.5	12.8	0.0090	0.0120	6.7
861014	1000	4	1.4	1.5	10.6	12.2	0.0080	0.0099	5.4
861015	900	7	1.1	1.3	9.9	10.2	0.0074	0.0087	4.7
861016	1120	26	1.2	1.7	5.4	6.9	0.0291	0.0400	9.7
861017	1010	47	1.2	1.7	5.0	5.6	0.0320	0.0435	10.3
861018	1204	53	1.3	1.6	7.0	9.8	0.0220	0.0564	8.4
861020	1212	101	2.1	2.7	8.5	11.1	0.0233	0.0488	11.1
861021	1650	59	1.2	1.6	10.6	11.6	0.0073	0.0107	4.9
861022	1150	37	1.0	1.2	11.3	12.2	0.0051	0.0088	3.8
861125	1440	295	1.0	2.7	7.7	13.5	0.0147	0.0455	6.3
861205	931	80	2.8	4.6	8.6	11.1	0.0252	0.0431	14.6
861218	1002	19	0.9	1.5	7.9	9.8	0.0117	0.0283	5.7
870106	1020	NO WAVE MEASUREMENTS							
870121	1150	46	1.5	2.7	7.3	12.2	0.0208	0.0498	10.4
870123	1144	21	1.5	2.8	8.9	11.1	0.0174	0.0433	9.4
870213	1345	236	1.3	4.0	8.6	23.3	0.0145	0.0677	7.7
870219	1155	118	2.4	5.2	8.0	10.7	0.0262	0.0499	14.7
870303	929	171	1.4	2.5	8.5	13.5	0.0150	0.0379	8.2
870318	1025	325	2.3	5.2	9.8	13.5	0.0169	0.0572	11.2
870326	1300	145	1.3	2.6	8.9	12.8	0.0121	0.0512	7.1
870402	1511	135	1.6	3.0	9.5	12.8	0.0140	0.0468	8.6
870430	1120	483	1.6	4.2	9.2	14.2	0.0148	0.0509	8.4
870511	916	179	1.0	3.2	8.9	14.2	0.0101	0.0414	5.3
870901	605								
870908	1357	117	1.4	2.5	7.1	11.1	0.0202	0.0543	8.1
870929	730	553	0.8	1.6	8.4	13.5	0.0080	0.0393	3.8
871105	1350	1085	1.2	3.6	8.2	23.3	0.0137	0.0590	6.5
871113	1155	253	1.2	2.9	7.3	11.1	0.0166	0.0653	7.1

871125	1138	379	1.0	2.3	7.4	12.8	0.0157	0.0453	6.6
871202	1148	221	1.7	2.6	9.0	12.8	0.0156	0.0451	8.7
871209	800	90	0.6	0.7	11.9	16.0	0.0036	0.0338	2.4
871223	1104	441	0.9	2.1	7.6	15.1	0.0153	0.0635	6.3
880104	1348	384	1.3	3.4	8.4	14.2	0.0171	0.0571	8.3
880112	1140	253	1.6	4.0	7.0	10.2	0.0228	0.0455	11.0
880202	824	658	1.1	3.4	9.8	17.1	0.0117	0.0722	6.1
880218	1302	412	1.3	2.9	8.3	15.1	0.0172	0.0661	8.6
880303	1107	243	1.2	3.5	7.5	12.8	0.0182	0.0689	8.0
880321	1016	412	1.1	2.6	7.5	12.2	0.0171	0.0528	7.9
880401	858	176	0.9	2.0	7.6	12.2	0.0121	0.0400	6.1
880415	1025	288	1.9	5.6	9.1	12.2	0.0175	0.0543	10.2
880421	800	114	1.1	2.9	9.2	16.0	0.0190	0.0679	7.5
880518	1005	430	1.0	2.4	8.6	16.0	0.0112	0.0470	5.6
880602	1012	195	0.9	2.2	7.9	12.2	0.0121	0.0562	5.5
880607	837	142	1.5	2.8	8.2	12.2	0.0188	0.0581	8.2
880621	935	237	0.7	1.7	7.5	13.5	0.0104	0.0437	4.4
880708	700	197	0.7	1.2	8.0	11.1	0.0093	0.0430	4.0
880720	913	189	0.6	0.9	7.8	10.7	0.0089	0.0715	3.5
880909	1015	807	0.8	2.3	7.5	19.7	0.0123	0.0714	5.0

APPENDIX D: CALCULATED WAVE CHARACTERISTICS FOR THE OUTER BAR

Date	Time	Values	$(H_o)_{mean}$ m	$(H_o)_{max}$ m	T_{mean} sec	T_{max} sec	$(H_o/L_o)_{mean}$	$(H_o/L_o)_{max}$	$(H_o/wT)_{mean}$
810126	850	23	0.9	2.7	7.9	11.9	0.0119	0.0400	5.7
810210	900	57	0.9	2.0	8.3	12.8	0.0126	0.0600	6.1
810224	1540	57	1.6	2.9	9.6	16.0	0.0136	0.0466	8.3
810310	1440	55	1.3	2.3	9.7	14.8	0.0122	0.0486	7.0
810325	1555	57	1.3	3.9	9.9	15.3	0.0128	0.0413	7.4
810406	1030	38	0.8	1.3	8.5	14.8	0.0096	0.0463	4.7
810415	1245	28	1.1	2.4	7.6	11.0	0.0149	0.0350	6.7
810427	1400	39	0.9	2.2	9.0	16.3	0.0123	0.0572	5.5
810511	1300	54	1.3	2.7	7.5	12.2	0.0193	0.0717	8.2
810526	1400	57	1.0	2.2	8.2	12.8	0.0133	0.0396	6.1
810609	1245	52	0.7	1.1	7.9	10.1	0.0080	0.0232	3.8
810622	1300	51	0.6	1.1	8.2	11.4	0.0074	0.0335	3.4
810701	1200	31	1.0	2.4	7.1	12.2	0.0156	0.0295	6.0
810717	1200	57	0.7	1.3	8.1	10.8	0.0093	0.0438	3.7
810928	1115								
811016	1700	73	1.4	3.1	7.9	14.4	0.0210	0.0600	8.3
811026	1530	35	1.3	2.7	8.3	12.8	0.0147	0.0414	7.0
811104	1500	30	1.6	2.7	8.8	12.8	0.0162	0.0501	8.1
811117	1415	33	2.0	4.2	9.1	14.0	0.0178	0.0426	9.5
811130	1200	50	1.2	3.3	7.8	14.8	0.0196	0.0572	7.4
811216	1100	58	1.3	2.5	7.6	14.2	0.0171	0.0438	8.0
820105	1300	73	1.2	3.6	7.3	13.8	0.0185	0.0457	8.3
820120	59	47	0.9	2.4	8.6	14.6	0.0155	0.0654	6.4
820128	1210	34	1.5	2.6	7.0	10.6	0.0221	0.0483	10.4
820209	845	48	1.1	1.7	8.9	12.0	0.0120	0.0442	6.4
820216	1430	28	1.2	2.8	8.3	12.0	0.0159	0.0441	7.8
820302	1045	54	1.7	3.7	8.9	17.0	0.0171	0.0783	9.5
820317	1435	54	1.1	2.3	8.2	12.0	0.0143	0.0640	7.1
820324	1130	26	0.9	1.5	7.5	12.0	0.0162	0.0361	6.8
820414	1115	77	1.0	1.8	7.4	11.0	0.0158	0.0712	6.8
820503	1430	75	1.0	2.8	7.6	12.0	0.0136	0.0623	6.5
820517	1515	51	1.0	2.0	9.7	14.0	0.0082	0.0427	4.7
820602	75	59	0.6	1.1	8.4	11.0	0.0064	0.0321	3.3
820616	1200	55	1.0	1.7	8.5	12.0	0.0104	0.0321	5.1
820701	1245	37	0.8	3.2	8.3	14.0	0.0099	0.0572	4.3
820714	1630	26	0.7	1.2	7.5	12.0	0.0116	0.0312	4.3
820726	1230	35	0.5	1.0	7.8	11.0	0.0072	0.0285	2.9
820810	1100	51	0.5	0.9	8.5	14.0	0.0061	0.0182	2.8
820824	1340	37	0.5	0.8	6.8	14.0	0.0095	0.0356	3.3
820901	1600	14	0.7	1.3	7.6	10.0	0.0094	0.0338	3.8
820913	1505	42	1.0	1.5	7.1	10.0	0.0152	0.0390	5.9
821007	1505	89	0.9	1.8	8.1	14.0	0.0127	0.0442	5.3
821014	1500	27	1.5	2.5	10.7	17.0	0.0089	0.0335	5.6
821015	1140	3	0.9	1.1	12.7	14.0	0.0037	0.0042	3.0
821016	1550	5	0.7	0.9	10.6	12.0	0.0056	0.0168	3.0
821017	1040	3	1.3	1.5	6.3	7.0	0.0221	0.0312	8.7
821027	1500	39	1.6	4.6	8.2	14.0	0.0186	0.0416	8.5
821108	1550	48	0.9	1.8	9.8	17.0	0.0092	0.0361	4.5
821206	1430	64	1.0	2.3	7.3	12.0	0.0145	0.0361	6.4
821214	1525	28	1.7	4.3	7.6	12.0	0.0220	0.0416	10.4
821222	1300	31	1.6	2.6	9.8	14.0	0.0150	0.0468	8.4
830113	1310	88	1.3	3.4	8.6	17.0	0.0176	0.0427	8.5
830124	1220	39	1.3	2.5	9.1	14.0	0.0158	0.0481	8.3
830208	1250	59	1.4	4.8	8.9	12.0	0.0140	0.0481	8.0
830224	1500	65	2.0	4.6	10.5	15.0	0.0150	0.0598	9.7
830322	1245	102	1.4	3.6	9.3	13.0	0.0124	0.0468	7.6
830328	1300	25	2.0	5.1	9.7	15.0	0.0174	0.0466	10.3

830412	1130	59	1.0	3.1	8.8	13.0	0.0113	0.0640	5.9
830505	845	84	0.9	3.2	8.7	14.0	0.0145	0.1441	5.7
830525	930	78	0.8	2.3	7.5	11.0	0.0122	0.0498	5.2
830614	900	79	0.8	2.2	8.0	14.0	0.0105	0.0391	4.8
830630	1245	62	0.8	1.8	7.8	14.0	0.0107	0.0361	4.5
830712	1610	46	0.7	1.3	8.1	17.0	0.0104	0.0569	4.1
830725	1155	51	0.5	1.4	8.9	17.0	0.0050	0.0280	2.4
830808	1245	53	0.7	1.0	8.7	14.0	0.0073	0.0361	3.3
830826	1230	72	0.8	2.2	8.1	14.0	0.0115	0.0391	4.8
830906	1410	45	0.8	1.4	8.1	14.0	0.0105	0.0364	4.3
830918	1240	46	0.9	3.2	9.0	14.0	0.0119	0.0520	5.0
831001	1130	52	1.5	4.1	8.4	12.0	0.0163	0.0481	7.2
831014	850	52	1.2	2.7	9.2	14.0	0.0145	0.0561	6.6
831024	1415	41	1.5	3.2	9.0	14.0	0.0158	0.0442	7.7
831107	1300	54	1.2	2.7	9.1	12.0	0.0133	0.0480	6.4
831121	836	53	0.8	2.3	7.9	17.0	0.0128	0.0361	5.3
831202	1000	43	0.6	1.7	8.4	14.0	0.0091	0.0442	3.7
831227	1415	94	1.2	3.6	8.6	14.0	0.0157	0.0428	7.6
840105	900	35	1.5	2.5	8.9	14.0	0.0164	0.0447	8.7
840117	1050	48	1.5	3.3	8.5	12.0	0.0166	0.0494	8.9
840202	1300	60	1.0	1.8	8.0	12.0	0.0139	0.0390	6.7
840209	850	27	1.0	2.1	8.2	11.0	0.0125	0.0372	6.6
840216	1145	26	1.0	3.4	9.2	11.0	0.0087	0.0240	5.5
840224	1015	16	1.0	3.1	7.9	12.0	0.0169	0.0569	7.0
840308	1025	33	1.1	2.1	6.5	12.0	0.0209	0.0468	8.6
840320	1200	39	1.4	2.4	9.5	14.0	0.0130	0.0442	7.5
840402	1405	51	1.0	1.7	9.7	12.0	0.0083	0.0442	5.2
840406	915	15	1.2	2.0	9.9	12.0	0.0096	0.0234	5.9
840413	845	28	1.1	1.7	9.8	12.0	0.0104	0.0481	5.6
840425	1330	47	0.9	1.7	8.9	12.0	0.0086	0.0280	4.8
840509	1230	51	0.7	1.6	8.6	12.0	0.0083	0.0321	4.1
840514	850	20	0.5	0.7	7.3	9.0	0.0074	0.0240	3.2
840524	1125	31	0.9	1.8	8.1	14.0	0.0116	0.0298	5.1
840601	1040	29	0.9	2.3	6.3	10.0	0.0155	0.0321	6.1
840613	1040	45	0.5	0.9	8.9	11.0	0.0043	0.0168	2.4
840628	800	60	0.7	1.2	7.1	11.0	0.0116	0.0361	4.5
840709	820	43	0.7	1.4	7.7	11.0	0.0093	0.0242	4.1
840721	1200	45	0.5	0.9	9.7	17.0	0.0045	0.0156	2.3
840727	1150	23	0.5	0.8	9.8	17.0	0.0085	0.0640	2.8
840811	800	59	0.5	1.0	8.3	12.0	0.0067	0.0361	2.6
840830	1330	70	0.6	1.2	7.1	10.0	0.0098	0.0401	3.7
840906	1310	23	0.7	1.4	8.7	14.0	0.0117	0.0312	4.3
840910	900	15	1.3	1.8	7.0	9.0	0.0180	0.0298	7.5
840920	1030	39	1.3	2.0	7.4	10.0	0.0177	0.0354	7.6
850105	1125	28	2.8	3.6	8.1	10.2	0.0285	0.0415	16.7
850125	1200								
850214	1430	94	1.6	4.2	7.6	13.5	0.0193	0.0453	9.9
850301	1054	59	0.8	2.3	9.0	15.1	0.0100	0.0430	5.2
850315	1210	54	1.0	2.9	8.3	16.0	0.0137	0.0475	6.9
850326	1430	60	1.8	3.5	8.3	15.1	0.0200	0.0429	11.1
850423	1005	125	1.2	4.6	9.2	16.0	0.0131	0.0691	6.7
850509	1138	69	1.1	3.1	7.5	12.2	0.0153	0.0611	6.7
850531	930	88	1.0	2.0	7.2	9.8	0.0144	0.0411	6.4
850620	1059	78	0.6	1.0	7.2	11.1	0.0113	0.0709	4.2
850715	945	96	0.8	2.3	8.0	14.2	0.0107	0.0447	4.4
850724	1710	38	0.9	2.0	7.5	10.7	0.0160	0.0665	5.8
850807	1000	63	1.2	2.7	8.1	12.8	0.0146	0.0415	6.5
850821	735	52	0.9	1.5	7.6	9.8	0.0125	0.0480	4.9
850903	1150	53	0.8	1.2	9.6	17.1	0.0093	0.0351	4.0
850906	1500	72	0.6	0.8	10.5	12.2	0.0035	0.0108	2.2
850909	1030	62	0.5	0.6	10.8	12.2	0.0029	0.0050	1.9
850911	1330	48	0.6	1.5	10.1	14.2	0.0072	0.0379	2.8

850911	1400	NO WAVE MEASUREMENTS							
850911	1600	2	1.7	1.8	5.9	6.0	0.0317	0.0325	11.7
850912	1408	21	1.8	2.1	6.5	7.8	0.0274	0.0377	11.0
850912	1705	3	1.6	1.6	8.0	9.1	0.0185	0.0311	8.3
850915	1350	50	1.9	2.6	7.4	10.2	0.0253	0.0489	10.9
850918	735	63	1.2	1.5	8.3	10.7	0.0132	0.0456	6.1
850927	1600	136	1.8	6.5	12.0	23.3	0.0090	0.0240	6.1
851015	1355	57	1.1	1.7	7.8	13.5	0.0147	0.0383	6.2
851019	945	22	1.0	1.8	7.0	12.2	0.0164	0.0397	6.3
851020	835	8	0.7	0.8	7.0	7.3	0.0096	0.0107	4.3
851023	1024	74	2.1	3.4	7.4	9.8	0.0251	0.0490	11.8
851106	1030	134	2.4	4.2	8.8	12.8	0.0203	0.0416	11.6
851121	820	59	1.1	2.0	9.5	17.1	0.0106	0.0379	5.5
860516	1224								
860602	1430	65	0.7	1.5	7.9	10.7	0.0082	0.0431	3.8
860611	1700	36	1.2	2.2	8.3	16.0	0.0160	0.0399	7.0
860623	1145	47	0.9	1.8	8.8	15.1	0.0097	0.0345	4.6
860709	1145	63	0.7	1.1	7.9	11.1	0.0088	0.0349	3.8
860723	1345	54	0.6	0.8	9.1	15.1	0.0062	0.0390	2.7
860813	920	86	0.6	1.0	6.6	9.1	0.0118	0.0723	3.9
860818	1115	39	1.6	4.4	7.4	10.2	0.0183	0.0383	8.4
860903	1500	61	1.2	2.3	8.6	14.2	0.0161	0.0473	6.7
860912	1235	40	0.9	1.6	7.4	23.3	0.0142	0.0399	5.3
860918	1115	28	1.2	1.9	8.1	13.5	0.0152	0.0450	6.4
860926	1130	26	0.7	1.1	10.0	12.2	0.0055	0.0196	2.9
861006	1405	75	0.6	1.9	8.0	13.5	0.0111	0.0556	3.8
861013	1300	164	1.7	3.8	7.7	12.8	0.0203	0.0462	9.4
861014	1000	4	1.4	1.5	10.6	12.2	0.0080	0.0099	5.4
861017	1010	80	1.2	1.7	5.6	10.2	0.0289	0.0435	9.6
861205	931	625	1.5	4.6	8.4	13.5	0.0168	0.0564	8.0
861218	1002	19	0.9	1.5	7.9	9.8	0.0117	0.0283	5.7
870106	1020	NO WAVE MEASUREMENTS							
870121	1150	46	1.5	2.7	7.3	12.2	0.0208	0.0498	10.4
870123	1144	21	1.5	2.8	8.9	11.1	0.0174	0.0433	9.4
870213	1345	236	1.3	4.0	8.6	23.3	0.0145	0.0677	7.7
870219	1155	118	2.4	5.2	8.0	10.7	0.0262	0.0499	14.7
870303	929	171	1.4	2.5	8.5	13.5	0.0150	0.0379	8.2
870318	1025	325	2.3	5.2	9.8	13.5	0.0169	0.0572	11.2
870326	1300	145	1.3	2.6	8.9	12.8	0.0121	0.0512	7.1
870402	1511	135	1.6	3.0	9.5	12.8	0.0140	0.0468	8.6
870430	1120	483	1.6	4.2	9.2	14.2	0.0148	0.0509	8.4
870511	916	179	1.0	3.2	8.9	14.2	0.0101	0.0414	5.3
870529	1053	216	1.1	2.3	8.2	16.0	0.0123	0.0556	6.1
870617	1033	280	0.6	1.3	7.6	13.5	0.0117	0.0635	4.1
870706	1325	305	0.7	1.6	7.6	14.2	0.0103	0.0558	4.2
870722	723	244	0.6	1.4	7.5	10.2	0.0098	0.0439	3.7
870731	920	155	0.6	0.9	7.4	15.1	0.0094	0.0388	3.4
870812	1100	192	0.7	1.5	7.3	14.2	0.0132	0.0642	4.6
870901	605	336	1.0	2.6	8.5	12.2	0.0124	0.0793	5.2
870908	1357	117	1.4	2.5	7.1	11.1	0.0202	0.0543	8.1
870929	730	553	0.8	1.6	8.4	13.5	0.0080	0.0393	3.8
871105	1350	1085	1.2	3.6	8.2	23.3	0.0137	0.0590	6.5
871113	1155	253	1.2	2.9	7.3	11.1	0.0166	0.0653	7.1
871125	1138	379	1.0	2.3	7.4	12.8	0.0157	0.0453	6.6
871202	1148	221	1.7	2.6	9.0	12.8	0.0156	0.0451	8.7
871209	800	90	0.6	0.7	11.9	16.0	0.0036	0.0338	2.4
871223	1104	441	0.9	2.1	7.6	15.1	0.0153	0.0635	6.3
880104	1348	384	1.3	3.4	8.4	14.2	0.0171	0.0571	8.3
880112	1140	253	1.6	4.0	7.0	10.2	0.0228	0.0455	11.0
880202	824	658	1.1	3.4	9.8	17.1	0.0117	0.0722	6.1
880218	1302	412	1.3	2.9	8.3	15.1	0.0172	0.0661	8.6
880303	1107	243	1.2	3.5	7.5	12.8	0.0182	0.0689	8.0

880321	1016	412	1.1	2.6	7.5	12.2	0.0171	0.0528	7.9
880401	858	176	0.9	2.0	7.6	12.2	0.0121	0.0400	6.1
880415	1025	288	1.9	5.6	9.1	12.2	0.0175	0.0543	10.2
880421	800	114	1.1	2.9	9.2	16.0	0.0190	0.0679	7.5
880518	1005	430	1.0	2.4	8.6	16.0	0.0112	0.0470	5.6
880602	1012	195	0.9	2.2	7.9	12.2	0.0121	0.0562	5.5
880909	1015								
881011	1028	512	1.1	3.1	8.4	16.0	0.0137	0.0524	6.1
881109	926	342	0.9	2.1	9.4	16.0	0.0098	0.0483	4.5
881121	1445	167	1.1	2.1	6.0	11.6	0.0215	0.0474	8.1
881205	952	279	1.2	3.1	6.8	14.2	0.0213	0.0538	8.2
881219	1135	223	1.1	2.4	7.8	23.3	0.0185	0.0581	7.4
890117	1222	458	1.2	2.9	8.0	23.3	0.0149	0.0551	7.5
890125	1226	135	1.5	3.5	8.7	11.6	0.0151	0.0531	8.5
890202	1347	113	0.8	1.5	8.3	16.0	0.0096	0.0408	4.9
890216	1343	223	0.9	2.2	6.4	9.8	0.0173	0.0545	7.1
890221	1130	138	2.1	3.6	8.0	10.7	0.0244	0.0465	13.3
890227	1210	175	2.1	5.0	9.8	13.5	0.0162	0.0494	10.4
890312	1300	275	2.4	4.6	9.3	13.5	0.0191	0.0549	12.4
890328	1348	321	1.3	2.8	7.6	16.0	0.0167	0.0431	8.5
890426	942	549	1.1	2.7	7.7	13.5	0.0143	0.0514	6.9
890508	1336	206	0.8	1.7	6.9	13.5	0.0136	0.0544	5.5
890516	1000	134	0.7	1.4	8.2	11.6	0.0080	0.0184	4.1
890517	1030	16	0.6	0.8	4.7	6.9	0.0231	0.0407	6.4
890524	938	112	1.0	1.7	9.9	17.1	0.0093	0.0396	5.0
890615	859	368	0.6	1.9	7.5	15.1	0.0105	0.0398	4.1
890629	1034	298	0.6	0.9	9.0	14.2	0.0056	0.0423	2.9
890719	1025	250	0.8	1.4	7.7	13.5	0.0115	0.0529	4.6
890726	840	110	0.7	1.0	10.8	17.1	0.0067	0.0214	3.3
890815	1620	327	0.9	2.3	7.9	15.1	0.0124	0.0408	5.3
890824	1620	120	0.7	1.0	8.4	12.2	0.0070	0.0370	3.4
890912	1010	404	1.5	2.9	11.2	17.1	0.0105	0.0448	5.7
891003	1342	468	1.7	3.6	10.4	23.3	0.0152	0.0467	7.6
891010	1350	109	2.1	3.1	14.5	23.3	0.0187	0.0720	7.6
891101	1326	351	1.9	3.4	10.2	23.3	0.0156	0.0713	8.2
891117	1130	260	0.9	2.3	8.4	16.0	0.0127	0.0516	5.5
891128	1540	89	1.0	2.4	7.3	18.3	0.0193	0.0622	6.9
891207	1050	68	1.1	2.7	6.6	23.3	0.0208	0.0558	7.9
891212	1025	NO WAVE MEASUREMENTS							
891221	1220	31	1.3	2.1	7.3	15.1	0.0231	0.0392	9.7
891228	1550	193	2.5	6.0	9.7	16.0	0.0227	0.0442	12.7

APPENDIX E: NOTATION

A = an empirical (shape) parameter

A_* = shape parameter in the offshore region of the profile

d = box dimension in box-counting method

D_o = equilibrium wave energy dissipation per unit volume in the inshore

D_∞ = equilibrium wave energy dissipation per unit volume in the offshore

D_{50} = sediment median grain size

dx_{cg}/dt = speed of bar movement

$Fr = w/(gH_o)^{1/2}$ = sediment Froude number

h = water depth

h_c = minimum bar depth

H = significant wave height

H_b = breaking wave height

H_{max} = maximum significant wave height

H_{mean} = mean significant wave height

H_o = deepwater wave height

H/L = wave steepness

H/wT = fall speed parameter

l_b = bar length

L = wavelength

L_o = deepwater wavelength

$N(r)$ = number of boxes of size r

r = size of boxes in box-counting method

r = correlation coefficient

T_{max} = maximum peak spectral period

T_{mean} = mean peak spectral period

V_b = bar volume

w = sediment fall speed

x = distance offshore (measured from the shoreline, $h = 0$)

x_{cg} = location of bar mass center

x_{end} = seaward limit of bar extent

x_s = location of shoreline

x_{start} = shoreward limit of bar extent

z_m = maximum bar height

Δh_{rms} = root-mean-square deviation in depth

ΔV_b = change in bar volume

λ = characteristic length describing rate at which D_o approaches D_∞

Subscripts

b = breaking; bar

c = (bar) crest

max = maximum value

$mean$ = mean value

min = minimum value

o = deepwater condition

rms = root-mean-square value

Waterways Experiment Station Cataloging-in-Publication Data

Larson, Magnus.
Analysis of cross-shore movement of natural longshore bars and material placed to create longshore bars / by Magnus Larson and Nicholas C. Kraus ; prepared for Department of the Army, US Army Corps of Engineers.
115 p. : ill. ; 28 cm. — (Technical report ; DRP-92-5)
Includes bibliographical references.
1. Sand bars. 2. Sediment transport. 3. Littoral drift. 4. Dredging spoil. I. Kraus, Nicholas C. II. United States. Army. Corps of Engineers. III. U.S. Army Engineer Waterways Experiment Station. IV. Dredging Research Program. V. Title. VI. Series: Technical report (U.S. Army Engineer Waterways Experiment Station) ; DRP-92-5.
TA7 W34 no.DRP-92-5